Integrated Flood Risk Analysis
and Management Methodologies

FLOODsite

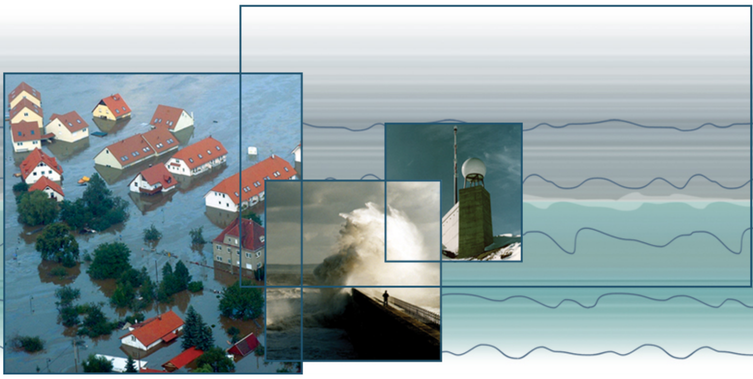

# Reliability Analysis of Flood Sea Defence Structures and Systems

## *APPENDICES 1 TO 5*

| | |
|---|---|
| **Date** | **April 2008** |
| **Report Number** | **T07-08-02** |
| Revision Number | 1_2_P01 |
| Deliverable Number: | D7.1 |
| Due date for deliverable: | February 2008 |
| Actual submission date: | April 2008 |
| Task Leader | 12 |

FLOODsite is co-funded by the European Community
Sixth Framework Programme for European Research and Technological Development (2002-2006)
FLOODsite is an Integrated Project in the Global Change and Eco-systems Sub-Priority
Start date March 2004, duration 5 Years

**Document Dissemination Level**

| | | |
|---|---|---|
| **PU** | **Public** | **PU** |
| PP | Restricted to other programme participants (including the Commission Services) | |
| RE | Restricted to a group specified by the consortium (including the Commission Services) | |
| CO | Confidential, only for members of the consortium (including the Commission Services) | |

Co-ordinator: HR Wallingford, UK
Project Contract No: GOCE-CT-2004-505420
Project website: www.floodsite.net

SIXTH FRAMEWORK PROGRAMME

## DOCUMENT INFORMATION

| | |
|---|---|
| **Title** | Reliability Analysis of Flood Sea Defence Structures and Systems Appendices 1 to 5 |
| **Lead Author** | Pieter van Gelder |
| **Contributors** | **TUD**<br>Foekje Buijs, Cong Mai Van, Wouter ter Horst, Wim Kanning, Mohammad Nejad, Sayan Gupta, Reza Shams, Noel van Erp<br>**HRW**<br>Ben Gouldby, Greer Kingston, Paul Sayers, Martin Wills<br>**LWI**<br>Andreas Kortenhaus, Hans-Jörg Lambrecht |
| **Distribution** | Public |
| **Document Reference** | T 0 7 -08-01 Appendix |

## DOCUMENT HISTORY

| Date | Revision | Prepared by | Organisation | Approved by | Notes |
|---|---|---|---|---|---|
| 01/01/08 | 1.1.p12 | P. van Gelder | TUD | | |
| 01/04/08 | 1.1.p12 | C. Mai Van | TUD | | |
| 09//04/08 | 1.1p12 | P. van Gelder | TUD | | Corrupted Word version replaced |
| 10/04/08 | 1.2P01 | Paul Samuels | HR Wallingford | | Formatted as a deliverable |
| | | | | | |
| | | | | | |


## ACKNOWLEDGEMENT

The work described in this publication was supported by the European Community's Sixth Framework Programme through the grant to the budget of the Integrated Project FLOODsite, Contract GOCE-CT-2004-505420.



## DISCLAIMER

This document reflects only the authors' views and not those of the European Community. This work may rely on data from sources external to the FLOODsite project Consortium. Members of the Consortium do not accept liability for loss or damage suffered by any third party as a result of errors or inaccuracies in such data. The information in this document is provided "as is" and no guarantee or warranty is given that the information is fit for any particular purpose. The user thereof uses the information at its sole risk and neither the European Community nor any member of the FLOODsite Consortium is liable for any use that may be made of the information.

© FLOOD*site* **Consortium**

# CONTENTS

# I. Appendix 1: Details of the PRA Thames

This appendix describes the reliability analysis applied to the Dartford Creek to Gravesend flood defence system in more detail. Section 1 provides a site description, which includes a definition of the floodplain boundaries and main structure types. Section 2 discusses the failure mechanisms and fault trees of the structure types in more detail. To enable probabilistic calculations the flood defence line is discretised into sections which are each over the whole length characterized by one cross section. The discretisation into flood defence sections and the probabilistic calculations is described in section 3. The results of the probabilistic calculations are discussed in section 4.

## 1. Site description

The Dartford Creek to Gravesend flood defence line protects one floodplain and consists of a wide variety of flood defence structures, figure 1.

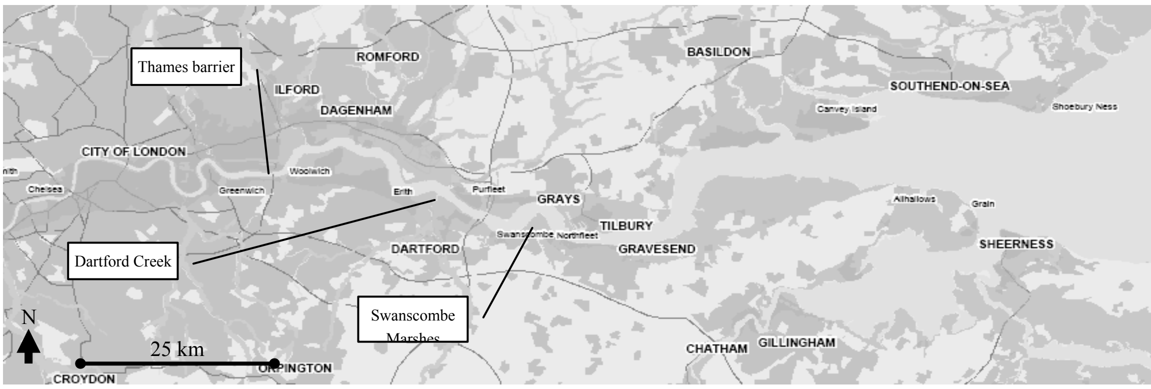


**Figure 1 The location of Dartford Creek, Gravesend and the Thames barrier at Greenwich in the Thames Estuary.**

The flood defence line in the reliability analysis is 10.6 km long, whereby the structure types represent the following proportions:

- Earth embankments: 6.7 km
- Reinforced concrete walls: 1.9 km
- Anchored sheet pile walls: 2.1 km

The elevation of the crest levels is shown in figure 2. The structure types and failure mechanisms are described in more detail in the following section. The hydraulic boundary conditions along the Dartford Creek to Gravesend flood defence line are governed by the tidal conditions rather than the fluvial discharges. A Monte Carlo simulation of joint wind speed and tidal water levels at the mouth of the Thames Estuary is combined with iSIS predictions to derive inner estuarial local water levels. A simple predictive model is applied to derive local wave conditions. The soil conditions are generally represented by a clayey peaty layer overlying a water conductive gravel or sand layer.

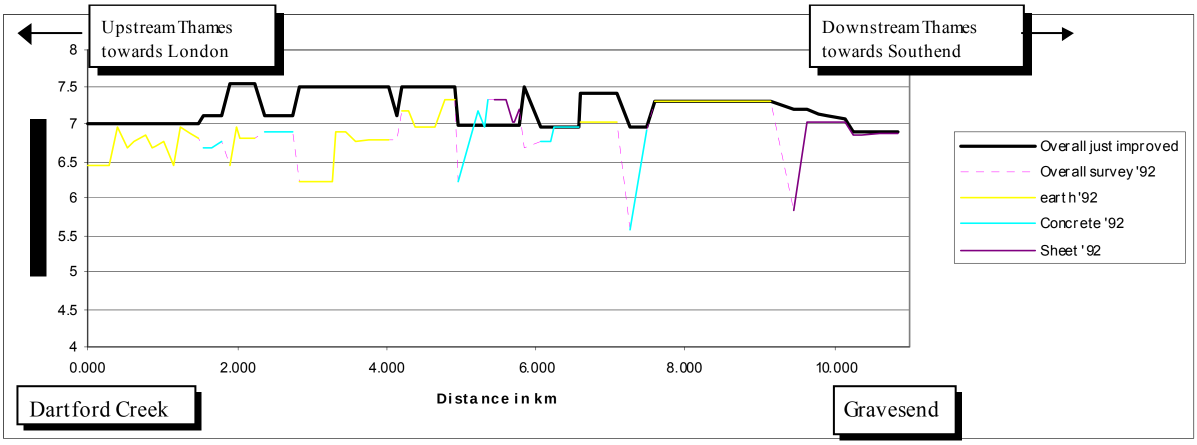


**Figure 2 Elevation of the defence line between Dartford Creek to Gravesend: after '70s / '80s improvements (in black) versus the recently surveyed defence line (dashed purple). The latter indicates the stretches of the different flood defence types.**

## 2. Structure types and failure mechanisms

### 2.1 Earth embankments

The primary function of earth embankments is flood defence. Two types of earth embankments occur along the Dartford Creek to Gravesend defence line: a combination of a riverward and landward earth embankment (referred to as double crested) and the regular earth embankment (referred to as single crested). Figure 3 shows a drawing of the double crested embankments. The basic failure mechanisms and equations of the single and double crested earth embankment are similar. Differences occur between fault trees and some of the details in the failure mechanisms.

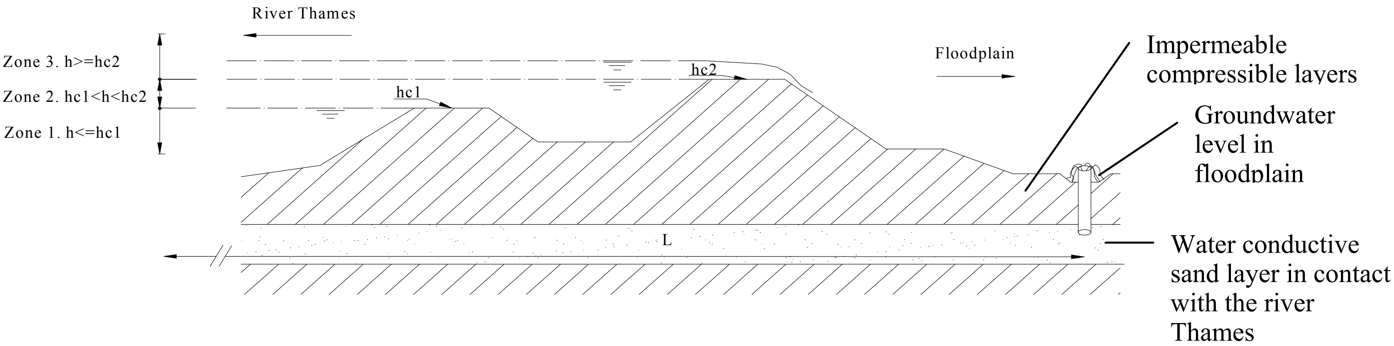


**Figure 3 Representation of double crested earth embankments. Characteristics of process models or fault trees change according to the three different water level zones**

The embankments are generally founded on impermeable layers overlaying a water conductive sand or gravel layer. At some locations the water overpressures in the sand / gravel layer are drained by a pipe, see figure 3.

The failure processes associated with the embankments along the Dartford Creek to Gravesend flood defence system are listed in table 1 along with the failure mechanisms that are implemented in the reliability analysis. Table 1 refers to the failure mechanisms in the Task 4 Floodsite report. The process models for grass erosion are slightly different from those applied in the reliability analysis.

Table 1 An overview of the site specific failure processes and the failure mechanisms included in the Dartford Creek to Gravesend reliability analysis.

| Site specific failure processes | Failure mechanisms in reliability analysis |
|---|---|
| • Overtopping / overflow causing erosion and slope instability<br>• Uplifting and piping<br>• Fissuring / cracking<br>• Long term crest level settlements: compressible layers and estuarial settlements<br>• Short term crest level settlements: off-road cycling<br>• Bathymetrical changes of Thames<br>• Third party activities loading embankment slopes | • (Wave) overtopping and erosion, Aa1.1, Ba2.4i<br>• Combination of uplifting and piping, Ba1.5aii and Ba1.5aiii |

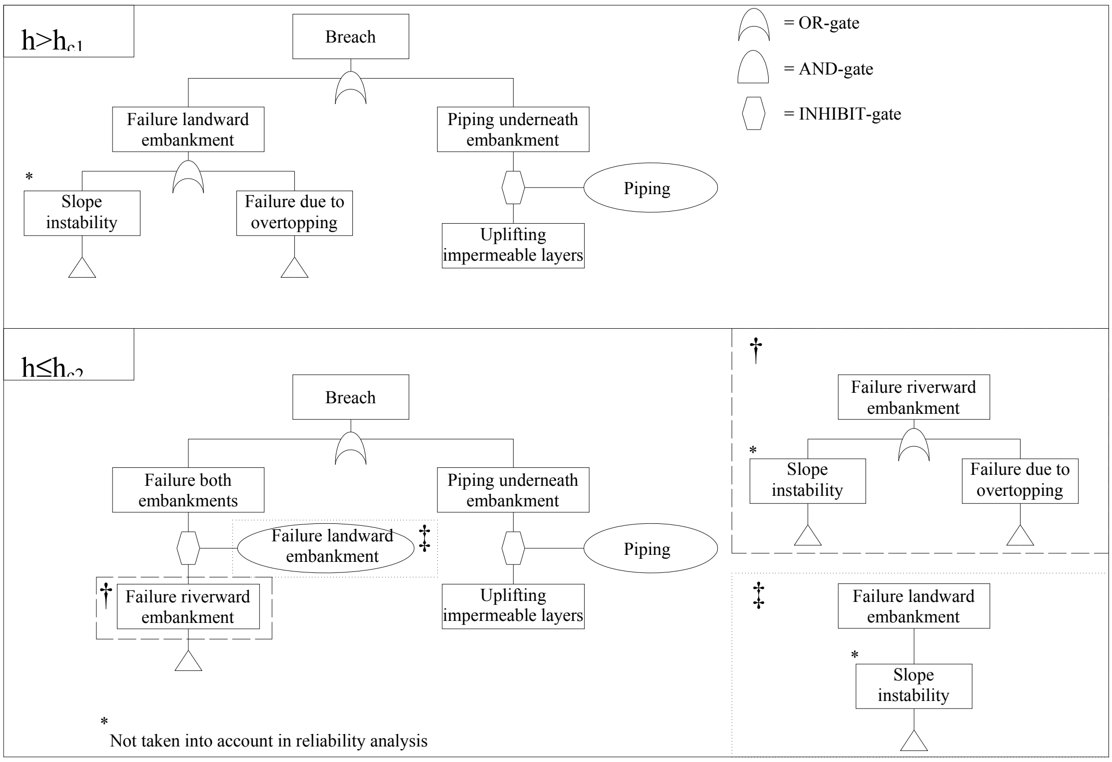


Figure 4 Fault trees for double crested earth embankments underpinning the reliability analysis. Explanation to top fault tree: if the water level is higher than the riverward crest level, $h_{c1}$, then the water level directly loads the landward embankment, $h_{c2}$. Inundation occurs in that case if the landward embankment fails, hence those failure mechanisms are relevant. Explanation to bottom fault tree: If the

## 2.2 Reinforced concrete walls

The primary function of reinforced concrete walls is flood defence, in many cases the reinforced concrete wall is part of a larger earth embankment. The reinforced concrete walls were built as part of flood defence improvements to the Thames Estuary in the ‘70s and ‘80s. There are a number of different types of reinforced concrete walls along the Dartford Creek to Gravesend flood defence line. The three types considered in the reliability analysis as well as a superficial picture are shown in figure 5. Sheet piles applied underneath the concrete structure prevent seepage/piping or in some cases mobilise the soil between the piles for extra stability.

Table 2 contains an overview of the failure processes for reinforced concrete walls along the Dartford Creek to Gravesend flood defence line. The table also indicates the failure mechanisms incorporated in the reliability analysis and reference to those in the Task 4 Floodsite report. Figure 6 presents the fault tree applied to the reinforced concrete wall in the Dartford Creek to Gravesend reliability analysis.

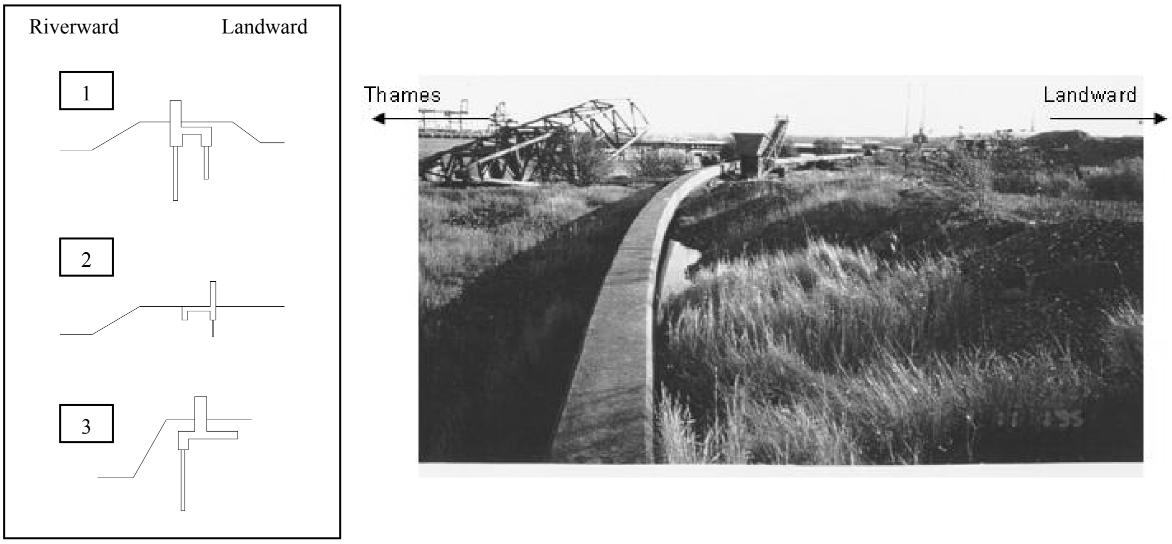


Figure 5 The three reinforced concrete wall types implemented in the reliability analysis (left), a picture of reinforced concrete walls along the flood defence line (right).

Table 2 Overview of site specific failure processes and failure mechanisms implemented in the reliability analysis.

| Site specific failure processes | Failure mechanisms implemented in reliability analysis |
|---|---|
| Damage by residential developments: concrete cracking, joint failure and settlements | • Uplifting and piping underneath overall earth embankment (only for types 1 and 2), Ba1.5aii and Ba1.5aiii<br>• Sliding of the concrete wall, Cc1.2aii<br>• Overturning of the concrete wall, Cc1.2b<br>• Reinforcement failure in the vertical concrete slab, Cc1.2c<br>• Shear failure in the vertical concrete slab, Cc1.2d<br>• Piping directly underneath seepage screen, Cc1.5 |

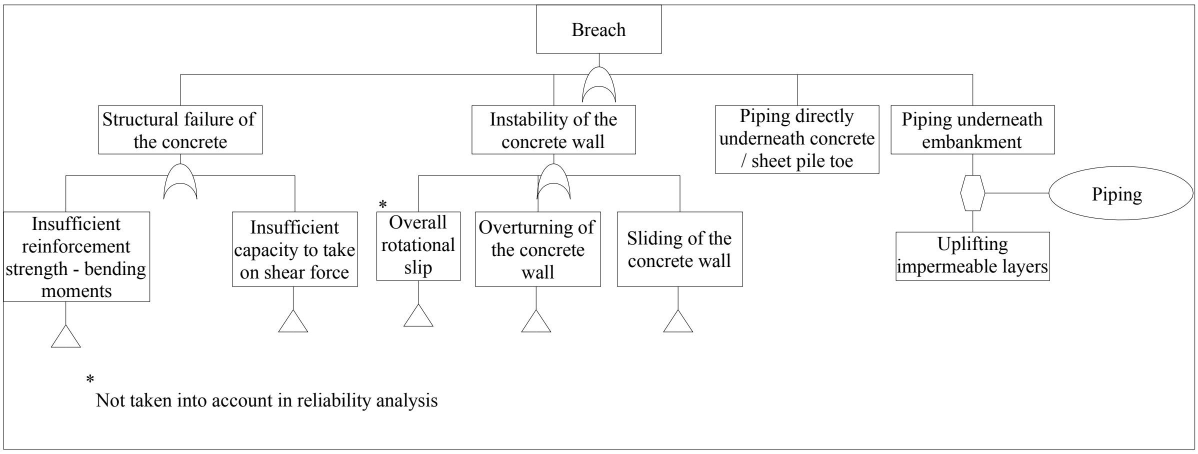


Figure 6 Simplified fault tree for reinforced concrete wall as applied in reliability analysis (top).

### 2.3 Anchored sheet pile walls

The primary function of anchored sheet pile walls is a ground retaining frontage which was previously used as docks. Sheet pile walls were refurbished as part of the Thames Estuary flood defence improvements in the ‘70s and ‘80s. Figure 7 shows an example of an anchored sheet pile wall applied along the Dartford Creek to Swanscombe Marshes defence line. In some cases old frontages in the form of for instance masonry walls are still present in the ground behind the current sheet pile walls, the space in between the walls backfilled with concrete. In other cases, the old frontage was used to anchor the sheet pile walls or the rubble of the old frontage was used as backfill material. The failure mechanisms are organized in a fault tree according to figure 8. Table 3 presents the site specific failure processes and the failure mechanisms taken into account in the Dartford Creek to Gravesend reliability analysis. The failure mechanisms refer to the Task 4 Floodsite report on flood defence failure mechanisms.

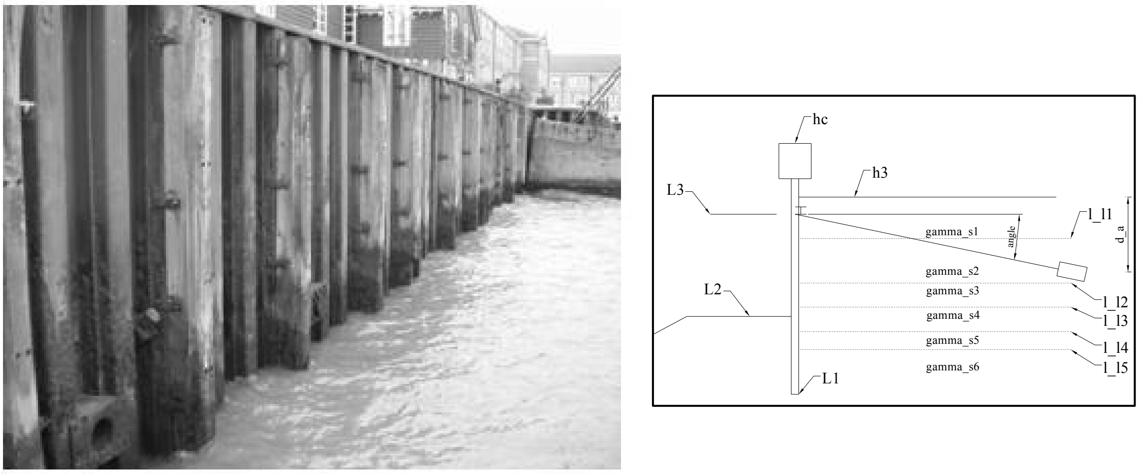


Figure 7 Example of a sheet pile wall along the Dartford Creek to Gravesend defence line.

*Table 3 Site specific failure processes and failure mechanisms implemented in the reliability analysis of anchored sheet pile walls.*

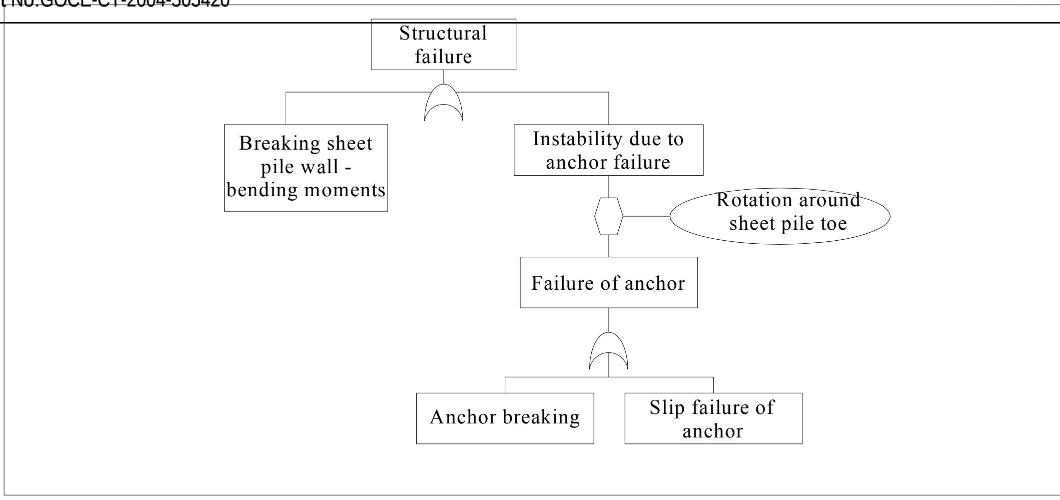


Figure 8 Simplified fault tree for anchored sheet pile wall as applied in reliability analysis

| Site specific failure processes | Failure mechanisms implemented in the reliability analysis |
|---|---|
| • Accelerated Low Water Corrosion in the splash zone<br>• Corrosion of the ground anchors | • Breaking of the ground anchor, Cb1.2a<br>• Sliding of the ground anchor due to insufficient shear strength of the soil, not included in Task 4 report<br>• Breaking of the sheet pile cross section, Cb1.2c<br>• Rotational failure of the sheet pile after failure of the ground anchor, Cb1.2d |

## 3. Discretisation and probabilistic calculations

After the site description the reliability analysis proceeds with the process model definition of the failure mechanisms for each structure type. In order to carry out the probabilistic calculations, the relevant flood defence information needs to be extracted. To this end, the flood defence line is discretised into flood defence sections with similar characteristics. Each flood defence section is represented by one cross section in terms of its geometry, revetment, soil properties, hydraulic boundary conditions etc. The information requirements are determined by the failure mechanisms that are taken into account for the structure type of the flood defence section. Figure 8 presents the flood defence sections in which the flood defence line is discretised.

Figure 9 shows a flow chart for the calculations of the annual probability of failure and the fragility of the earth embankments, reinforced concrete walls and anchored sheet pile walls.

## 4. Discussion of the results of the reliability analysis

Figure 10 and 11 present fragility curves for earth embankments and reinforced concrete walls. Anchored sheet pile walls are more likely to fail for lower water levels. During a storm with increasing water levels the probability of failure therefore remains equal to the initial failure probability. The probability of failure of the anchored sheet pile wall equals 0.15 due to jointly anchor breaking and rotational failure of the sheet pile wall. The probability of failure does not always cover all the relevant failure mechanisms or the probability of breach. The probability of failure of earth embankments does not take slope instability into account. The probability of failure of reinforced concrete walls does not take failure of the embankment underneath the concrete wall into account and therefore does not

represent the probability of breach. The probability of failure of anchored sheet pile walls represents the probability of ground instability and damage to the assets behind the anchored sheet pile wall.

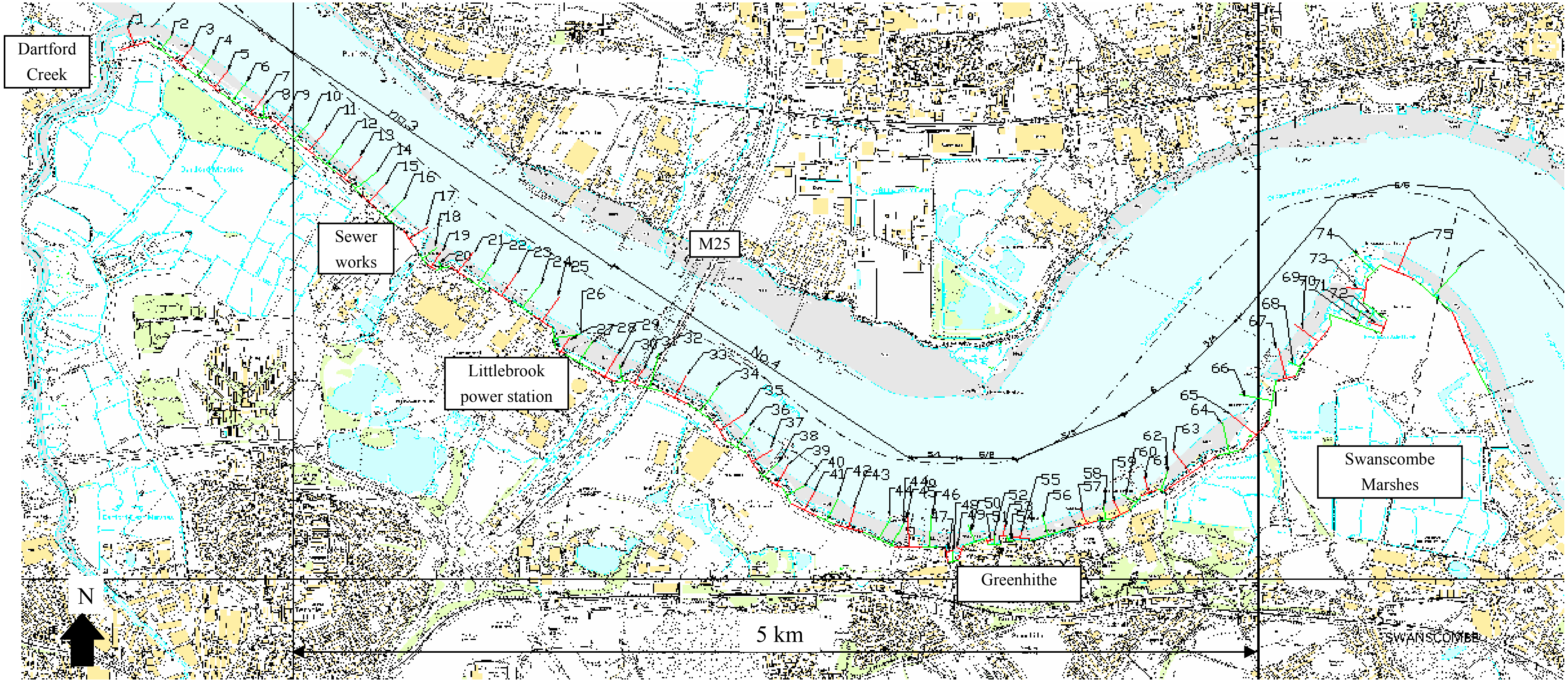


Figure 9 Flood defence sections 1 to 75 in the Dartford Creek to Swanscombe Marshes flood defence system, sections 1 to 67 are included in the time-dependent system reliability analysis.

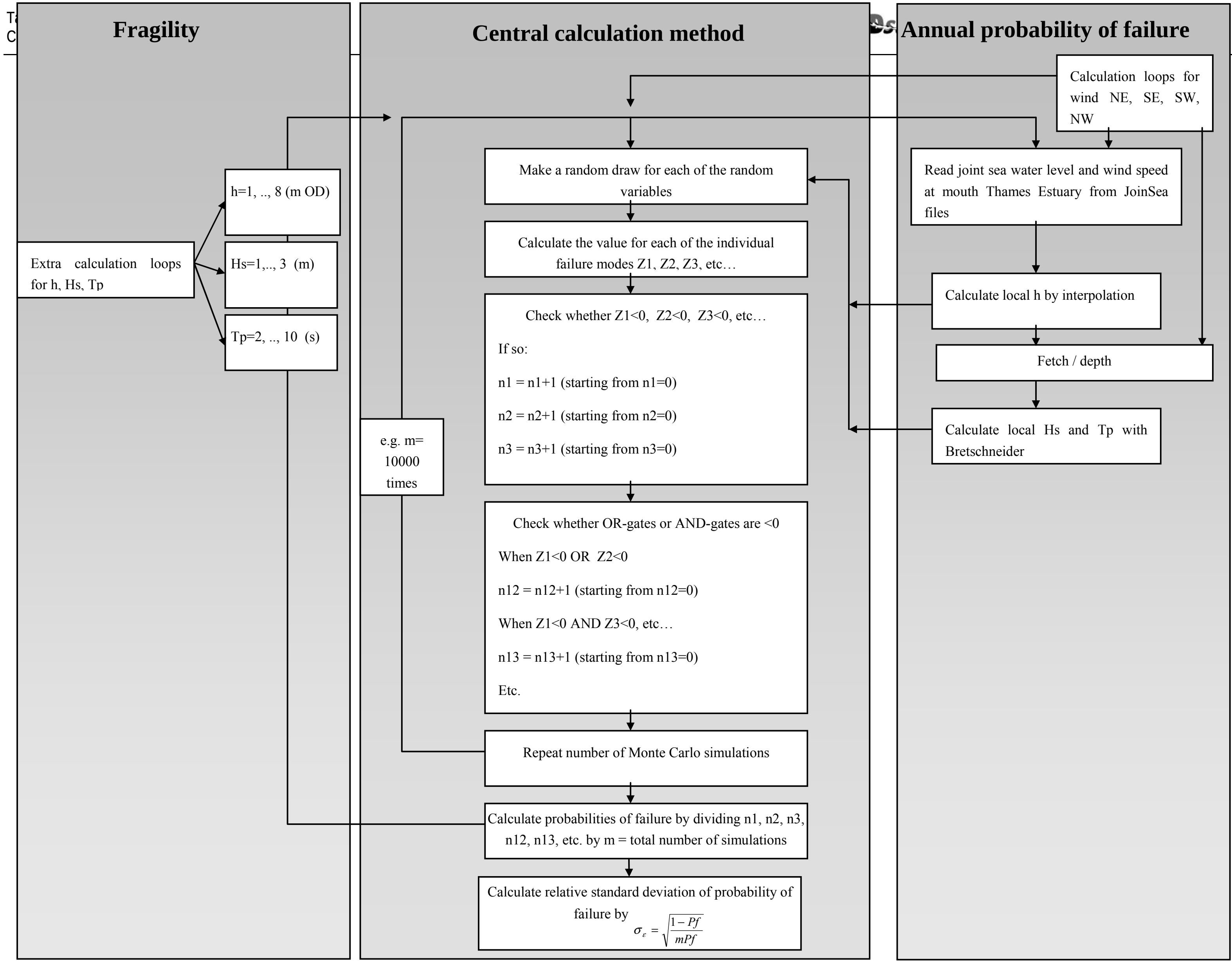


Figure 10 Flow chart with steps to calculate fragility and the annual probability of failure

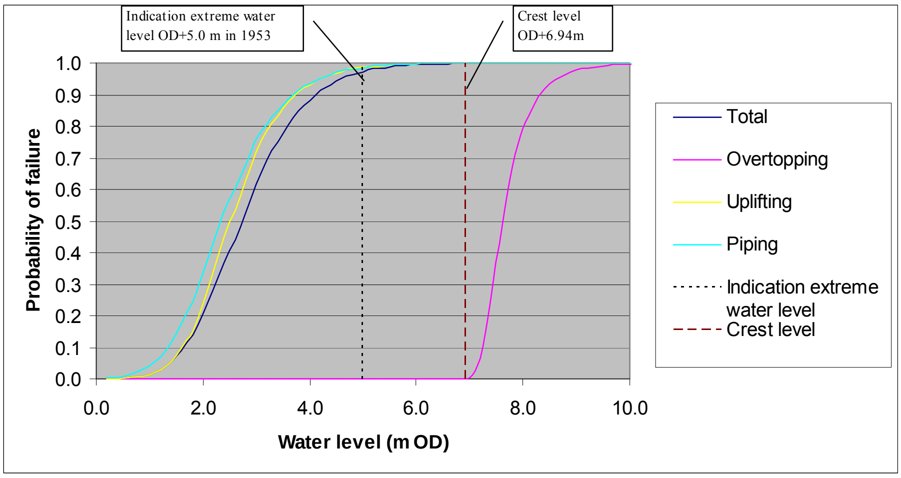


Figure 11 Fragility for earth embankment section 4. The failure mechanism driven by a combination of uplifting and piping

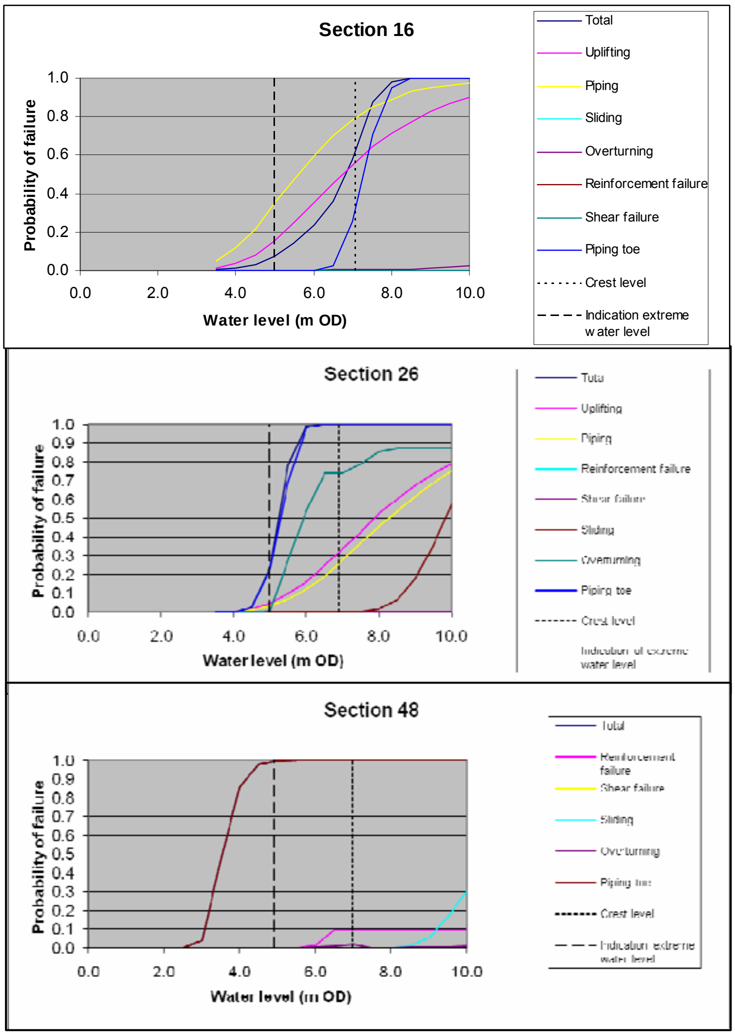


Figure 12 Fragility curves for three different types of reinforced concrete walls.

# II. Appendix 2: Details of the PRA Scheldt

## II-1 INTRODUCTION

### *Background*

FLOOD*site* is aiming for Integrated Flood Risk Analysis and Management Methodologies. New research efforts in this field will be undertaken to fill gaps in knowledge and to achieve a better understanding of the underlying physics of flood related processes.

Any new knowledge developed in FLOOD*site* will be developed and tested at selected pilot sites in Europe which will help to identify missing elements in research. These pilot sites are

- River Elbe Basin
- River Tisza Basin
- Flash Flood Basins
    - the Cévennes-Vivarais Region (France);
    - the Adige River (Italy);
    - the Besos River and the Barcelona Area (Spain);
    - the Ardennes Area (Trans-national);
- River Thames Estuary
- River Scheldt Estuary
- River Ebro Delta Coast
- German Bight Coast

It can be seen that pilot sites are well distributed over the types of waters like rivers, estuaries and coasts as well as types of floods like plain and flash floods. For each of those sites at least two pilot areas with different properties have been selected to test as many newly developed tools as possible. The 'Scheldt' has been selected as a typical North Sea area which is protected against coastal flooding by means of different flood defence structures such as forelands, sea dikes, dunes and other constructions.

The methodologies developed under FLOOD*site* are partly based on a probability based risk analysis. This analysis will require a set of failure modes and related limit state equations for each of the flood defence structures under question. The aim of this report is to provide a first calculation of the overall failure probability of flood defence structures in the Scheldt area. The limit state equations which will be used within this report is based on available LSEs outside FLOOD*site*. These equations will be updated when more information is available from Task 4 of FLOOD*site*.

At the beginning of a reliability analysis of a flood defence system, a very limited physical knowledge will be available on failure modes, their interactions and the associated prediction models, including the uncertainties of the input data and models. Therefore, a detailed flood risk assessment based on a

sound physical understanding of the failures and the possible flooding of the protected area will not be feasible at this stage. Therefore, initially, the reliability analysis focuses on providing support to feasibility level decisions.

In order to identify the relative importance of the gaps in the existing knowledge and to help to optimise research objectives, it is necessary to perform a very preliminary flood risk analysis using a holistic approach (feasibility level). For this purpose, three selected pilot sites in different countries and from different areas (coast, estuary, river) will be used (HRW, TUD, and LWI). The main outputs and benefits from this preliminary study will identify more precisely (i) the relative importance of the uncertainties and their possible contributions to the probability of flooding, (ii) the gaps related to prediction models and limit state equations by means of a detailed top-down analysis; (iii) the uncertainties which are worth reducing by the generation of new knowledge, (iv) the priorities with respect to the allocation of research efforts for the various topics to be addressed in the other sub-projects, (v) the areas of high, low and medium uncertainty.

There is potential for significant differences in the PRA approach between the 3 pilot studies. TUD/HR/LWI need to review before any work starts to ensure that, at minimum, there is a common understanding of each PRA approach, and at best, that a common approach is adopted for all three.

The preliminary analysis in this report will assess the probabilities of flooding and related uncertainties in the south-western province of the Netherlands. Dike ring area 32 will be examined to see how reliable the flood defences are and to identify any weak points. In particular attention will be paid to the special elements in the dike rings; hydraulic structures such as locks, weirs and pumping stations. To date, little is known about the safety of these elements.

Existing techniques (among others the PC Ring approach) will be applied in first instance. Refined techniques will be proposed in case the resulting failure probability from PC Ring is too inaccurate.

The Western Scheldt forms the entrance to the harbour of Antwerp (Belgium). Water levels are influenced by the wind surges on the North Sea, as well as the river discharges from the Scheldt. There are four surrounding dike ring areas along the Western Scheldt (no. 29 to 32).

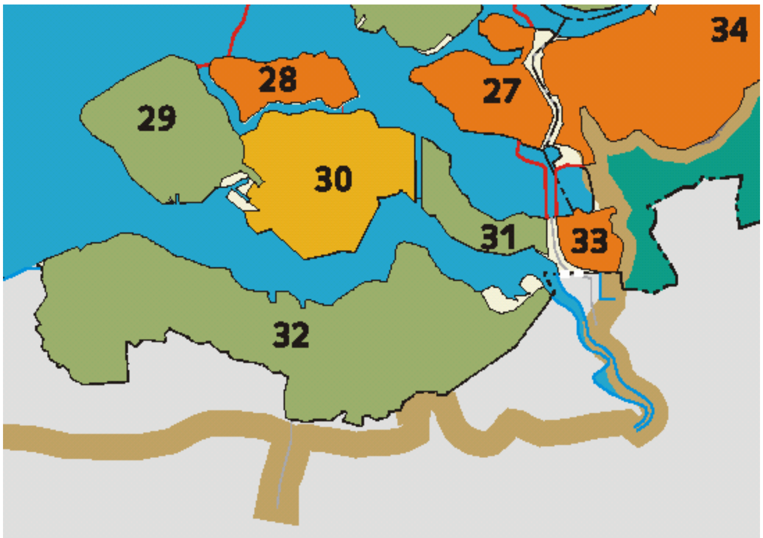


Figure 1 Dike ring areas in the southern part of the province Zeeland, along the estuary Western Scheldt: no. 29 = Walcheren, no. 30 = Zuid Beveland West, no. 31 = Zuid Beveland Oost, no. 32 = Zeeuwsch Vlaanderen

The water board Zeeuwse Eilanden (http://www.wze.nl) has provided the problem identification and data with respect to problematic dike sections along the western Scheldt. The study of VNK (Ministry of Water Management) will serve as a basis for further investigations of this test pilot site.

# II-2 PILOT SITE ‘SCHELDT’

This section provides a description of dike ring area 32, Zeeuws-Vlaanderen, and the schematizations of the various dike sections. The assessment of the water board is given in this section as well.

Section 2.1 provides general information concerning the location and the characteristics of the dike ring followed by an overview of the dikes and structures in section 2.2. Sections 2.3 to 2.8 take a closer look at the schematization of the dikes and dunes. Section 2.9 finally gives an overview of the assessment of the water board. Calculations have been made by DHV with checks by VNK and assessments by WZE.

## *Location and characteristics*

Dike ring area 32 encompasses all of Zeeuw-Vlaanderen with primary embankments of category a, these are embankments that enclose the dike ring areas – either with or without high grounds- and directly retain outside water, along the North Sea and Westerschelde. The length of primary embankments in Zeeuws-Vlaanderen amounts to 85 kilometers, of which 8 kilometers of dune coast. The exceedance frequency for this area equals to 1/4000 years. The dike ring is border-crossing with Belgium. The embankments in Belgium are of category d. Its length is unknown. A system of regional (secondary) embankments is situated at a variable distance from the primary embankments along the whole North Sea coast and Westerschelde.

An overview of the dike ring area is given in figure 2-1.

The dike ring is enclosed by the following embankments:

- The dike along the Westerschelde
- The dike along the Schelde
- The high grounds in Belgium and Northern France
- The sea retaining dunes or dikes of Belgium, Northern France and the Netherlands

## *Dikes, dunes and structures*

An overview of the embankments in dike ring 32 is given on the overview map primary and regional embankment of dike ring area 32. The following important water retaining structures can be distinguished:

- Dike with stone covering
- Dike with grass covering
- Dike with asphalt covering

- Dune
- Sea walls RWS (Public Works and Water Management)
- Engineering structure

The following division can be made:

- 0 - 0.8 km : dike with stone covering
- 0.8 - 4.3 km : dike with grass covering
- 4.3 - 20.1 km : dike with stone covering
- 20.1 - 22.0 km : sea wall RWS
- 22.0 - 40.2 km : dike with stone covering
- 40.2 - 44.7 km : sea wall RWS
- 44.7 - 67.0 km : dike with stone covering
- 76.0 - 68.2 km : dune
- 68.2 - 69.7 km : sea wall RWS
- 69.7 - 70.1 km : dike with stone covering
- 70.1 - 71.2 km : dune
- 71.2 - 76.3 km : dike with stone covering
- 76.3 - 77.3 km : dune
- 77.3 - 78.8 km : dike with grass covering
- 78.8 - 79.8 km : dike with stone covering
- 79.8 - 82.7 km : dune
- 82.7 - 82.9 km : dike with stone covering
- 82.9 - 84.3 km : dune
- 84.3 - 84.6 km : dike with stone covering
- 84.6 - 85.1 km : dune
- 85.1 - 85.7 km : grass

The division and selection of dike and dune section is looked further into in section 2.3.

14 Structures are present in dike ring area 32. An overview of these structures is given in table 2-1.

| | |
|---|---|
| 1 | Pumping station Cadzand |
| 2 | Pumping station Campen |
| 3 | Pumping station Nieuwe Sluis |
| 4 | Pumping station Nummer Een |
| 5 | Pumping station Othene |
| 6 | Pumping station Paal |
| 7 | Sluice station Terneuzen Oostsluis |
| 8 | Sluice station Terneuzen Middensluis (schutsluis) |
| 9 | Sluice station Terneuzen Middensluis (spuiriool) |

| | |
|---|---|
| 10 | Sluice station Terneuzen Westsluis |
| 11 | Sluice station Terneuzen Westsluis (spuiriool) |
| 12 | Discharge sluice station Braakman |
| 13 | Discharge sluice station Hertogin Hedwigepolder |
| 14 | Discharge sluice station Nol Zeven |

*Table 2.1: Structures in dike ring 32*

### *Division in 33 dike and 4 dune sections*

The dike ring area "Zeeuws-Vlaanderen" was initially divided into 287 dike sections according to the VNK-schematization. These were mainly dikes, but encompassed a number of dunes and structures as well. Because calculating the probability of failure for this number of dike sections with PC-Ring is very elaborate, a selection has been made by DHV. This selection is based on the presently existing sections in PC-Ring. Thus no routes with representative dike sections have been selected.

The chosen 33 dike and 4 dune sections are dike ring covering and are deemed to be representative for the total dike ring.

The dike ring area is divided into parts for the selection, each with their own characteristic orientation. One or more dike sections are selected within these parts, where thought is given to the following aspects:

Length of the dike section

Height of the crown

Height of the toe

Orientation of the dike section

Presence of shoulder and/or bend (in other words type of dike section)

Dike covering

The results of the already calculated overflow/wave run-up and bursting/piping of PC-Ring are considered for the choice of dike sections. The dike sections with a significant higher probability of failure have been selected. It was decided to add two more weak links, in consultation with the District Water Board Zeeuws-Vlaanderen. These are dike sections 7009 and 7023. This brings the total number of sections that are taken into account in PC-Ring to 37, of which 33 dike and 4 dune sections. This

number is without the water retaining structures (14 structures). The location of the selected dike sections is shown in figure 2-1 (in which dike section 2 represents dike section number 7002 etc). The selected dune sections are given in figure 2-2 (dune section 8 represents dune section number 7008 etc).

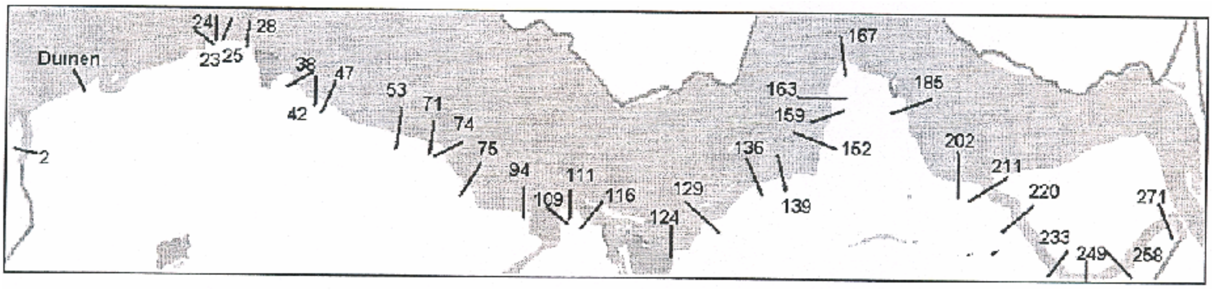


Figure 2-1 Selected dike sections

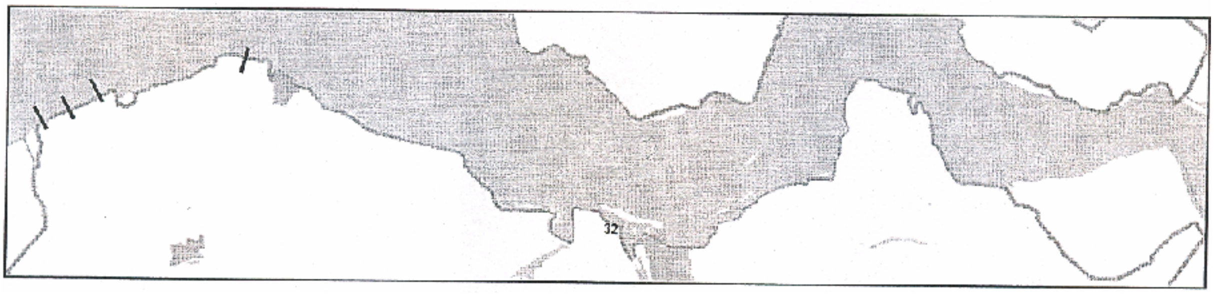

Figure 2-2 Selected dune sections

The 33 dike sections are numbered according to the following distances in kilometer :

| | | | | | | | | | | | | | | |
|---|---|---|---|---|---|---|---|---|---|---|---|---|---|---|
| 7002 | 7009 | 7023 | 7024 | 7025 | 7028 | 7038 | 7042 | 7047 | 7053 | 7071 | 7074 | 7075 | 7094 | 7109 |
| 85.2 | 82.4 | 71.7 | 71.6 | 71.2 | 70.1 | 65.1 | 64.1 | 63.6 | 61.9 | 57.6 | 56.9 | 55.7 | 51.7 | 47.4 |

| | | | | | | | | | | | | |
|---|---|---|---|---|---|---|---|---|---|---|---|---|
| 7111 | 7116 | 7124 | 7129 | 7136 | 7139 | 7152 | 7159 | 7163 | 7167 | 7185 | 7202 | 7211 |
| 46.4 | 45.7 | 39 | 36.7 | 33.3 | 32 | 28.2 | 27.1 | 25.6 | 24.2 | 18.8 | 14.1 | 12.6 |

| | | | | |
|---|---|---|---|---|
| 7220 | 7233 | 7249 | 7258 | 7271 |
| 11.5 | 8.8 | 6.4 | 3.9 | 0.9 |

### Adjustments of profiles

DHV has made several adjustments to the PC-Ring database during the calculations. Apart from the adjustment of the dike section selection, as discussed in the previous section, the dike profiles are adjusted to recently measured cross-sections of the water board . The adjustments of the profiles is further commented on in appendix A.

### Schematization of coverings

Often more than one type of covering on a dike section is present in dike ring 32. PC-Ring is unable to perform calculations for more than type of covering for 1 dike section. In case more than one type of covering is present, VNK calculates all types individually and determines which one is governing (also in relation to concurrent design points). This governing covering is consequently accounted for when calculating the probability of flooding.

Only 1 type of covering per section is calculated in the calculations for dike ring 32:

Dike sections 7002 (024-Dp7), 7258 (074-Dp99) and 7271 (072-Dp69) for grass covering

Dike sections 7024 (006a-Dp11) and 7025 (006a-Dp15) for asphalt covering

The other sections for stone covering

The types of covering for which the various sections have been calculated are familiar to the water board.

There are 2 options for schematization in case more than one type of stone covering is present in 1 section:

Take the average along the total section

Take the worst part for a shorter length of the section

In order to be able to compare the results it should be possible to insert both values in the overall spreadsheet.

### Schematization of dunes

It was agreed upon with engineering bureau VNK to perform calculations on the measured dune sections of 2004 (5 pieces) because these provide a conservative image (a 5-annual supplement is not planned until 2005). The choice of dune sections to be calculated is done based on the 2004 report of RIKZ. The choice is commented on in appendix A.

### Schematization foreland of Saeftinghe

Shallow foreland is present in the land of Saeftinghe (6 most easterly located sections 7211 to 7271). This foreland is not accounted for in the calculations in this dike ring report. The boundary condition points (SWAN-points) are 100 meter from the coast (300m apart), so the influence of the foreland will be partially included in these. Foreland over 100 meter is of no use anyway.

### Selection of profiles for sliding mechanism inner slope

Because calculating the sliding mechanism is an elaborate process, this calculation is not performed for all sections. The district water board has made a selection of 7 cross-section profiles (out of a series of 40 that were used for the testing) during the process of schematization. From these only 1 matches with one of the 33 selected dike sections. Therefore only one result will be calculated for the sliding mechanism of the inner slope.

### Assessment of the water board

In accordance with the “Law on water retention 1996” the District Water Board Zeeuws-Vlaanderen reported on the condition of the embankments in dike ring 32 to the County Council of the Zeeland Province, at the end of 2000. This concerned the first report from a series of the 5-annual safety tests.

*Dikes*

The assessment of the water board for dike ring 32, based on the results of the first test, is summarized in table 2-2 for the selected sections. In this table the Ht_score represents the score for overflow and

wave run-up, STPI_score represents the score for bursting and piping, STBI_score represents the score for stability of the inner slope. In case of an even score, one can assume that the overflow and wave run-up mechanism is governing. For the covering damage and erosion body of a dike mechanism the result of the 'old' testing is not provided. The calculated probabilities of failure for this mechanism are discussed during consults with the water board and related to the temporary results of the 'new' testing (see section 4).

| 7002 | 7009 | 7023 | 7024 | 7025 | 7028 | 7038 | 7042 | 7047 | 7053 | 7071 | 7074 | 7075 | 7094 | 7109 |
|---|---|---|---|---|---|---|---|---|---|---|---|---|---|---|
| suf | insuf | suf | suf | suf | suf | suf | suf | suf | suf | suf | suf | suf | suf | suf |
| suf | suf | suf | suf | suf | suf | suf | suf | suf | suf | suf | suf | suf | suf | insuf |
| suf | suf | suf | suf | suf | suf | suf | suf | suf | suf | suf | suf | suf | suf | suf |

| 7111 | 7116 | 7124 | 7129 | 7136 | 7139 | 7152 | 7159 | 7163 | 7167 | 7185 | 7202 | 7211 |
|---|---|---|---|---|---|---|---|---|---|---|---|---|
| insuf | insuf | insuf | suf | suf | suf | insuf | suf | suf | suf | suf | suf | insuf |
| insuf | suf | suf | suf | suf | suf | suf | suf | suf | suf | suf | suf | suf |
| suf | suf | suf | suf | suf | suf | suf | suf | suf | suf | suf | suf | suf |

| 7220 | 7233 | 7249 | 7258 | 7271 |
|---|---|---|---|---|
| suf | suf | suf | suf | suf |
| insuf | insuf | suf | suf | insuf |
| suf | suf | suf | suf | suf |

*Table 2-2 Assessment of the water board for dikes in dike ring 32 (the first row shows the section number, the second row the Ht_score which represents the score for overflow and wave run-up, the third row shows the STPI_score which represents the score for bursting and piping, and the fourth row the STBI_score which represents the score for stability of the inner slope. Suf stands for sufficient and Insuf for insufficient.*

*Dunes*

Recent research established that one has to reckon with heavier wave action than was assumed so far along the Dutch coast. This could imply that embankments of Zeeuws-Vlaanderen no longer comply with the legal requirements. The calculated weak spots, based on the given boundary conditions,

provide a true representation of the locations with the greatest strength deficiencies. These are determined by the water board and the assessment of the water board, based on unambiguity in boundary condition sections and the shape of the coastal sections, leads to the following strength deficiencies (see figure 2-3).

- The dune area of Cadzand, west of the outlet with the adjoining sea dike of the Kievitspolder East (coastal length 940m, test crown height deficiency 2.00m) (Figure 2-4, top left).
- The sea dike of the Jong Breskenpolder between Nieuwe Sluis and the lighthouse (coastal length 1060m, test crown height deficiency 0.50 to 1.00m) (Figure 2-4, top right).
- The addition to the artificial dune in Breskens at the Veerhaven (coastal length 470m) (Figure 2-4, bottom left).
- 4 junctions of constructions of sea dikes and/or dune toe defense on the adjacent dune area (coastal length 600m at Schoneveld, the Kruishoofd and Nieuwe Sluis).
- The slopes of stone on sea dikes and connection constructions (coastal length 8100m, tested under Project Zeeweringen).

1. The dune area of Cadzand, west of the outlet with the adjoining sea dike of the Kievitspolder East.
2. The sea dike of the Jong Breskenpolder between Nieuwe Sluis and the lighthouse
3. The addition of the artificial dune in Breskens at the Veerhaven

Figure 2-3 Weak spots according to the assessment of the water board

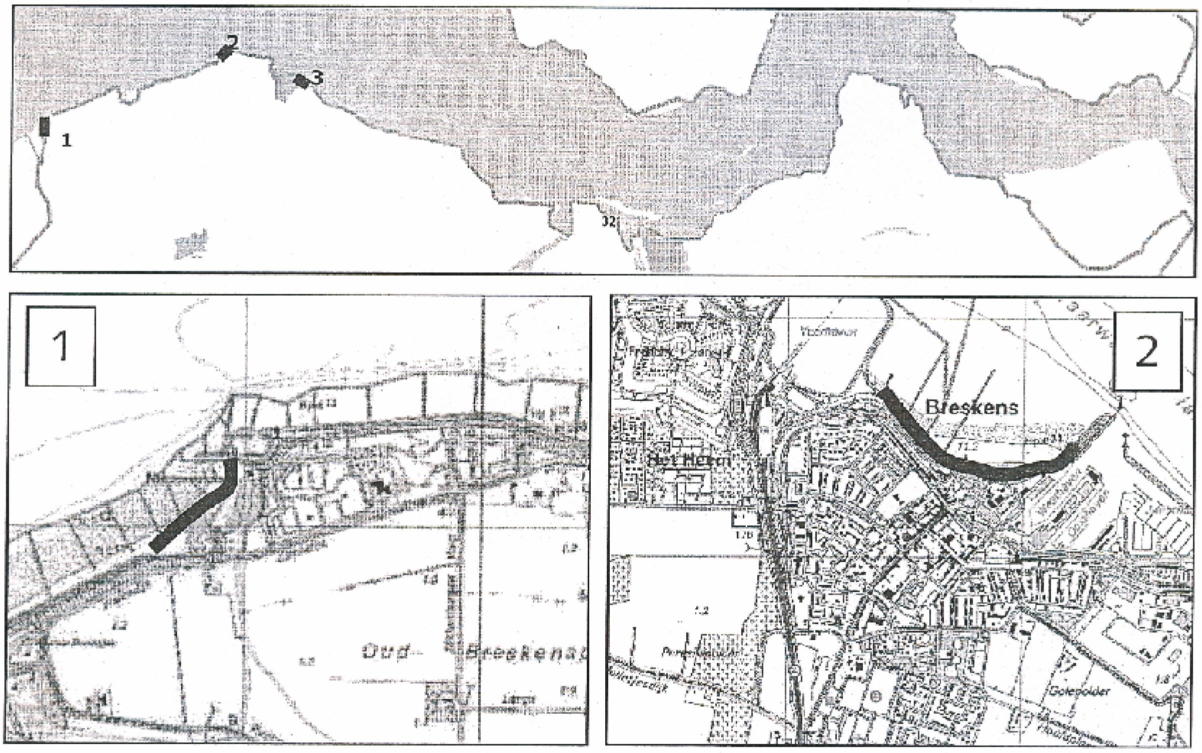

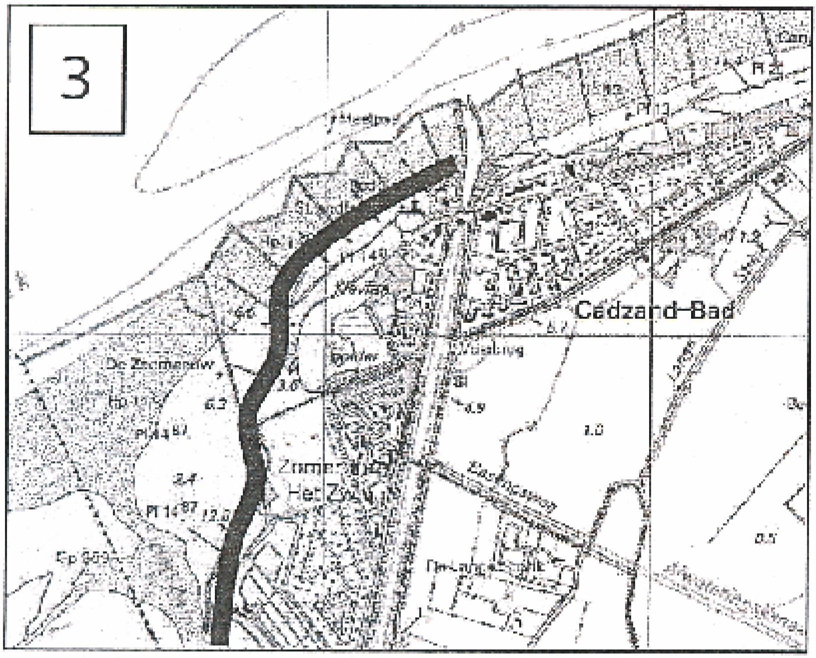
3
Cadzand-Bad

## II-3 LEVEL III PROBABILITY OF OVERTOPPING CALCULATION DIKE RING AREA 32

The probability of a dike failure due to overtopping is considered of dike ring 32. Overtopping is assumed to take place due to extreme sea levels, extreme river discharge or a coincidence of both. The levels of the river and sea are modelled as random variables and the water level along a dike section is obtained as a nonlinear function of these random variables. The height of the dike is assumed to have spatial uncertainty variation. A Monte Carlo simulation based approach is considered for the reliability analysis of the dike. The computation of the local water level involves calculation through a computationally intensive hydrodynamic model and is carried out using commercially available software. Efforts to reduce computational time in the reliability analysis are explored through the use of importance sampling technique. Further reduction in computational efforts is achieved by adopting a novel response surface based method. This strategy involves using available response database for the local water levels corresponding to observed boundary conditions. In the importance sampling based Monte Carlo simulations carried out in this study, the local water levels are computed by interpolating from the available response database rather than using the hydrodynamic model. The proposed method is observed to bring about significant reduction in computational efforts.

### *Introduction*

The reliability analysis of a dike at a lower reach of the tidal Scheldt river is considered.  In this study, it is assumed that dike failure occurs due to overtopping only. Overtopping of the dike is assumed to take place due to (a) extreme sea levels, (b) extreme river discharge and (c) coincidence of both of the above extremal events. This has been illustrated by the schematic diagram in Figure 3-1. The stochastic nature of the input variables, in this case, the extreme levels of the sea and river discharge and the time of their occurrence, implies the necessity for using probabilistic methods for the analysis.

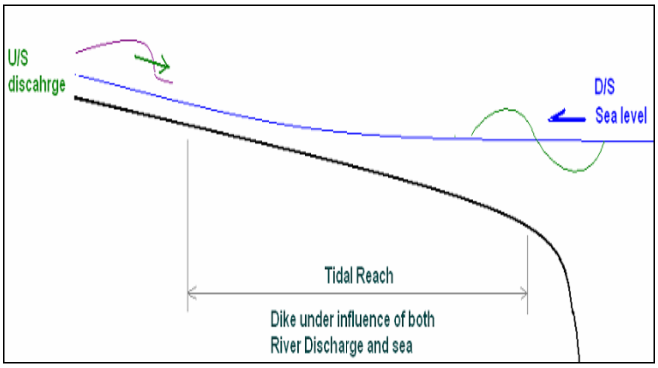


Figure 3-11:Dike on tidal reach of a river subjected to both discharge and sea level variations.

Use of Monte Carlo simulations for reliability analysis lead to accurate estimates of the failure probabilities. Here, the basic steps involved are (i) digital generation of an ensemble of loading conditions that obey specified probabilistic laws, (ii) treatment of each realisation of the problem using deterministic procedures, and (iii) statistical processing of the ensemble of sample solutions for the problem, leading to estimates of the failure probability. Thus, in principle, the method is applicable to any problem where it is possible to digitally generate an ensemble of loading

conditions and deterministic solution methods for a sample problem are available. The method, however, can be computationally intensive.

For the river dike problem considered in this study, the water levels along the dike segment are computed using a hydrodynamic model. This requires nontrivial computational effort. In Monte Carlo simulations, repeated analysis of the hydrodynamic model for each realization of the random boundaries makes Monte Carlo simulations very expensive. This implies that there is a need to explore the use of alternative less computationally intensive techniques for reliability analysis. One such method, the importance sampling technique, is used in the study carried out in this paper. The method is applied to estimate the two-days overflowing probability of a dike of length 80 km along the Western Scheldt, Province of Zeeland, The Netherlands. Three variables, namely, the dike height, sea level and Scheldt river discharge are considered as randomly distributed variables. The limit state is idealized as a function of these three mutually independent random variables. Probability distributions for these three random variables are constructed from analysis of data based on observations from the site (Pandey *et al.*, 2003). Calculations through the hydrodynamic model are carried out with a commercially available software (SOBEK). Additionally, the use of a response database in lieu of the hydrodynamic model for calculating the water level along the dike is explored (Dahal, 2005).

### *Importance sampling*

First, a brief review of the method of importance sampling is presented. Assume that the uncertainties associated with the problem are represented through a vector of random variables X. The performance function is given by g(X), such that, g(X)<0 indicates failure, g(X)>0 indicates safe region and g(X)= 0 denotes the limit state. Using Monte Carlo simulations, an estimate of the failure probability, $P_f$, is obtained as

$$P_f = \int_{-\infty}^{\infty} I[g(\mathbf{X}) \le 0] p_{\mathbf{X}}(\mathbf{x}) d\mathbf{x} = \frac{1}{N}\sum_{i=1}^{N} I[g_i(\mathbf{X} \le 0)] \,. \quad (1)$$

Here, $I[.]$ is an indicator function which takes values of unity when $g(\mathbf{X}) \le 0$ and zero otherwise. The minimum number of samples required for target coefficient of variation $V(P_f)$ is given by

$$N > \frac{1}{V(P_f)^2}\left(\frac{1}{P_f} - 1\right). \quad (2)$$

Thus, it follows that to reduce the estimate of variance to acceptable levels, for low failure probability levels, sample size, N, needs to be large. This has led to the development of a number of variance reduction techniques (Kahn, 1956). In implementing the importance sampling technique, Eq.(1) is rewritten as

$$P_f = \int_{-\infty}^{\infty} \frac{I[g(\mathbf{X}) \le 0] p_{\mathbf{X}}(\mathbf{x})}{h_{\mathbf{Y}}(\mathbf{x})} h_{\mathbf{Y}}(\mathbf{x}) \mathrm{d}\mathbf{x} \,, \quad (3)$$

and an estimate of the failure probability is obtained as

$$P_f = \frac{1}{N}\sum_{i=1}^{N} \frac{I[g_i(\mathbf{X}) \le 0]}{h_{\mathbf{Y}}^{(i)}(\mathbf{X})} p_{\mathbf{X}}^{(i)}(\mathbf{X}). \quad (4)$$

Procedures that estimate $P_f$ with specifically chosen $h_Y(\mathbf{x})$ as sampling density functions are called important sampling procedures and $h_Y(\mathbf{x})$ is called the importance sampling function. Here, the sampling is done in the $h_Y(\mathbf{x})$ region rather than $p_X(\mathbf{x})$. A major step in implementing the procedure lies in choosing an appropriate importance sampling probability density function $h_Y(\mathbf{x})$. The importance sampling density function could be Gaussian or non-Gaussian and is centred over an appropriately defined multi-dimensional region covering the region of likelihood around the design point (Shinozuka, 1983). Considering non-Gaussian importance sampling functions, however, lead to difficulties when the random variables are mutually correlated. These problems can be circumvented by transforming the problem to the standard normal space and constructing Gaussian importance sampling functions (Schueller and Stix, 1987). This is especially true when the location of the design point is not known *apriori* (Bucher, 1988).

### *Model setup*

The overflowing of the dike triggers erosion in inner slope, breach starts to grow which leads to the ultimate failure of the dike. Thus, in the study reported in this paper, failure is defined as the overtopping of the dike and the performance function is taken to be of the form

$$g(h_k, h_s, Q_r) = h_k - h(h_s, Q_r), \qquad (5)$$

where, $h_k$ is crest height of dike and $h$ is the local water level obtained as a function of $h_s$ and $Q_r$, representing, respectively, the extreme sea-level and extreme river water discharge.

The relationship between the local water level and the boundary parameters $h_s$ and $Q_r$ is through a nonlinear hydrodynamic model. The parameters $h_k$, $h_s$ and $h_r$ are modeled as mutually independent, random variables. The extreme values of the sea-water levels and the river discharges are assumed to be non-Gaussian random variables. The dike crest height along the entire stretch of the dike is modeled as a Gaussian random process with a specified auto-correlation function. The length of the dike is discretized into smaller segments. The dike crest height is assumed to be constant throughout each segment and is modeled as a Gaussian random variable. The probability of overtopping is calculated for each segment using the performance function in Eq.(5). The dike segments are assumed to be in series and the bounds on the failure probability estimates for the series system are obtained (Cornell, 1967).

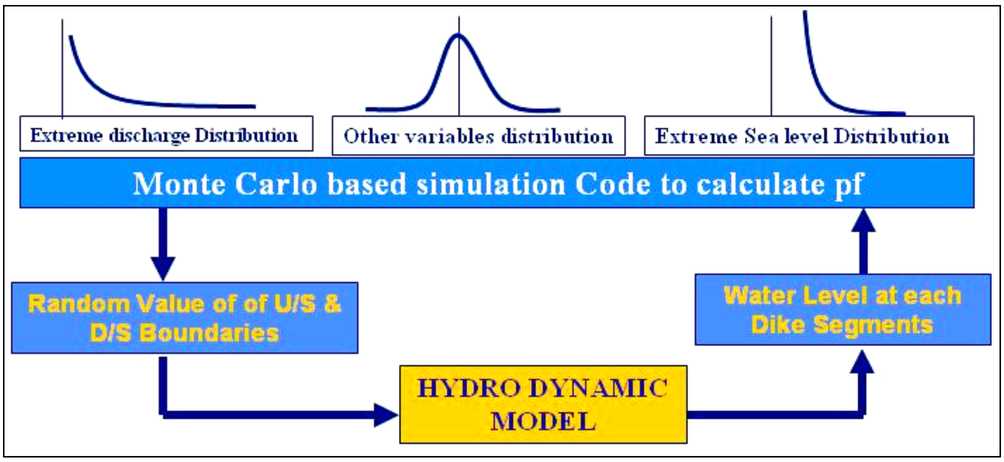


Figure 3-2: Probabilistic loops through hydrodynamic model for stochastic simulation

During Monte Carlo simulations, first, an ensemble for the random variables are generated and deterministic calculations are carried out, using the hydrodynamic model is necessary, for each realization. Figure 3-2 illustrates a schematic diagram of the simulation procedure and loop through hydrodynamic model. The computation time for one sample realization through the hydrodynamic model is non-trivial. An importance sampling based Monte Carlo approach is adopted for estimating the probability of dike overtopping.

### *Response database*

Despite adopting an importance sampling strategy, computation of the water level at the dike section requires significant computational effort. In this study, we explore the possibility of further reduction in computational time using a response database. This is possible if there exists a database of observations of water levels corresponding to different boundary conditions. During Monte Carlo simulations, first, the program searches into the database for the set of boundary conditions which have the closest correspondence to the particular realization. The local water level is then calculated by interpolation. This strategy for computing the river water level ensures (a) that the costly computations through the hydrodynamic model can be avoided, and (b) the database of observations already existing is of use. Figure 4 illustrates a schematic framework for the use of response database instead of probabilistic loop in this study.

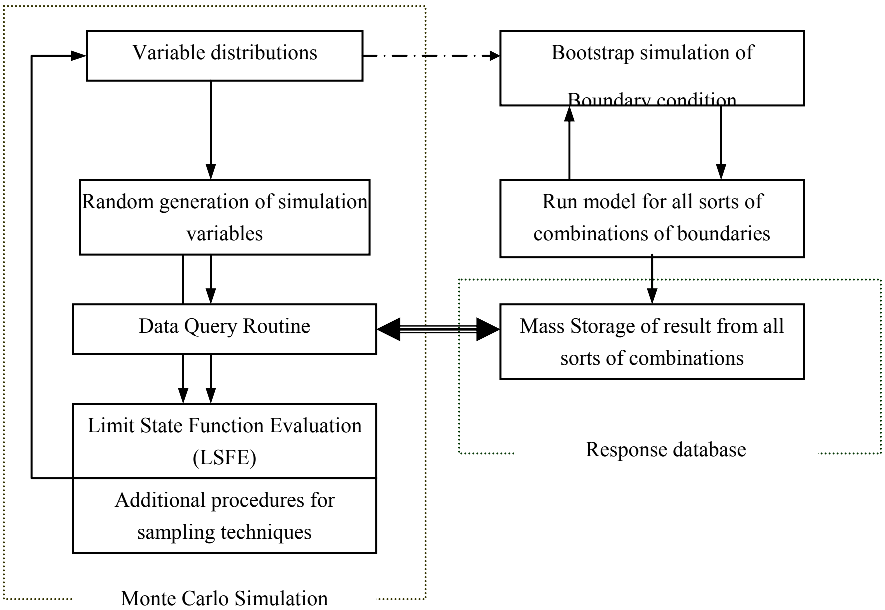


Figure 3-3: Block Diagram of conceptual framework for response database used in Monte Carlo simulation

The method of estimating the river water levels along the dike sections through interpolations from the response database is somewhat, in principle, similar to the response surface method. It must be noted that the response surface based methods are used to develop approximating functions that surrogate for long running computer codes (Khuri and Cornell, 1987). In this study, the interpolation functions used to estimate the water levels along the dike sections can be viewed as response surface functions for the particular realization.

### *Simulation details and results*

The overflowing failure mechanism of dike ring No 30, 31 from Western Scheldt, Province of Zeeland, is studied. The water levels of North Sea recorded at station Vlissingen were used to construct probability distribution functions of downstream levels. The data analysed are daily records from 1863 to 2004; see figure 3-4. Bestfit package was used to rank the distribution and find the parameters based on method of moments. A Pareto distribution was observed to lead to a realistic description for the observed data; see figure 3-5.

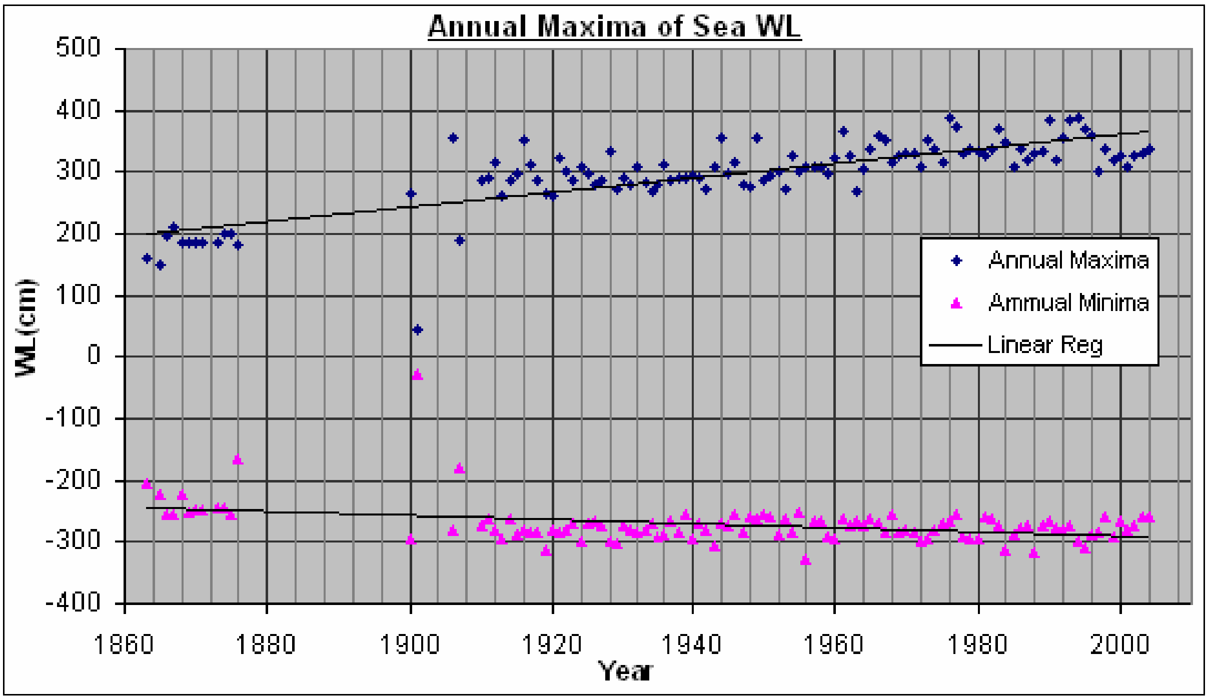


Figure 3-4:Annual maxima and minima of Sea Water level at Vlissingen, Western Scheldt

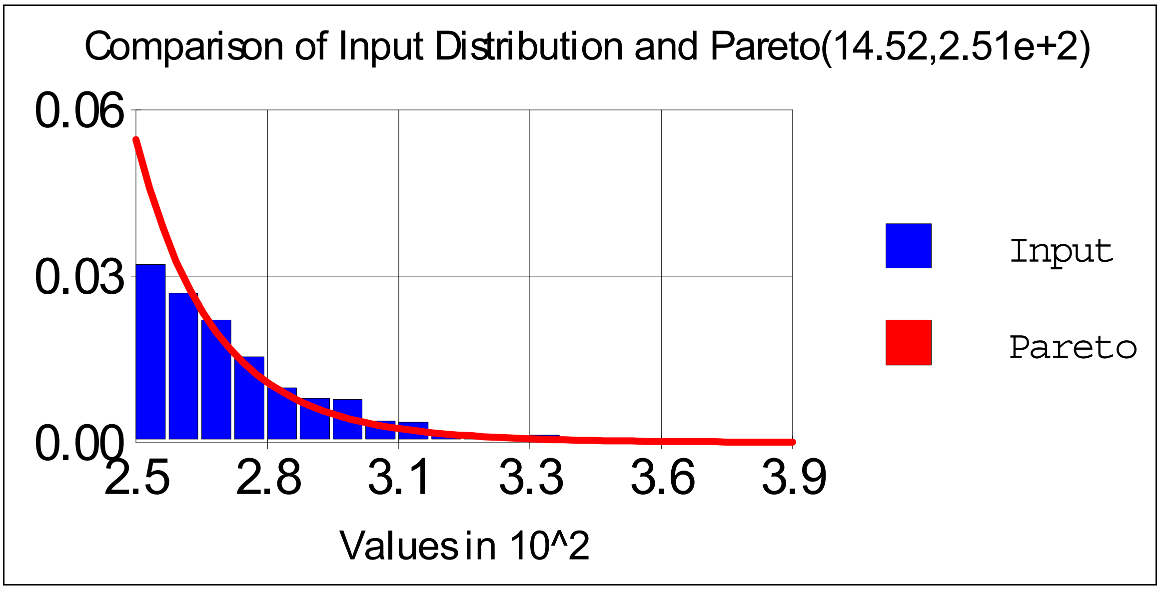


Figure 3-5: Pareto distribution representing sea level flactuation

A family of Pareto distributions were obtained depending on the threshold level selected while constructing the Pareto distributing using peak over threshold (POT) analysis; see figure 3-6

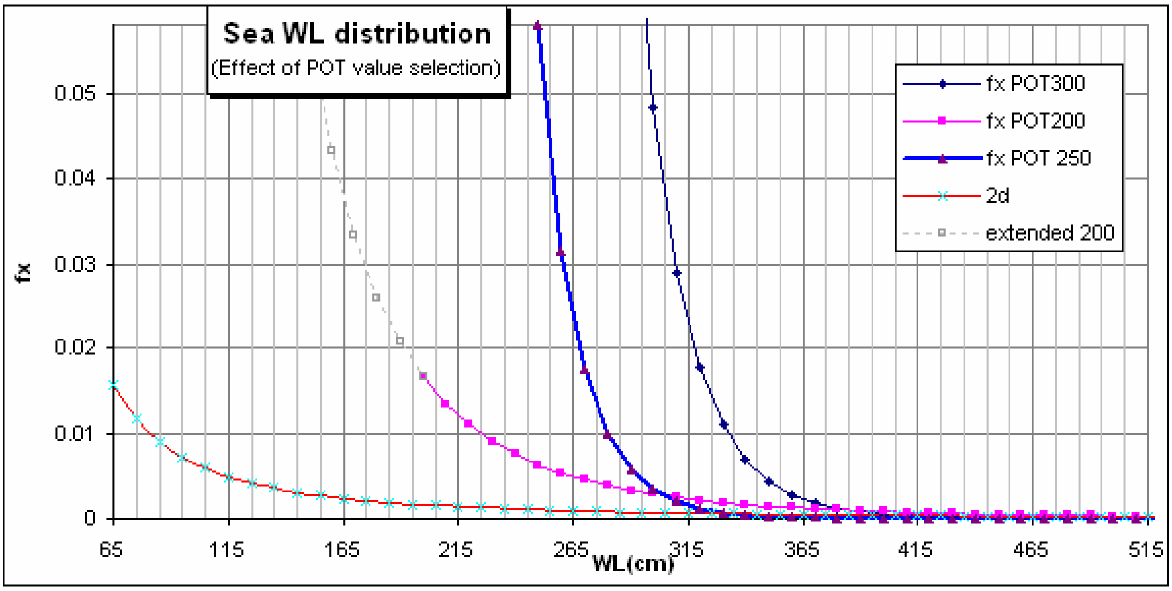


Figure 3-6: Effect of Choice of POT value on distribution

Parameters of exponential distribution, calculated by Bestfit, are based on zero position of the location parameter. For corresponding 2 days maxima, POT analysis is carried out by changing location and scale parameters successively. Figure 3-7 illustrates the effect of changing the threshold during POT analysis, on the location and scale parameters.

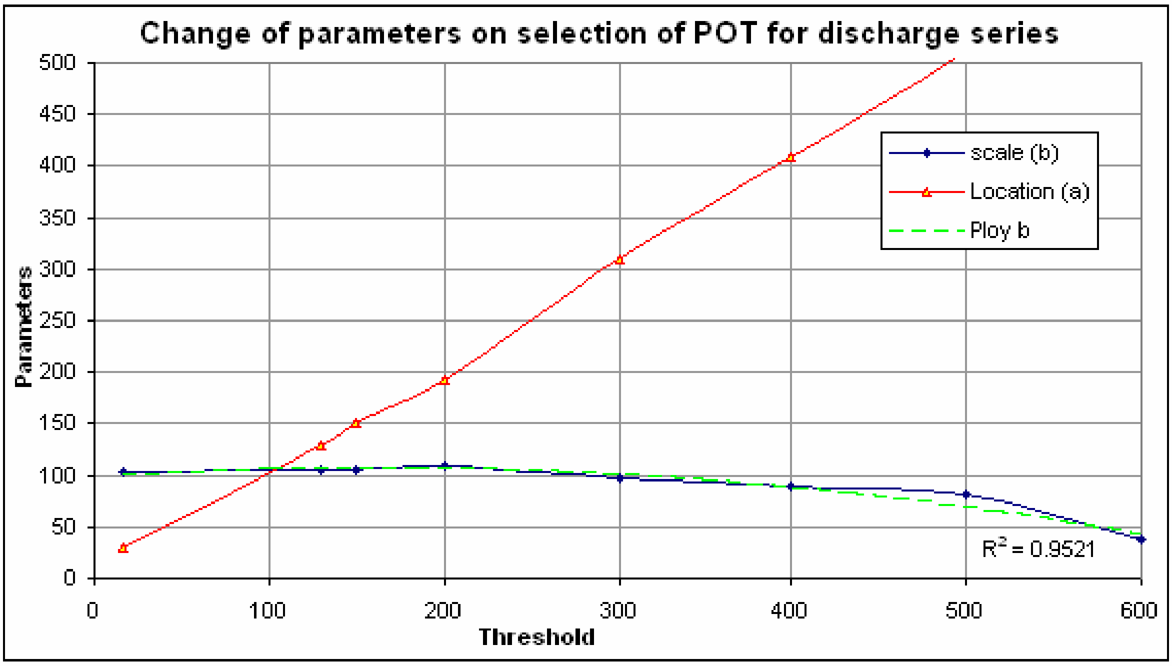

Figure 3-7:Change in location and scale parameter with different POT values

The dike length is discretized into segments such that, each segment could be considered independent of each other. The length of each segment was taken equal to the correlation length of the random process modelling the spatial randomness of the dike height. The autocorrelation function considered is as follows:

$$\rho_{X,X+L}(L) = e^{-\left(\frac{L}{D}\right)^2 \frac{\pi}{4}}, \qquad (6)$$

where, $D$ is the fluctuation scale given by

$$D = \int_0^\infty \rho_{x,x+L}(L)dL. \qquad (7)$$

Figure 3-8 illustrates the auto-correlation function for the dike height. The fluctuation scale is found to be 3532 m and the dike segments were taken to be of length 3500m.

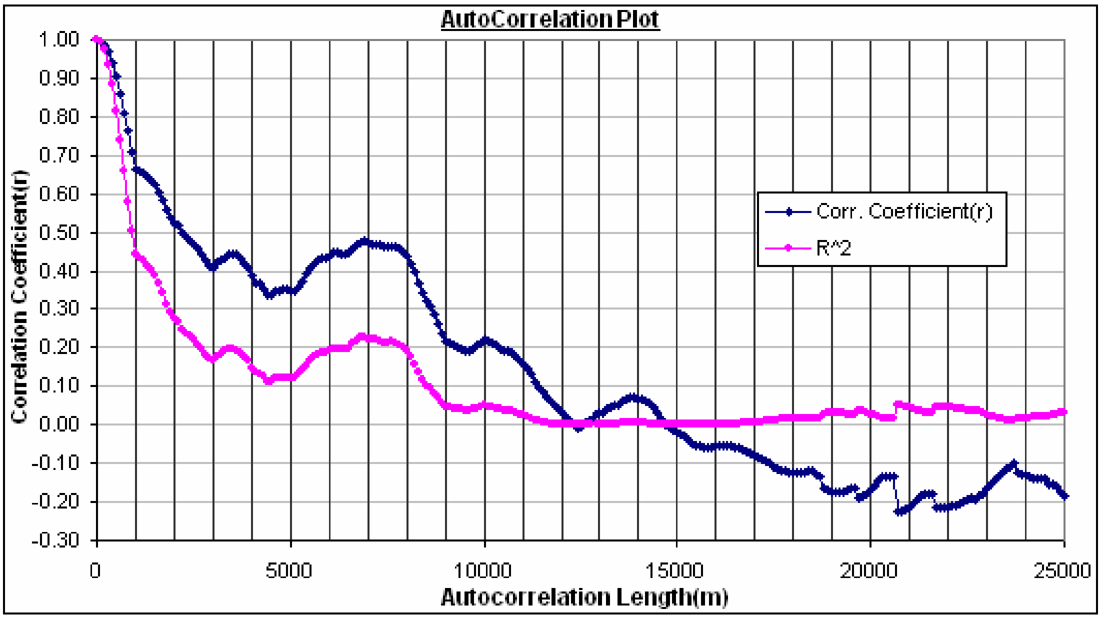


Figure 3-8: Autocorrelation for dike height

A new sea level is assumed to take place every 2 days (48 hours). The typical travel time of a flood wave along the length of the dike is approximately one hour. Thus, the river water levels, along the dike, are measured every hour. Calculations through the hydrodynamic model are carried out using SOBEK. A node is selected in each dike segment in SOBEK 1D schematisation.

For the purpose of illustration, the response database was built up using Sobek for a set of observed random boundary conditions. In practice, it is expected that the response database would be available. Importance sampling is subsequently carried out for estimating the failure probability for each dike segment. All the dike segments are assumed to be in series configuration and Cornell's bounds are computed for the system reliability. These bounds are observed to be $2.56 \times 10^{-7}$ and $8.75 \times 10^{8}$. The use of importance sampling in reliability analysis of the dike reveal that the sample size required is considerably less than full scale Monte Carlo simulations.

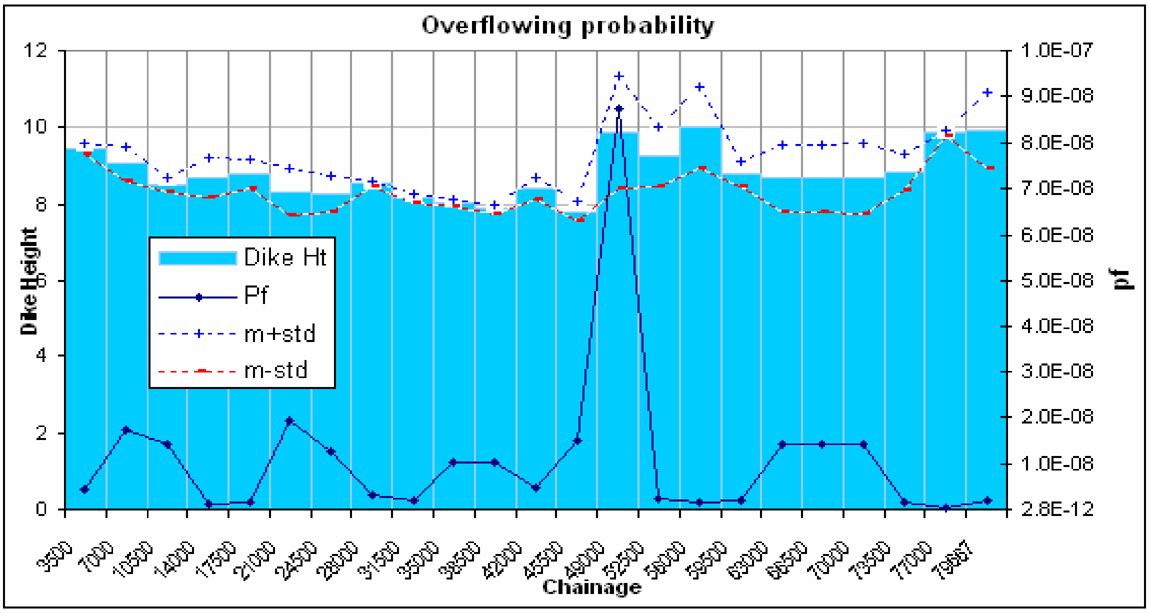


Figure 3-9: Overflow probability of the 80km long dike

### *Concluding Remarks*

The probability of overtopping of the 80 km long dike, due to the occurrence of extreme sea levels and river discharge, either concurrently or otherwise, is estimated. The reliability computations are carried out using importance sampling based Monte Carlo simulations. A novel response surface based method, based on already existing database, is adopted while computing the performance functions. The procedure shows promise in significantly reducing the computational effort.

# II-4 PROBABILITY OF FLOODING CALCULATION DIKE RING AREA 32

This section describes the approach and results of the performed calculations for determining the probability of flooding. With the presentation of the results, a distinction is made between contributions to the probability of flooding of dunes, dike sections and structures, and of different failure mechanisms within them. The calculated results are compared with the judgment of the water board. The computer model used to calculate the probabilities of flooding for dike ring 32 is PC-Ring version 4.3 (February 2005). Calculations have been made by DHV with checks by VNK and assessments by WZE. It proved to be difficult to perform good calculations of the probability of flooding, due to the variation in loads and the complexity of the dike profiles.

## *Approach and assumptions of the calculations*

### *1.1.1 General*

The calculations of the probability of flooding of the dike ring and the probability of failure of dike section and dunes have been performed using the computer program PC-Ring (version 4.3). Input for this program are the schematization and the data as discussed in chapter 2. The program calculates a probability of failure for each dike section, based on the contributions of each separate failure mechanism, and eventually the total probability of flooding for the entire dike ring.

Additionally the program provides insight in to what amount the various variables (e.g. the length of seepage present or the height of the dike) contribute to the calculated probability of failure. This is an important factor for conducting sensitivity analyses. The reliability index (beta) is often used for calculating with probabilities. The probability of failure is a function of this reliability index. PC-Ring also calculates with betas.

The probabilities of failure of structures are calculated using different procedures without PC-Ring. The calculated probabilities of failure per structure do form input for PC-Ring for calculating the probability of flooding of the entire dike ring based on the contributions of the distinguished dike sections and structures.

Statistic data of wind and water level are used for calculating the probability of flooding of dike sections. Based on these data the load models are defined, which are implemented in PC-Ring. The load models in question are adjusted to the valid hydraulic boundary conditions.

Please note that a clear difference has to be made between probability of exceedance, probability of failure and probability of flooding. The probability of exceedance is the probability that the water level at a dike section reaches higher than the test level. This is used in the present safety approach. The probability of failure is the probability that a dike section actually yields to one the failure mechanisms. The probability of flooding is the probability that the dike ring floods as a result of failure of a dike section on one or several places. A comparison between these latter two probabilities

and the probability of exceedance is not possible. The fact that in this report weak links are indicated when the probability of failure of that specific link is greater than 1/1250 does not relate to the fact that the probability of exceedance of this area is 1/1250 as well.

### 1.1.2 Failure mechanism dikes

For calculating the probabilities of failure of dikes, the hydraulic load of water levels and waves is confronted with the relevant characteristics of the embankment that are governing for the strength of the embankment. Both the load and the characteristics of the embankment are described in terms of probability distributions. Uncertainties in the input data are accounted for using these probability distributions.

Calculations of the probability of failure of a dike are based on the following failure mechanisms:

- Overflow and wave overtopping
- Covering damage and erosion body of the dike
- Bursting/piping
- Sliding inner slope

**Overflow and wave overtopping**

With this failure mechanism the dike fails because large amounts of water run or sweep over the dike. In case of offshore wind of otherwise very small wave heights, the yielding is described by the failure mechanism overflow. In other cases the yielding is described by the failure mechanism wave overtopping.

**Covering damage and erosion body of the dike**

With this failure mechanism the dike fails because the covering is damaged by wave action first, after which the cross-section of the dike core is diminished by erosion.

**Bursting/piping**

With this failure mechanism the dike fails because the sand is washed away from underneath the dike. The sealing layer, if present, will first burst due to the pressure of the water. Consequently so-called “pipes” can occur, causing the sand to be washed away and the dike to collapse.

**Sliding inner slope**

With this failure mechanism the dike fails because a part of the dike becomes unstable as a result of high water levels for a long period of time and consequently slides.

The possible failure mechanisms liquid settlement, buoyancy, sliding of the foreland, sliding of the outer slope, micro-instability and weakening are not taken into account because these failure mechanisms do not directly result in flooding. An assessment model is used per failure mechanism in order to be able to compare loads and strengths or otherwise to be able to calculate the probability of failure for the failure mechanism in question.

### 1.1.3 Failure mechanisms structures

For determining the probabilities of failure for structures, the exceedance frequency line of water levels is confronted with the strength of the embankment. For the structures, the uncertainties in the input data are also accounted for explicitly. For determining the probability of failure of a structure, the following failure mechanisms are accounted for:

- Overflow and wave overtopping
- Not-closing of the closing elements
- Constructive failure

The failure mechanisms are briefly described below.

**Overflow and wave overtopping**

With the failure mechanism overflow and wave overtopping the structure fails because water runs over the structure. The assessment of the structure is based on a comparison of the retaining height in relation to the exceedance frequency line of the outside water level.

**Not-closing of the closing elements**

With the failure mechanism not-closing of closing elements the structure fails as a result of the closing elements not being closed off in good time. The assessment of the structure is based on a comparison between the exceedance frequency line of the outside water level and the “open retaining level” (OKP), taking into account the probability of the not-closing of the closing elements.

For determining the probability of not-closing of the closing elements the VNK-method follows the Guideline Structures 2003. This guideline distinguishes four main causes of failure:

- Failure of the high water warning system: failure water level registration, failure alarm, etc.
- Failure of mobilization: operating personnel is not present at the retaining structure in time.
- Failure due to operating errors: faulty or omitted acts.
- Technical failure of the closing elements: motion device fails, etc.

**Constructive failure**

With the failure mechanism constructive failure the structure fails as a result of loss of strength or stability of (parts of) the structure. The assessment of the structure is based on a consideration of constructive strength and stability of the structure in relation to the loads when retaining high water. For this assessment the following mechanisms are applicable:

- Constructive failure of the retaining devices resulting from drop load
- Constructive failure of the concrete construction
- Constructive failure of the foundation
- Chance of loss of stability due to instability of the bottom protection
- Failure due to loss of stability as a result of a collision
- Failure due to general loss of stability
- Failure due to under or rear seepage (piping)

**Method of assessment**

Within the project VNK a method has been developed for several types of structures to calculate the probability of flooding for different failure mechanisms. It concerns the following types of structures: navigation locks, discharge sluices, cuttings, tunnels and pumping stations.

The failure of a structure by overflow and wave overtopping or not-closing of the closing elements does not inevitably result in the arising of a breach in the embankment and with that the flooding of a dike ring area. The water flowing in can often be stored in the adjacent water system behind the structures that are linked to the inland water, without resulting in flooding. Also the structures can often handle large flows without loss of stability. Therefore the initially calculated probabilities of failure as a result of overflow and wave overtopping and not-closing of the closing elements respectively are tightened in the assessment system to probabilities where the start of a breach occurs. These are smaller probabilities by definition. This tightening requires extra effort and is thus only executed when the first approach results in relative large probabilities compared to the existing standard frequency for design water levels.

With the mechanism constructive failure, it is assumed that the stability is directly lost when breaching occurs. The corresponding probability of failure is therefore considered the probability of breaching.

### *1.1.4 Probability of flooding of the dike ring area*

The probability of flooding of a dike ring area is made up of the calculated probabilities of failure of the dikes, dunes and structures in question. First the probability of failure is determined per dike section of structure based on the contributions of the various failure mechanisms. Consequently the probability contributions of the various dike sections and structures are combined into the probability of flooding of the dike ring. With combining the various contributions, possible dependencies in probabilities of failure of nearby dike sections are accounted for.

### Process description

- The collecting of data on dike ring 32 is done by the water board in cooperation with VNK. The quality of the data is checked by both VNK (roughly) and the Bouwdienst (during the conversion of the data from the overall spreadsheet to the database). The result of this is recorded in various checklists and reports overall spreadsheet dike ring 32.
- With executing the first calculations for dikes and dunes, several adjustments to the PC-Ring database were performed. The greatest adjustments concerned the selection of dike sections (see section 2.3) and the schematization of the dike profiles. With the selection of dike sections, 33 dike sections and 4 dune sections were chosen out of 287 sections that were schematized by the water board. With the schematization of the profiles, the schematized profiles (done by the water board) in the PC-Ring database were compared with recently measured cross-sections of the water board. All profiles were schematized again because anomalies occurred between the measured and the schematized profiles.
- DHV both did the initial calculation and a further analysis for dikes and dunes in principle. With the calculations one ran into many difficulties concerning amongst others the schematization, the complexity of the dike profiles, the variation in loads and the programming, due to which doing good calculations for this dike ring turned out to be difficult.
- VNK checked and corrected all DHV's calculation for the dikes together with TNO. This resulted in the fact that a probability of failure has been calculated for (almost) all mechanism for the selected sections.
- The calculated probabilities of failure are discussed with the water board. VNK processed the results of these discussions in this dike ring report.
- The structures are assessed by DHV. The results are tested and checked by VNK and the water board.
- The MproStab calculations are performed by DHV and checked by GeoDelft.

### Results of the calculations of the probability of flooding

#### 1.1.5 Introduction

In this section an insight is provided in the calculated probabilities of failure for dike ring 32. It concerns preliminary results, since the results have not been analysed thoroughly. These preliminary results have been discussed with the water board. Because it concerns preliminary results, a so-called reference sum is not yet presented for dike ring 32.

#### 1.1.6 First results per dike section

The (preliminary) results per dike section in beta are provided in table 4-1. These results are discussed with the water board (see section 4.3.4). As a result of this discussion, it was concluded that a number of sections can be left out of consideration for now. These are results that are unidentifiable for the water board and have to be analysed further or weak spots that are nominated to be improved. These sections are shaded grey in the table.

| | | | | | | | | | | | | | | |
|---|---|---|---|---|---|---|---|---|---|---|---|---|---|---|
| 7002 | 7009 | 7023 | 7024 | 7025 | 7028 | 7038 | 7042 | 7047 | 7053 | 7071 | 7074 | 7075 | 7094 | 7109 |
| 5.0 | 6.6 | 5.7 | 5.6 | 6.0 | 7.4 | 5.2 | 5.8 | 5.8 | 5.7 | 5.4 | 4.8 | 4.9 | 5.0 | 5.5 |
| 6.7 | 6.5 | 11.3 | 11 | 11 | 7.3 | 6.7 | 6.3 | 9.8 | 10 | 6.3 | 6.1 | 6.2 | 7.0 | 6.4 |
| 3.4 | 3.7 | 5.0 | 4.6 | 9 | 2.4 | | 6.2 | 9.3 | 7.6 | 5.1 | 7.0 | 7.8 | 7.8 | 6.0 |

| | | | | | | | | | | | | |
|---|---|---|---|---|---|---|---|---|---|---|---|---|
| 7111 | 7116 | 7124 | 7129 | 7136 | 7139 | 7152 | 7159 | 7163 | 7167 | 7185 | 7202 | 7211 |
| 5.2 | 4.9 | 3.9 | 5.0 | 5.6 | 4.9 | 4.9 | 4.4 | 4.8 | 3.0 | 4.1 | 4.8 | 3.9 |
| 6.7 | 6.6 | 7.1 | 6.3 | 8.0 | 6.1 | 5.3 | 5.2 | 4.5 | 7.5 | 4.1 | 4.8 | 4.5 |
| 5.4 | 6.5 | 8.5 | 5.3 | 5.7 | 37 | 6.8 | 5.2 | 14 | 13 | 36 | 6.1 | 14 |

| | | | | |
|---|---|---|---|---|
| 7220 | 7233 | 7249 | 7258 | 7271 |
| 4.5 | 4.8 | 4.5 | 4.5 | 4.6 |
| 5.7 | 4.6 | 5.2 | 6.0 | 6.4 |
| 37 | 8.9 | 37 | 1.8 | 2.2 |

*Table 4-1 Reliability indices (preliminary) per section (in first row) calculated by VNK based on the following failure mechanisms:*

- Second row: Overflow and wave overtopping
- Third row: Bursting/piping
- Fourth row: Covering damage

The reliability index of section 7249 for the mechanism sliding inner slope has been calculated as 2.1. Indices for dune erosion has been calculated for the following sections 7008, 7010 and 7013 with beta values equal to 4.4, 4.4 and 4.9.

### 1.1.7 Sliding inner slope

7 Profiles have been selected for calculating the probabilities of failure for the failure mechanism sliding. DHV calculated these 7 profiles with MproStab. Only 1 profile is part of the 33 selected sections for the PC-Ring calculations (EMMA118 belongs to section 7249 (076-dp124)). A result for the mechanism sliding inner slope is incorporated in table 3-2 for only this section. An overview of the calculated safety factors and reliability indices at different water levels for all 7 sections is provided in table 4-2.

DHV consequently considered with which of the profiles from table 4-2 each of the 33 sections matches best. A profile is linked to each selected section and a probability of failure has been calculated for each section using PC-Ring. Since the used method is not correct, the results are not displayed here. The coupling is based on height of the crown, gradient of the inner slope, MHW and thickness of the covering layer, but doesn't account for the structure of the soil. The coupling of the sections and the profiles does thus not match the routes for which the profiles are deemed to be representative according to the water board.

| Bestandsnaam | Dijkvaknummer | MStab | MproStab | | |
|---|---|---|---|---|---|
| | | | MHW Fn / β | MHW –0,5m Fn / β | MHW –1,0m Fn / β |
| TIENH15.STI | 1320007012 | 0,97 | 1,19 / 1,53 | 1,22 / 1,65 | 1,24 / 1,74 |
| NISLU17.STI | 1320007014 | 1,06 | 1,31/ 2,53 | 1,33 / 2,68 | 1,36 / 2,80 |
| HOOFD37.STI | 1320007052 t/m 1320007063 | 0,94 | 1,21 / 1,92 | 1,24 / 2,13 | 1,28 / 2,29 |
| PAULIN4.STI | 1320007079 | 0,80 | 1,04 / 0,97 | 1,08 / 1,27 | 1,13 / 1,55 |
| WIL206A.STI | 1320007204 t/m 1320007208 | 1,10 | 1,31/ 2,43 | 1,34 / 2,53 | 1,36 / 2,62 |
| ALS166B.STI | 1320007226 | 0,56 | 0.93 / 0,21 | 0,96 / 0,42 | 0,94 / 0,29 |
| EMMA118.STI | 1320007249 t/m 1320007252 | 0,90 | 1,17 / 1,874 | 1,19 / 1,95 | 1,23 / 2,18 |

*Table 4-2 Comparison safety factors according to Bishop from MStab and MproStab (results by VNK)*

When considering this latter, next to section 7249 (076-dp124) DHV made the right coupling for sections 7109 (123-dp26), 7111 (122-dp16), 7116 (121a-dp9), 7233 (078-dp148), 7258 (074-dp99) and 7271 (072-dp69). For the latter three sections the MHW (almost) matches with the MHW of the representative profile. This is not the case for the first three. The probabilities of failure that DHV calculated for these sections are provided in table 4-3.

| Dijkvak | Bèta afschuiven | Faalkans afschuiven |
|---|---|---|
| 7109 – 123-Dp26 | 1,905 | 1/35 |
| 7111 – 122-Dp16 | 1,906 | 1/35 |
| 7116 – 121a-Dp9 | 1,891 | 1/34 |
| 7233 – 078-Dp148 | 2,140 | 1/62 |
| 7258 – 074-Dp99 | 2,159 | 1/65 |
| 7271 – 072-Dp69 | 2,135 | 1/61 |

*Table 4-3 Reliability index Beta and the failure probability for the mechanism sliding (DHV results)*

These results provide an indication of the probabilities of failure to be expected. Before the results are incorporated in the calculation of the probability of failure for dike ring 32, it should be checked whether coupling of the dike sections from PC-Ring to representative profiles with another MHW is possible.

### 1.1.8 Feedback results per section to water board

The results of the calculations per dike section are discussed with the water board. An overview of its findings per mechanism is given below. The results are compared with the results of the testing in 2000 (table 2-2) and the preliminary results of the 2005 testing as far as these are available. As a result of this, it is concluded that a number of results should left out of consideration for the time being (these results are shaded grey in table 4-1).

*Overtopping and wave overrun*

- Dike section 7167 (097-dp290), Molenpolder, has a relative bad score for the mechanism overtopping/wave overrun (beta is 3,03). This result is not recognisable for the water board. Possibly the sandbank ahead is not schematised correctly (this is no foreland), due to which too little wave reduction is accounted for. Other cause could be the calculated profile. A further analysis of required here.

→ The water board thinks the present result should not be considered in the calculations of the probability of flooding of the dike ring, because it doesn't recognise the results.

- For sections 7009 (020-dp16), 7111 (122-dp16), 7116 (121a-dp9), 7124 (113-dp87), 7167 (097-dp290), 7211 (083a-dp186) and 7233 (078-dp148) the water board separately indicated that these score well for height in the (preliminary) results of the 2005 testing. A number of these sections scored unsatisfactory in the 2000 testing (see table 2-2).
- The section 7152 (100a-dp330) scored unsatisfactory in the 2000 testing, but is strong according to the VNK calculations. If this section still appears to be unsatisfactory in the new testing, the result of VNK will have to be examined further.

*Bursting and piping*

- The results of VNK do not indicate weak spots for the mechanism bursting/piping.
- A number of sections scored unsatisfactory with the first testing. No improvement works related to the phenomenon bursting/piping have been executed since. Works have been executed to drainage and better soil research has been done. For now, a number of sections do not yet score satisfactory for this mechanism with the second testing.
- For the sections 7109 (123-dp26), 7111 (122-dp16), 7220 (081a-dp175) the water board has separately indicated that they score well for the mechanism bursting and piping in the (preliminary results) of the 2005 testing. The section 7223 (078-dp148) scored unsatisfactory in the 2000 testing. Both sections are strong according to the VNK calculations. If it appears from the final results of the new testing that these sections still score unsatisfactory, the result of VNK will have to be analysed further.
- Result from VNK mainly agrees with the assessment of the water board and the testing.

*Covering damaging and erosion body of the dike*

- The sections 7002 (024-dp7) for grass, 7009 (020-dp16) for stone, 7028 (004-dp25) for stone, 7258 (074-dp99) for grass and 7271 (072-dp69) for grass score relatively bad for the mechanism covering damaging and erosion body of the dike.
- For the section 7028 (004-dp25), as for 7038 (139a-dp17), insufficient data for the stone covering were initially put into the overall spreadsheet to calculate a result with PC-Ring.
  - For dike section 7028 the data were copied from dike section 7042 (after consult with the water board concerning the type of stone covering). This results in a large probability of failure. By principle it should be verified whether the copied data match the reality. The water board indicates that this section is nominated for improvement concerning the stone coverings. Thus the bad result is identifiable.

  → *The water board thinks that the present result should not be taken into the calculation for the probability of flooding of the dike ring, because the section is part of a running improvement project.*

  - No other data have been put in for dike section 7038 and thus no result has been calculated.
- The testing is being performed now. On this moment additional data are gathered for an advanced testing (amongst others on the grass quality). The water board has already indicated the state of affairs of the (preliminary) results of the 2005 testing for a number of sections. In many cases the type of covering for which these sections were tested differs from the type that VNK has calculated (and which was identifiable for the water board (see section 2.5)). This assessment of the water board with the mechanism for which the section is calculated at VNK next to it is given in table 3-5.
- Comments can thus be given on the results for the mechanism covering damaging and erosion of body of the dike. Further research on the various types of covering (a dike is always constructed from a combination of multiple types of covering (dry stone, stone, asphalt and grass) that are present on a dike section seems necessary. All types will need to be calculated separately and consequently it has to be determined which one is governing (also in relation to the associated design criteria). Even better would be if multiple types of covering on 1 dike section could be calculated with PC-Ring.
- For section 7159 (099a-dp319) it is indicated that it is nominated to be improved. With testing this section doesn't make it based on its age. The water board thus doubts the calculated result, which is relatively good (beta = 5,2). The section partly consists of asphalt and partly of stone. Both types should be calculated.
- The water board has indicated that transition structures often form a weak spot. VNK does not calculate these.

| Section | Judgement water board | VNK Calculations based on: |
|---|---|---|
| 7002 | Stone revetment after inspection considered good | Gras |
| 7023 | Stone revetment insufficient | Stone |
| 7024 | Stone revetment insufficient | Asphalt |
| 7025 | Stone revetment insufficient | Asphalt |
| 7042 | Stone revetment excellent | Stone |
| 7071 | Excellent grass | Stone |
| 7074 | Excellent grass | Stone |

| | | |
|---|---|---|
| 7075 | Excellent grass | Stone |
| 7111 | Stone revetment excellent | Stone |
| 7129 | Excellent grass | Stone |
| 7136 | Stone revetment excellent | Stone |
| 7139 | Excellent grass | Stone |
| 7159 | Asphalt insufficient | Stone |
| 7163 | Asphalt insufficient | Stone |

*Table 4-4 Assessment of the water board based on preliminary results 2005 testing*

*Sliding inner slope*

- VNK assesses the sliding of the inner slope. This mechanism is calculated correctly for 1 section (7249 - 076-dp124), for which a large probability of failure is calculated. Other indicating calculations also indicate large probabilities of failure (betas around 2).
- The water board has seen sliding of the outer slope, but no real problems for the inner slope have ever arisen.
- The cause of the bad results can be found in the conservative data that are used for the 1st testing (due to a lack of data). These data were also used for VNK. This results in a pessimistic picture.
- On this moment one is busy doing additional soil research for the 2nd testing (gathering of test samples (borings), measurements of water pressures, foundation). The sub-soil is mapped out better with these methods. It is expected that this will lead to better results for sliding. The model of the sub-soils used for the Mstab calculations also seems conservative. For the long term the water board expects to be able to take this into account better (and consequently calculate better results).
- Apart from that, it needs noticing that the dikes around dike ring 32 are high and steep and that additionally the sub-soil is not very good (weak layers are present). Based on that fact it is not unlikely that sliding will appear as a relatively weak mechanism. For less conservative data as well, it is expected that this mechanism will score relatively bad (beta around 2,5-3).
- For sections 7012 (019a-dp20), 7052 (137a-dp23), 7079 (130-dp16) the water board has separately indicated that these score well for the mechanism sliding in the (preliminary) results of the 2005 testing. For the sections 7226 (080-dp169), 2749 (076-dp124) applies that they need advanced testing for the mechanism sliding of the inner slope. These are sections that are part of the selected cross-sections and thus (except for the latter section) are not part of the 33 dike sections that are selected for calculation.
- For section 7025 (006a-dp15) the water board also indicated that it needs advanced testing for the mechanism sliding of the inner slope. The profile of this section is not assessed on this mechanism within VNK.
- At the 200 testing, none of the selected section scored unsatisfactory for the mechanism sliding of the inner slope.
- It is recommended to couple the other selected profiles, which do not match the selected sections, to the right section in PC-Ring (section that is thus not in the selection). It concerns the sections 7012 (019a-dp20), 7014 (013-dp8), 7052 (137-dp23), 7079 (130-dp16), 7204 (084-dp199), 7226 (080-dp169). Next to that it is recommended to use the results of the additional soil research for these calculations.

→ The water board thinks that the present results should not be taken into the calculations of the probability of flooding, since research is now being done to improve the input data.

*Dunes*

- No single dune sections scores unsatisfactory in the 2005 testing with the new graver boundary conditions for waves (also see section 2.9). The results of the 4 sections that VNK calculated (with the old lees grave boundary conditions), seem to be correct (beta 4,37 to 5,26).
- A suppletion policy is pursued along the whole North Sea coast for both the dunes and the dikes to maintain the basic coastline. VNK can't directly calculate such dikes. One should assume a coupled failure mechanism; the dike is addressed only after the dune is swept away.

*Sliding outer slope*

- Stability outside the dike (dike and shore drops) is not considered by VNK. The water board expects that especially this mechanism is a threat to the safety of dike ring area 32 (and consequently has a large influence on the probability of flooding).
- Sliding of the outer slope occurs at low tide. Depending on the degree of sliding, this leads to a threat to safety or not.
- The water board indicates that dike ring area 32 has a closed system of regional flood defences with closable constructions to counteract this phenomenon. This system is controlled and maintained by the water board.

### Results per structure

The results per structure are given in table 4-5. The results that can be left out of consideration in connection with consult with the water board are shaded grey here as well.

| No. | Structure | Overflow and overtopping | Non-closure | Structural failure |
|---|---|---|---|---|
| 1 | Pumping station Cadzand | 4.4 | 6.0 | 4.5 |
| 2 | Pumping station Campen | | 5.5 | 4.4 |
| 3 | Pumping station Nieuwe Sluis | | 5.9 | 6.1 |
| 4 | Pumping station Nummer Een | | 6.0 | 4.9 |
| 5 | Pumping station Othene | 4.1 | 3.5 | 1.7 |
| 6 | Pumping station Paal | 5.0 | 5.8 | 4.7 |
| 7 | Sluice station Terneuzen Oostsluis | 4.1 | 6.6 | 5.3 |
| 8 | Sluice station Terneuzen Middensluis (schutsluis) | 3.9 | 4.8 | 4.3 |

| | | | | |
|---|---|---|---|---|
| 9 | Sluice station Terneuzen Middensluis (spuiriool) | | 5.1 | 4.3 |
| 10 | Sluice station Terneuzen Westsluis | 3.9 | 5.3 | 5.2 |
| 11 | Sluice station Terneuzen Westsluis (spuiriool) | | 5.2 | 5.2 |
| 12 | Discharge sluice station Braakman | 4.7 | 4.3 | 4.5 |
| 13 | Discharge sluice station Hertogin Hedwigepolder | 4.0 | 4.7 | 5.2 |
| 14 | Discharge sluice station Nol Zeven | 4.6 | 4.5 | 4.5 |

*Table 4-5 DHV Results of the assessed structures in dike ring 32*

*Structures*

- The pumping station Othene scores very bad for the mechanism constructive failure (beta of 1,96, probability of failure 1/22). This has to do with the mechanism bursting and piping. This appears to be a problem if one assumes that the ground sills and aprons are not fully watertight. In case one can prove this is the case, or if physical measures are taken to achieve this, the norm can be complied with.

→ *In consultation with GeoDelft, this structure has been tested correctly in the meanwhile. The result can thus be left out of consideration.*

- For the mechanism not-closing the pumping station scores relatively bad (beta of 3,5, probability of failure of 1/4300). Not-closing results in a high probability of failure due to the large number of requests for closing (almost daily) on one hand and the presence of 2 flood defences on the other hand. The failure situation concerns the blocking of the mitre gates due to sedimentation or obstacles, after which the emergency gate can’t be closed in time. Improving the situation is possible by installing an additional set of mitre gates. Next to that, one can think of further investigating the probabilities of failure for the not-closing (advanced method), possibly in combination with optimizing the controls.

  → *Further inspection showed that this inflow is not possible, due to which a lower probability of failure than is now calculated can be expected. This result can thus be left out of consideration.*

- For the pumping station Cadzand the result of VNK seems too good for the mechanism overtopping and wave overrun (beta is 4,39, probability of failure < 1/100.000). From the structures report the following follows: VNK calculates a large probability of failure for this structure, but this probability of failure is adjusted to a much lower probability of flooding. With failure, water (waves) runs over the valve chamber. This overrun flow does not directly result in a loss of stability of the structure and thus to flooding. The overrun flow ends up on a hardened surface the behind the valve chamber and, on both sides, runs into the outlet channel lying behind. The stability of the structure is not lost until a flow runs over that is associated with a much higher water level (and with that a much smaller probability of failure) than the water level at which failure (overrunning) of the structure occurs.

## *Overall probability of flooding dike ring 32*

Let us assume that a dike stretch of length L is schematised into n sections by:

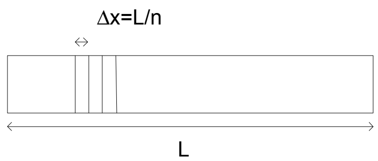


If the following autocorrelation function for the dike strength R at section x is assumed:

$$\rho\left[R(x), R(x+\Delta x)\right] = e^{-\left(\frac{\Delta x}{d}\right)^2}$$

And the reliability index for the i-th section is beta (for i=1,…, n):

$$P(F_i) = \phi(-\beta)$$

Then, we can write the overall failure probability as:

$$P(F) = \phi(-\beta) + (n-1)\left\{\phi(-\beta) - 2\phi(-\beta)\phi\left(-\beta\frac{1-\rho}{\sqrt{1-\rho^2}}\right)\right\}$$

Since $\max\limits_{j<i} P(F_i \text{ en } F_j) = P(F_j \text{ en } F_{i-1})$ and $\rho = e^{-\left(\frac{\Delta x}{d}\right)^2} \approx 1 - \left(\frac{\Delta x}{d}\right)^2$, as well as

$\rho^2 \approx 1 - 2\left(\frac{\Delta x}{d}\right)^2$, whereas $\phi(u) = \frac{1}{2} + \frac{u}{\sqrt{2\pi}}$ for small u .

Therefore $P(F) = \phi(-\beta)\left\{1 + \frac{n-1}{d}\frac{\beta\Delta x}{\sqrt{\pi}}\right\}$

since $\Delta x = \frac{L}{n}$ and $\frac{n-1}{nd}\frac{\beta L}{\sqrt{\pi}} \rightarrow \frac{\beta L}{d\sqrt{\pi}} (n \rightarrow \infty)$

Therefore:

$$P(F) = \phi(-\beta)\left\{1 + \frac{\beta}{\sqrt{\pi}}\frac{L}{d}\right\}$$

Which is independent of the number of sections n.

If all results from table 4-1 and table 4-5 are taken into consideration, a preliminary probability of flooding of >1/11 per year (COMBIN 1) is calculated for dike ring area 32, Zeeuws-Vlaanderen. This would mean that flooding is to be expected more than once each 11 years for dike ring area 32. Since the results have not been analysed thoroughly, one can not speak of a so-called reference sum of dike ring 32 in this case.

| Mechanism | COMBIN1 | COMBIN2 |
|---|---|---|
| Overflow / overtopping | 1/794 | 1/11312 |
| Bursting and piping | 1/30211 | 1/30211 |
| Revetment damage and dike erosion | 1/22 | 1/574713 |
| Overflow and overtopping of hydraulic structures | 1/16920 | 1/16920 |
| Non-closure of hydraulic structures | 1/3984 | 1/3984 |
| Structural failures of hydraulic structures | 1/22 | 1/34364 |
| Overall failure probability | 1/11 | 1/1996 |

*Table 4-6 Probability of flooding dike ring 32 according to DHV.*

When the 6 weakest spots for the dikes (7167-097-dp290 for overtopping and wave overrun), 7002-072-dp7, 7009-020-dp16, 7028-004-dp25, 7258-074-dp99 and 7271-072-dp69 for covering damaging and erosion body of the dike) and the weakest spot for the structures (constructive failure of pumping station Othene) are left out of consideration, a probability of flooding of 1/2000 per year (COMBIN 2) is calculated. According to the water board this approaches the value it would expect.

In both cases the mechanism sliding is not taken into account in the calculated probability, whilst it is clear that stability problems are a real threat in this case, because the dikes are high and steep and stand on weak layers in the sub-soil.

Because of the reasons a probability of flooding of <1/100 for dike ring area 32 is presented in the main report and the management summary of the project VNK. Herewith it is indicated that the probability of flooding is mainly determined by stability problems at the pumping station or at the dikes. In relation to the pumping station, it is consequently also indicated that this can be approved based on recent information with the second testing.

### *Possibilities of sensitivity analyses*

For dike ring area 32 no sensitivity analyses have yet been performed. In the section discusses in which way it can be determined which sensitivity analyses can be of interest.

The calculated probability of flooding of the dike ting is determined by a large number of dike sections, dune sections and structures, various failure mechanisms and a large number of stochastic variables per failure mechanism. The possible number of sensitivity analyses is in that way endless. It is therefore important to focus the sensitivity analyses on those factors that determine the level of probability of flooding most. For the dike sections it concerns the relatively weak dike sections. For those dike sections the attention is consequently given to the failure mechanisms that contribute to the probability of flooding most. And for those failure mechanisms the stochastic variables are looked at that have the largest contribution to the probability of flooding. On top of that it is important that these stochastic variables can be decreased by means of further research in reasonable time and with reasonable effort. The latter is an important restriction, for dike ring 32 the stochastic variable ‘Water level Vlissingen” contributes most by far to the probability of failure for the mechanism overtopping and wave overrun. It is however a stochastic variable for which further research will generate little new insights. Even 10 years of additional observations will only be of limited influence on the stochastic variable insecurity with which this stochastic variable is afflicted. Decreasing the probability of flooding by reducing insecurities by means of additional research will thus have to focus on other stochastic variables.

Information on the most influential stochastic variables can be derived from PC-Ring. PC-Ring calculates an influence-coefficient (alpha) per stochastic variable, also called sensitivity-coefficient. The magnitude of the alpha-value is determined by a combination of the influence of the average value and the magnitude of the standard deviation (or variation-coefficient). A low alpha-value for a parameter does not inherently mean that this parameter has little influence on the result. For a small variation-coefficient (or standard deviation), the variation of the average value can still have a significant influence on the result. For a parameter with a small variation-coefficient however, the value of this parameter is relatively ‘certain’. This means that it can not be expected that the average value will change a lot as a result of new insights. Varying the average values of those kinds of

parameters is possibly interesting for the calculating of measures. The alpha-values (influence-coefficient) are not beatific.

Sensitivity analyses and influence-coefficients are to be considered ‘together’.

The alphas thus represent the contribution of the stochastic variable to the probability of failure for a sub-mechanism. These can take effect both on the side of the load (negative alphas) and on the positive side (positive alphas).

# REFERENCES

1. Bucher, C.G. (1988), *Adaptive sampling - an iterative fast Monte Carlo procedure*, Structural Safety, 5, 119-126.

2. Cornell, C.A. (1967), *Bounds on the reliability of structural systems*, Journal of Structural Division, ASCE, 93(ST1), 171-200

3. Kahn, H. (1956), *Use of different Monte Carlo sampling techniques*, Symposium on Monte Carlo methods, (Ed: Meyer, H.A.), John Wiley and Sons, New York, 146-190.

4. Khuri, A.I. and Cornell, J.A. (1987), *Response surfaces: design and analyses*. Marcel and Dekker, New York.

5. Pandey, M.D., Van Gelder, P.H.A.J.M. and Vrijling, J.K.(2003), *Dutch Case Studies of the estimation of extreme quantiles and associated uncertainty by bootstrap simulation*, Environmetrics DOI: 10, 1002/env.656.

6. PC RING Manual 4.3. QQQ Delft and Demis bv, September 2004.

7. Schueller, G.I. and Stix, R. (1987), *A critical appraisal of methods to determine failure probabilities*, Structural Safety, 4, 239-309.

8. Shinozuka, M. (1983), *Basic analysis of structural safety*, Journal of Structural Engineering, ASCE, 109(3), 721-740.

9. VNK Report, *Safety in the Netherlands mapped*, Flood risks in dike ring area 32 Zeeuws-Vlaanderen, December 2005.

# APPENDIX II-A SCHEMATIZATIONS AND ADJUSTMENTS BY DHV

*Selection dike sections*

- In consultation with the water board two weak links in the dikes are added to the selection of DHV. It concerns weak links near:
  - Hm 72.000: this section was already in the original schematization (section 7023)
  - Hm 83.000: this section has eventually been added as section 7009 (dike section 7008 was chosen at first. This has been changed because the choice between 7008 and 7009 didn't matter that much according to the water board (both weak) and 7008 has later been converted into a dune).
- Consequently the total number of dike sections amounted to 33.

*Adjusting profiles*

- The profiles used in the first calculation in PC-Ring were based on old measurements by the water board. Next to that several adjustments were done in the profile in the first calculation, to be able to calculate them in PC-Ring, without data of the water board at hand to check the adjustments in the profiles. Because of that the input profiles were still compared to the recent measurements provided by the water board;
- The recent measurements of the water board are based on a hectometering of the dike (after a recent merging the water board switched from dike pole numbering to hectometering);
  -The dike pole numbering has been re-numbered to a hectometering, based on a conversion table (provided by the water board). With this a difference occurs in the exact position of the dike profiles of less than 50 meters. On a location a difference of 80 meters occurs;
- From the comparison it appeared that there were differences between the schematization and the recent profile measurements at several points:
  - For more than one profile the crown height differed 20 to 70 cm;
  - For more than one profile there were differences in sloping;
  - On several points the profile type in PC-Ring didn't quite match reality.
- In consult with VNK it was decided to adjust all 33 profiles in PC-Ring and to put them in based on recent measurements by the water board;
- Adjustments of profiles resulted in the fact that the profiles used for calculations in this report differ from the profiles used for the first calculation.
- For the new schematization the following assumptions were made:
  - For the toe of the dike one assumed the sand line;
  - If no foreland is present, the second point is the toe. An extra point appears than, which is located 2 meter in front of the toe, on the same level as the toe;
  - The choice between a bend or not on the crown is made based on a visual estimation;
  - If a berm is indicated in the file of the water board, but is it steeper than 1:15 it has to be adjusted for this schematization. In PC-Ring a slope than has to be steeper than 1:10 and a berm than less than 1:15. Everything steeper than 1:10 is considered a slope. With this berm

disappears and one obtains a slope with a bend. Everything below 1:10 becomes a berm. One considered up to one digit behind the comma for this;

- With the downgrading to a berm, an adjustment in height is made for the lowest point on the berm. This way the gradient of the attacked upper slope stays the same. The shift is not done in the line of the slope. The y point is vertically lifted of lowered (it is one or the other, because for extending the line of the lower slope the berm width changes, it is better to adjust the gradient of the lower slope);

- Applying a bend in the outer slope is done in such a way that the gradient of the upper slope doesn't change. The upper slope point is used as point of inflection. This is done for Ds numbers 7094 and 7159;

- For the point on the inner slope one assumed the first point on the inner slope that is given by the water board;

- Of Ds number 7028 the adjustment is done differently in order to be able to fit the profile in one of the schematizations. The berm has been lengthened, increasing the gradient of the upper slope and can be considered a slope. Other options for adjusting would mean adjustments for several points, due to which the profile would differ even more from reality;

- Ds number 0747 can't become category 8b, because the gradients of the crown are too high in case of an extra point on the crown. Thus one did eventually decide for a category 7a;

- Of the sections 7047, 7094, 7139 one would say that there's a bend in the crown. Copying 1 on 1 however means that the gradients of the crown planes become too steep (steeper than 1:15). Getting the gradients below 1:15 however means that one has to adjust the points in such a way that it either won't work or the bend becomes next to nil. In these cases one has chosen for a flat crown, and the levels are adjusted in such a way that the schematization is conservative.

*Dunes*

- At firs it was agreed upon to calculate 5 dune sections. With this it was agreed upon to calculate the dune sections of 2004. These provide a conservative picture, because the next (5-annual) suppletion is carried out in 2005;
- The choice of the dune sections to be calculated was made based on the Base Coastline Report of the RIKZ. The choice is based on a comparison of the base coastline (BCL), the coastline to be tested (TCL) and the trend the BCL has. When a probability of failure is calculated that contributes a lot to the total probability of flooding of the dike ring, possible nuances can be made based on information from the report on the base coastline. The calculated profile namely provides a lower limit of the probability of failure of the dune in question (dunes are calculated based on section measurements of a weak year);
- For the location of the dune sections one considered the maps of the Base Coastline Report and maps of the water board with the location of the dikes and dunes on them. The dike ring schematization in PC-Ring was also considered (where is a dune and where is a dike schematized);
- Eventually, considering the schematization present in PC-Ring, this lead to the choice of 4 dune sections to be calculated. In consult with VNK one has chosen to convert 2 profiles,

which at first were schematized as dikes in PC-Ring, into a dune profiles in order to be able to calculate 4 dune sections. Possibly a fifth dune section could have been calculated, if a dune section was divided into two dune sections. In consult with VNK it was decided not to do this;

- Of these 3 sections are weak and 1 section is a strong section. The strong section was chosen to see whether the outcomes in PC-Ring provide the same picture of the safety as the present situation of the section;
- Eventually the sections 7008, 7010, 7013 and 7027 were calculated as dune section. See the following schematization also:

- It needs noticing here that:

  - At first it was decided to calculate section 71 (Breskens) as well, since this is a weak section (which was indicated by the water board as well). In consult with VNK however it was decided not to calculate this section, because the section (and the rest of the dune site of which section 71 is a part) can't be schematized properly. The site is in between two jetties that have a strong reducing effect on the waves. Wave conditions are used that serve as input for the SWAN-calculations for dunes. For the Westerschelde these are the wave conditions for platform EUR. This is a deep water location at a considerable distance from the coast. In practice this means that the wind directions W to NNE are governing for the dunes. This was assumed because other conservative loads were not yet available. The deep water waves will in reality not reach the foot of the dune as a result of protection by the dams and possibly also because the coast is located in the shade of Walcheren (orientation of the dune is northerly, zero degrees). Expectation is thus that the wave loads will be less than follows from the calculations. Next to that stone covering is present at the foot of the dune. All considered, section 71 can not be taken into account properly in the calculations at this moment, despite it being a weak section;

  - Section 1354 was chosen as well. After consult with the water board this appeared to be a dike.

  - Dune section 1401 is put in on the original dike section 7008. Originally the x-y coordinates of dike pole 020-dp15 were used for 7008 in the schematization of dike ring 32 in PC-Ring. This dike pole is located roughly 500 meters east of section 1401. Because of this, one calculated with wave conditions specified for a location 500 meters away for section 1401.

- In connection with the schematization, several adjustments to PC-Ring have been carried out:

  - Two dike sections are converted to a dune, by:
    - Putting in type 2 for DS;
    - Profile type is 7;
    - River normal 999;
    - All fetch sections switched on (landside also)
    - Location codes are adjusted;
    - Profile overwritten by the Jarkus profiles.

  - For the four dune sections the right location codes have been put in the table dike section (with this also load model 10 has been added);

| (section) | loc.code | loc.code 1 | loc.code 2 | intpolation % |
|---|---|---|---|---|
| (230) | 7770028 | 7770028 | 7770029 | 85% |
| (851) | 7770028 | 7770028 | 7770029 | 40% |
| (1242) | 7770028 | 7770028 | 7770029 | 15% |
| (1401) | 7770028 | 7770028 | 7770029 | 5% |

- With respect to the boundary conditions it applies that the dunes of dike ring 32 are to be coupled to the load model of the Westerschelde. For this input files were added to the existing input files for the sandy coast.

- With the adding of the files mentioned above, two locations were added. The locations concern:

- 7770028 Bresken coordinates 27502 380752 test level = 5,25 m + NAP

- 7770029 ‘t Zwin coordinates 15013 378273 test level = 5,05 m + NAP

*MHW check*

- At the MHW check of DHV, an error was found in the location codes in PC-Ring. As a result of this, the right location codes were put in. The MHW check was done once more by DHV (see appendix B).

*Calculations DHV*

- The country setting of the computer is set to English to guarantee that the values that are put in the database are read correctly by PC-Ring. Decimal values have to be put in with a dot, so 0.4 in stead of 0,4;
- The stochastic variables for the calculations with coverings were all switched on, except for the deviation of wave direction;
- All calculations for probabilities of flooding are performed with the FORM*DS calculations method; VNK has used other techniques later on as well.
- For the covering calculations certain model settings were used. Possible adjustments are indicated by VNK in appendix B.

[1] According to PC-Ring (VNK) asphalt has to be chosen at all time for residual strength calculations, however this doesn’t lead to any results.

- DHV has switched off a large number of wind directions (by putting the number of fetch sections to zero) in order to obtain results for the stone coverings. This lead to the fact that

sometimes only three to seven wind directions were taken into account for calculating the probability of failure, this is in principal not correct. VNK has switched all these wind direction back on again at the start of its calculations. For the results for stone coverings, this doesn't this didn't matter too much. For the overtopping/wave overrun it did have somewhat more influence.

- With the help of the program MProStab calculations were done from which the probabilities of failure followed for the mechanism sliding, which can be combined with the other mechanisms of failure;
- The probabilities for the structures are determined using a method by hand. The sto.files obtained this way serve as input for PC-Ring which calculates the alphas en betas. The influence coefficients for both the mechanism constructive failure and not-closing of the closing elements were weighed based on probability contributions of the related mechanism and the residual strength. The values used for the mechanism overtopping and wave overrun and the other mechanisms are based on the ISO-norm. The sto.files serve as input for PC-Ring which calculates the values of the alphas, betas and the probabilities of failure. These values are consequently combined with the other probabilities to determine the total probability of flooding for the dike ring.
- After studying the values in the overall spreadsheet of the Water Board Zeeuws-Vlaanderen it appeared that the length of the seepage path was not represented correctly. The significantly greater length of the seepage path was determined based on the geometry of the dike for several dike sections (one assumed that the seepage path is minimal from toe to toe).

| DVNummer | Naam | Kwelweglengte WS | Kwelweglengte geometrie |
|---|---|---|---|
| 1320007002 | 024-Dp7 | 53,8 | 88,2 |
| 1320007009 | 020-Dp16 | 51,5 | 98,4 |
| 1320007023 | 006a-Dp10 | 42,2 | 120,5 |
| 1320007024 | 006a-Dp11 | 42,3 | 124,7 |
| 1320007025 | 006a-Dp15 | 50,3 | 101,6 |
| 1320007028 | 004-Dp25 | 40 | 100,2 |
| 1320007038 | 139a-Dp17 | 26,2 | 85,9 |
| 1320007042 | 138-Dp2 | 26,6 | 79,3 |
| 1320007047 | 137b-Dp7 | 19,9 | 191,4 |
| 1320007053 | 137a-Dp24 | 18,7 | 188,8 |
| 1320007071 | 133a-Dp67 | 23,8 | 77,4 |
| 1320007074 | 132a-Dp74 | 17,8 | 62,0 |
| 1320007075 | 131-Dp7 | 16,4 | 52,2 |
| 1320007094 | 127c-Dp69 | 28,6 | 69,4 |
| 1320007109 | 123-Dp26 | 26,8 | 81,3 |
| 1320007111 | 122-Dp16 | 25,4 | 84,9 |
| 1320007116 | 121a-Dp9 | 24,4 | 73,8 |
| 1320007124 | 113-Dp87 | 25,2 | 147,5 |
| 1320007129 | 111a-Dp12 | 33,3 | 99,0 |
| 1320007136 | 105-Dp10 | 30,6 | 86,1 |
| 1320007139 | 103-Dp23 | 29,3 | 79,7 |
| 1320007152 | 100a-Dp330 | 26,9 | 73,5 |
| 1320007155 | 095a-Dp319 | 25,5 | 84,2 |
| 1320007163 | 098b-Dp404 | 25,8 | 58,6 |
| 1320007167 | 097-Dp290 | 20,2 | 75,9 |
| 1320007185 | 090-Dp248 | 14,4 | 58,4 |
| 1320007202 | 085a-Dp201 | 18,9 | 74,7 |
| 1320007211 | 083a-Dp186 | 15,8 | 63,8 |
| 1320007220 | 081a-Dp175 | 15,8 | 58,1 |
| 1320007233 | 078-Dp148 | 16,3 | 63,0 |
| 1320007249 | 076-Dp124 | 16,0 | 61,6 |
| 1320007258 | 074-Dp99 | 15,1 | 63,8 |
| 1320007271 | 072-Dp69 | 14,7 | 61,1 |

Seepage path lengths for all sections (first column) given by Water board (3rd column) and based on the dike geometry (4th column).

# APPENDIX II-B ADAPTATIONS BY VNK

VNK has performed all calculations again (based on the database of DHV). In the scheme below it is indicated per section what has been altered relative to the database that was supplied by DHV.

| Section | Actions/notes related to database after delivery by DHV |
|---|---|
| All | In the calculations of DHV many wind directions have been turned off because these would not be relevant for the mechanism overtopping/wave overrun (this would be valid for offshore wind).<br>Offshore wind can be neglected in the river area (Bretschneider is used in that case). Along the coast the boundary conditions are determined using SWAN (in which also heave and diffraction etc are present). Herewith it could be that 1 or 2 wind directions do not converge. These wind directions could than possibly be turned off. For this one should first check whether these wind directions are not governing for overtopping/wave overrun. **Action 1: all wind directions are turned back on for all selected sections.** |
| | For the land of Saeftinghe a foreland of 5 kilometer is put in. the SWAN-points however are located 100 meters in front of the coast (and 300 meters apart). Foreland of 5 kilometer is useless. Foreland is turned off in the calculations of VNK. |
| | If the foreland is located >4 meter, there are no waves and thus no result. |
| | At a MHW-check, water levels are related to the RVW-book. This is not correct. There are different values with which should be checked. For this a file has been delivered by TNO in the past. No set-up is ipc expected along the coast. The values from table 4 are thus not correct. **Action 2: all wind set-up has been removed.** (in the database the dike section set-up is set to zero everywhere, as is the number of sections due to newer MHW-check). One does not save alterations (because then the new assortment is not saved, but the altered values are). |
| All | MHW-check performed according to the prescribed procedure. Foreland is turned off at sections 211, 220, 233, 249, 258, 271. See tab MHW-check → 2.pcr |

New PCR-file produced → results VNK → let everything be calculated by FORM-DS with 1 foreland point. If no good result was obtained, one looked whether this could be solved by adapting various things.

| | |
|---|---|
| 249 | Result seems to be caused by a strong covering. With the DS calculation the number of 5000 samples is too little with the higher beta values. These calculations thus have to be performed again with 100000 samples. Sections will not suddenly turn out weak. |
| 109 | No result for overtopping/wave overrun → initial value altered (from 8 to 1) and calculated with 6DS*FI instead of 8FORM*DS. |
| 38 | No data input on stone covering → thus no result |
| 24,25 | Level of GWL was set as 5,35. This should be 0 (is sea). Has been adapted. Factor fmGWS was set as 0,15 River, has been adapted into 0,25 Sea. |
| 42 | Covering: at wind direction 330 the residual strength crashed. 330 is governing wind direction for wave overrun, can not be turned off. Start method has been adapted from 8 → 1. Ov/ov keeps functioning. |
| 74 | Covering: crashes on the residual strength with the Combin calculation. Start method adapted from 8 → 1. Ov/ov keeps functioning. |
| 116 | Covering: crashes at residual strength. Start method has been adapted from 8 → 1. Result for covering, but now ov/ov does not function well. Southern wind direction (180 degrees) turned off. Now result for both mechanisms. |
| 139 | Gets stuck on residual strength. Start method adapted from 8 → 1. This results in a beta of 36. Covering seems very thick. Possibly a number of samples need to be calculated. Ov/ov keeps functioning. |
| 152 | Initial value adapted from 8 → 1. Result for covering, but now ov/ov does not function well. Southern wind direction (180 degrees) turned off. Now result for both mechanisms. |

| | |
|---|---|
| 159 | Initial value adapted from 8 → 1. Result for covering, but now ov/ov does not function well. It is not allowed to turn off the northern wind direction and even with 6DS*FI no good result follows. This should be solved manually. Thus ov/ov with initial value 8 and covering with initial value 1. → **both with FORM-DS** |
| 163 | Initial value adapted from 8 → 1. This does lead to result for the covering. Ov/ov keeps going well. Wind directions North, 30, 60, 90 turned off (not governing for ov/ov) → now result for both mechanisms |
| 167 | Initial value adapted from 8 → 1. Result for covering, but now ov/ov does not function well. It is not allowed to turn off wind direction 60 degrees and even with 6DS*FI no good result follows. This should be solved manually. Thus ov/ov with initial value 8 and covering with initial value 1. → both with FORM-DS. |
| 185 | Initial value adapted from 8 → 1. Ov/ov keeps functioning. Now result for the covering |
| 202 | Initial value adapted from 8 → 1. No result yet for covering, stops at 150. Ov/ov keeps functioningSouthern wind direction turned off → now result for covering. |
| 211 | Initial value adapted from 8 → 1. Result follows for both covering and overtopping/wave overrun. |
| 23 | Covering: crashes. Start method adapted from 8 → 1. Ov/ov keeps functioning. |
| 124 | Covering: crashes. Start method adapted from 8 → 1. Ov/ov keeps functioning. |
| 129 | Covering: crashes. Start method adapted from 8 → 1. Ov/ov keeps functioning. |
| 233 | Covering: crashes. Start method adapted from 8 → 1. Ov/ov keeps functioning. |
| All | Number of samples adapted from 5000 → 10.000 for all sections |

| | |
|---|---|
| Selection | For selected sections checked whether level GWL and Factor fmGWS are filled in correctly. Appeared this was often not the case. Adapted if necessary. Level GWL was set at 5,35. This should be 0 (is sea). Has been adapted. Factor fmGWS was set at 0,15 River, has been adapted to 0,25 Sea. |
| 28, 38 | For these sections no covering data were put in. |
| 28 | For 28 data input based on section 42.<br>Width stone 0 → 0,2<br>Length stone 0 → 0,2<br>Porosity filter 0 → 0,35<br>This results in a beta of 0,2<br>Section 28 has a very high toe |
| All | Calculate all sections for all mechanism. Initially all with FORM*DS, initial value 8 or 1 (resulting from action for 23, 42, 74, 116, 124, 139, 152, 163, 167, 185, 202, 211 and 233) |
| | For the following sections no or odd results have been calculated: |
| 28 | covering beta is 0,2057 |
| 109 | covering |
| 136 | overtopping/wave overrun + covering |
| 159 | overtopping/wave overrun |
| 167 | overtopping/wave overrun |
| 159, 167 | Adapt initial value from 1 → 8, then a result for overtopping/wave overrun; adapting manually per mechanism. Thus covering with initial value 1 and overtopping/wave overrun with initial value 8. |
| 109, 136 | Calculate with DS*FI with initial value 8 gives a result for all mechanisms |

28 If 3 (residual strength not relevant) is chosen in stead of 6 for the type number of the residual strength model, the same beta is calculated. Thus there are no data concerning residual strength in calculation.

Based on 42 more data adapted

Measure for acceleration of erosion in core of the dike: 1 (equal to the cover layer) → 3 (sand core)

Crack width: 0,001 → 0,015 (is standard in overall spreadsheet, was not put in for 28)

Relative density stone (average value): 1 → 1,8

Thickness granular filter layer: 0,04 → 0,1

Grain size 15% fraction of the filter material: 0,001 → 0,02 (is standard in the overall spreadsheet, was not put in for 28)

Residual strength model → 6 as in 42.

# III. Appendix 3: Details of the PRA German Bight

Within Action 3 of Activity 1 a preliminary reliability analysis (PRA) of the pilot site 'German Bight Coast' was performed the results of which are summarised in Kortenhaus & Lambrecht (2006). The reliability analysis was performed using the German 'ProDeich' model for coastal dikes as described in Kortenhaus (2003) and laser scan data of the flood defences made available by the coastal authorities of Schleswig-Holstein.

This section describes the approach to derive the overall probability of failure for all flood defences in the area. This comprises:

- a description of the flood prone area and the flood defence structures;
- the methodology to obtain geometrical parameters from laser scan measurements of the defence line;
- the development of an algorithm how the defence line can be split into different sections which can be treated independently;
- the calculation of the failure probability for each section of the flood defence line.

The methodology applied here is following the source-pathway-receptor model used in FLOOD*site* . The result of assessing the risk sources and the risk pathways is the probability of the flood defence failure, as highlighted in this figure.

St. Peter-Ording is a large community at the Schleswig-Holstein North Sea coast with the character of a tourist seaside resort. The community is located on the west (=exposed) coast of Eiderstedt peninsula (Figure 3.6). The size of the study area is approximately 6000 ha; from these about 4000 ha are considered to be flood-prone with the respective height distribution (NN = Ordinance Datum = regional Mean Water Level).

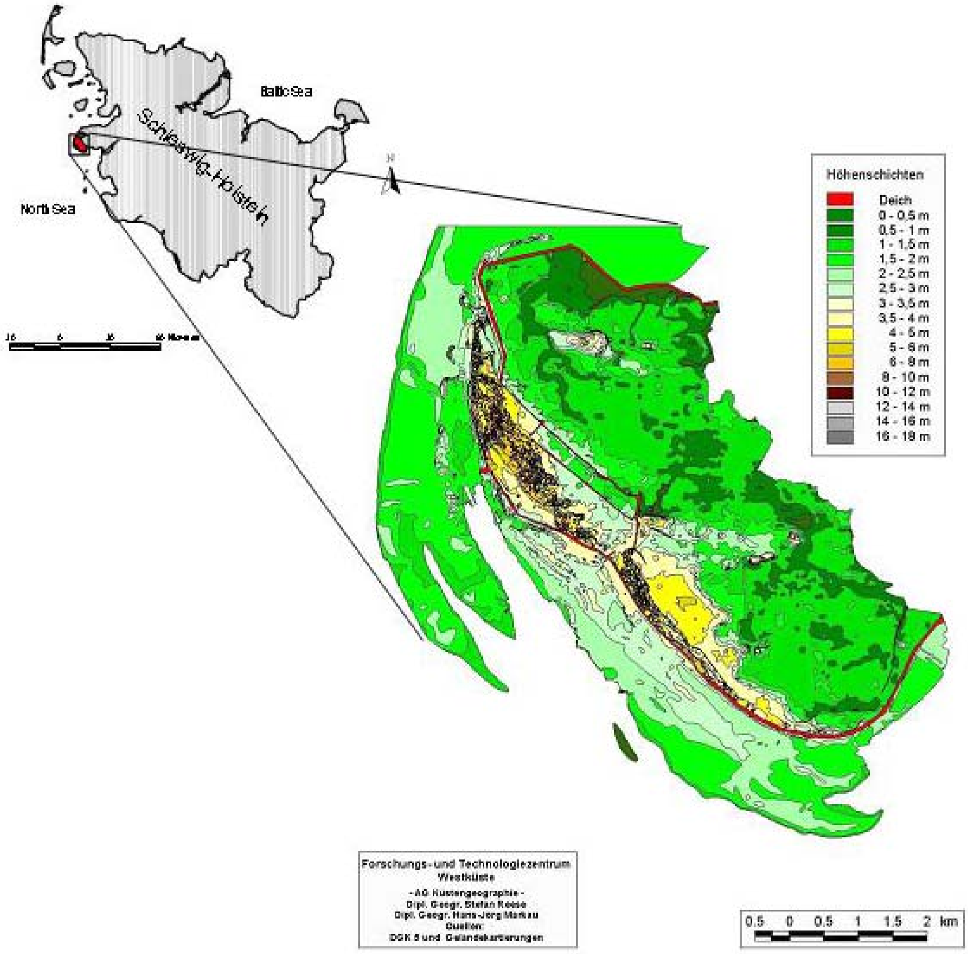


Figure **Error! No text of specified style in document.**.12: Map of pilot site 'German Bight' (red line illustrates the coastal dike)

The territory of the community amounts to 2800 ha with about 6300 inhabitants. In this area the irregular topography with intermittent small hills and dunes makes it difficult to draw flood-distance boundaries. Presently, flood protection is provided by a major dike (12.5 km long, about 8.0 m high) as well as dune structures 800 m, about 10 m and up to 18.0 m high), surrounding the community on three sides over a length of more than 15 km. The height of the dike line is not constant as shown in Figure 3.7.

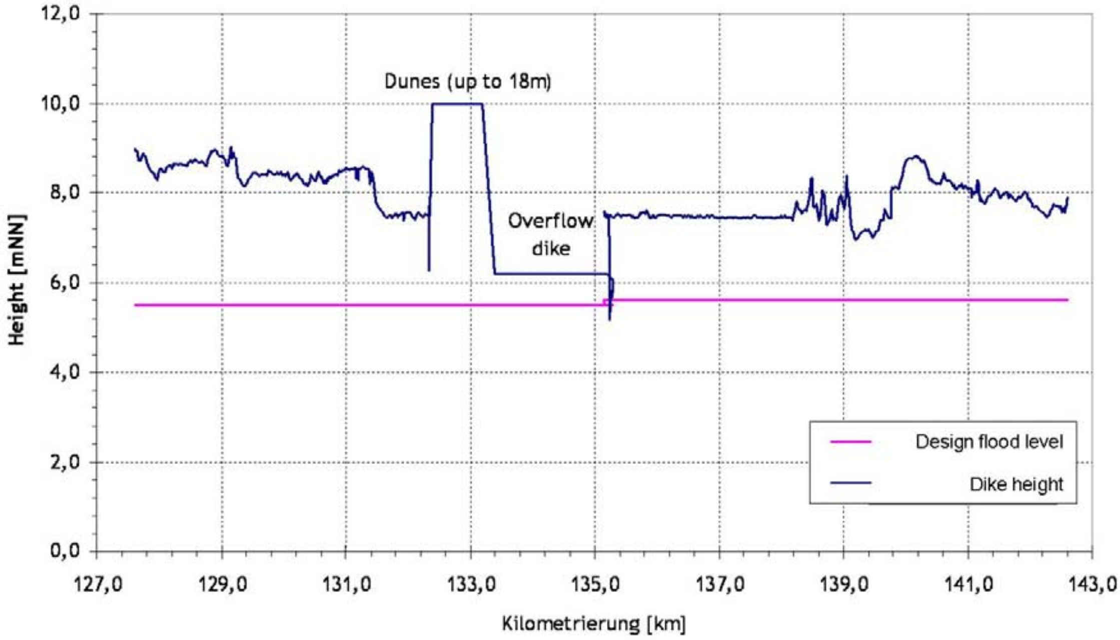


Figure **Error! No text of specified style in document.**.13: Height of costal defence structures at pilot site 'German Bight'

*Risk sources* at the German Bight are resulting from storm surges in the North Sea associated with high water levels and storm waves at the flood defences. Typically, storm surges last not longer than 12 to 24 hours but may increase the water level considerably (up to 3.5 m in the North Sea). The interaction of normal tides (water level differences in the range of 1-2 m are normal in the North Sea region), storm surges, and waves is crucial for the determination of the water level at the coast. In addition, the foreshore topography plays a major role when determining the waves at the flood defence structure. In case of the German Bight the limited water depths over a high foreland will cause the waves to break and will therefore limit the maximum wave heights which reach the flood defence structures. However, the PRA has only considered single probability distributions for each of the governing variables such as water level, wave height and wave period. No joint or conditional probability density functions were considered.

As for *risk pathways* in the German Bight Coast pilot site, flood defences comprise more than 12 km of dikes (grass and asphalt dike) and a dune area of about 2.5 km length. The PRA has however focussed on the dikes as the key flood defence structure since the dune belt is extraordinary high and wide and is regarded as significantly safer than the dike protection.

Before starting the probabilistic analysis the dike geometry and laser scan data have been used to define different sections of the flood defences. Criteria for distinction of different sections were the type of flood defence, its height, its orientation, the key sea state parameters like water level and waves, and geotechnical parameters. Thirteen sections have been identified using these criteria (see Kortenhaus & Lambrecht, 2006). Each of these sections is assumed to be identical over its entire length and hence will result in the same probability of failure.

The PRA has used a full probabilistic approach starting from the input parameters at the toe of the dike and applying early versions of the failure modes and fault trees which have been developed under FLOOD*site* for the specific type of flood defences. Time dependencies of limit state equations have been considered. Figure 3.8 shows a simplified version of the fault tree used for one of the sections at German Bight Coast for a typical sea dike. Most of the required input parameters for the failure modes are of stochastic nature which means that not only mean or design parameters but also a statistical distribution of this parameter describing the uncertainty is provided. The result of this analysis is an annual probability of flooding of the hinterland for each dike section which has been selected. These flooding probabilities were typically found to range from a probability of $10^{-4}$ to $10^{-6}$ which means a return period of flooding in the range of 10,000 or 1,000,000 years. The overall flooding probability using a fault tree approach for all sections results in $P_f = 4{\cdot}10^{-3}$.

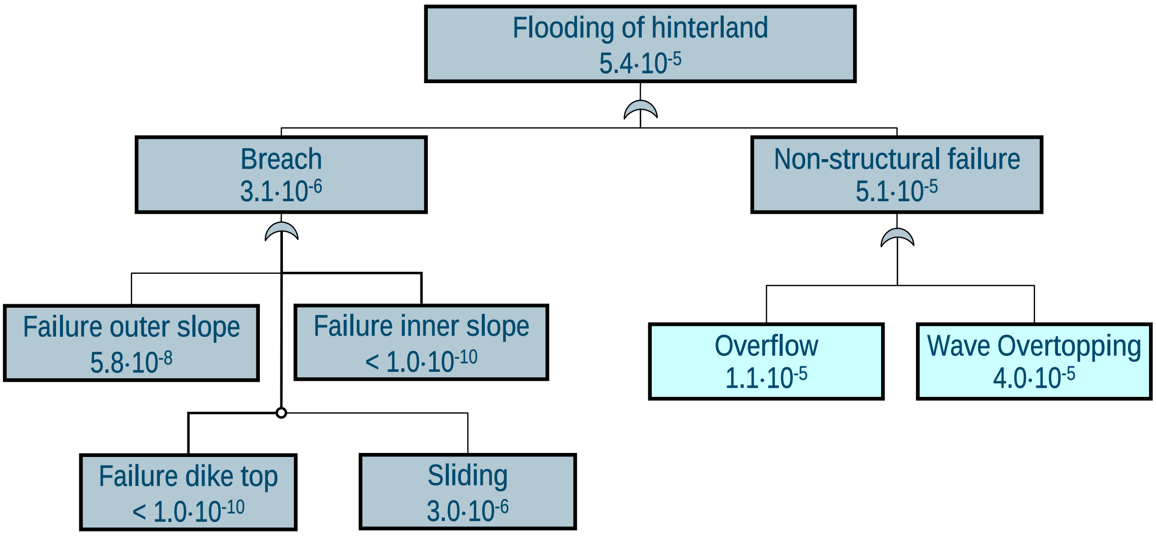


Figure **Error! No text of specified style in document.**.14: Typical fault tree for a dike section at “German Bight Coast”

The following lessons have been learned from performing this study for the German Bight Coast pilot site:

- The given results should only be used carefully since results depend on variations of parameter settings which still have to be performed.
- A limit state equation for dunes is still missing and needs to be implemented.
- The wide foreland in the German Bight Coast will induce heavy wave breaking under design conditions (and also for lower water levels of course). Results might therefore be dependent on morphodynamic processes and changes of these forelands. Breaker criteria should always be used when waves approaching the structure.
- Updated and harmonised limit state equations are needed to compare reliability calculations of pilot sites to each other.
- A wide range of input parameters are not directly available and had to be estimated. Therefore, sensitivity analyses of the influences of parameters have to be performed.

- Criteria for splitting the defence line into various sections need to be automatically derived in the model. Up to now, this is done semi-automatic (with some manual checks of the section at the end). Any change in key parameters of a dike section is therefore not directly leading to a re-calculation of the distinction of all the sections.
- Distinction between different sections was based on the assumption that the sections can be treated independently when calculating the overall failure probability of the system. This still needs verification or improved methods considering the length effect between sections.
- Dependencies between failure mechanisms or scenarios have not been considered yet. A first simple step to consider dependencies might be sensitivity calculations for different degrees of dependencies resulting in a range of possible failure probabilities. However, since the overall failure probability seems mostly dependent on section 8 (overtopping dike) inclusion of dependencies at this stage will probably not influence the result significantly.

# IV. Appendix 4: Uncertainty database

## IV-A: FAILURE MECHANISMS

The computer program PC-RING is used in the Netherlands to failure probabilities of dike sections (Steenbergen and Vrouwenvelder, 2003). In order to calculate the failure probability, a dike ring system is cut in several dike sections. The reliability of the dike sections with respect to the failure mechanism is calculated, after which the total failure probability of the dike ring is determined. The following failure mechanism are examined in PC-RING (Steenbergen and Vrouwenvelder, 2003B):

- Overflow/overtopping
- Slope instability
- Heave/piping
- Erosion revetment and erosion dike body
- Piping structures
- Not closing structures
- Dune erosion

Other mechanism have not been considered important enough to incorporate. The failure mechanism are elaborated in the following sections. The remaining part of this appendix is based on Steenbergen and Vrouwenvelder (2003A) and (Steenbergen and Vrouwenvelder, 2003B). A list with all the random variables in PC-RING is provided in Appendix B. The variable numbers in Appendix B correspond to the variable numbers below.

### 1.1.1.2 General

The geometry parameters apply to more than one failure mechanism. The geometric variables are listed in Table A 1.

Table A 1: General parameters (Steenbergen and Vrouwenvelder, 2003B)

| Variable nr. | symbol | description |
|---|---|---|
| 1 | $h_d$ | Dike height |
| 4 | $h_t$ | Toe height |
| 5 | $\tan \alpha_{u;b}$ | Angle outer slope (top) |
| 6 | $\tan \alpha_{u;o}$ | Angle outer slope (bottom) |
| 7 | $\tan \alpha_i$ | Angle inner slope |
| 2 | $h_B$ | Berm height |
| 3 | $B$ | Berm width |
| 131 | $\Delta d$ | Error in determination ground level |

### 1.1.1.3 Overflow/overtopping

The mechanism overflow/overtopping occurs in case to much water is flowing or topping over the dike, see Figure A 1. Failure due to overflow/overtopping occurs either if the revetment of the inner

slopes fails, or due to saturation of the inner slope. Saturation occurs when the overflow/overtopping discharge is larger than the critical discharge and when the inner slope slides.

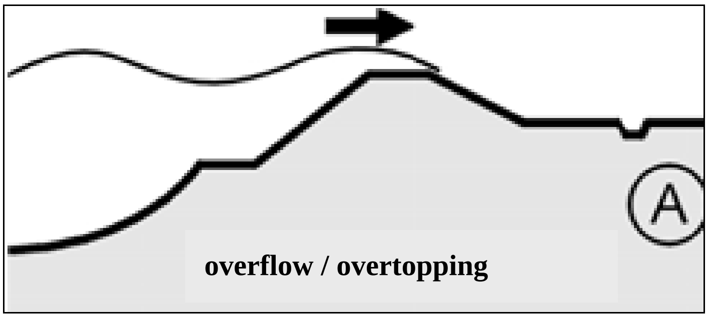


Figure A 1: Overflow / overtopping (Technical Advisory Committee on Water Defences, 1998)

The following variables (above the geometry variables) apply to the mechanism overflow/overtopping, see Table A 2. For more information about this mechanism is referred to (Steenbergen and Vrouwenvelder, 2003B)

Table A 2: Variables for overflow/overtopping (Steenbergen and Vrouwenvelder, 2003B)

| Variable nr. | symbol | description |
|---|---|---|
| 9 | $k$ | Roughness inner slope |
| 10 | $f_b$ | Factor for determination $Q_b$ |
| 11 | $f_n$ | Factor for determination $Q_n$ |
| 8 | $m_{qc}$ | Model factor critical overflow discharge |
| 12 | $m_{qo}$ | Model factor for occuring overflow discharge |
| 13 | $c'$ | Cohesion (Clay layer inner slope) |
| 14 | $\varphi'$ | Friction angle (Clay layer inner slope) |
| 15 | $\rho$ | Soil density (Clay layer inner slope) |
| 16 | $d_k$ | Layer thickness (Clay layer inner slope) |

#### 1.1.1.4 Slope instability

Slope instability occurs in case the dike becomes unstable and cannot supports its own weight anymore, see Figure A 2. This mechanism usually occurs due to infiltration of water in the dike and/or due to water pressure in sand layers below the dike. Slope instability can occur both on the inner side and on the outer side. However, slope instability of the inner slope is usually assumed to be the dominant mechanism.

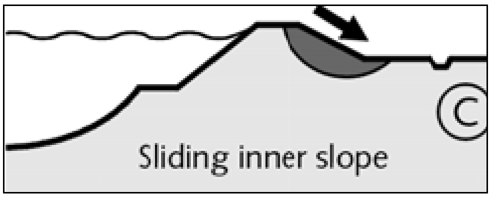


Figure A 2: Slope instability (Technical Advisory Committee on Water Defences, 1998)

The following variables (above the geometry variables) apply to the mechanism slope instability, see Table A 3. For more information about this mechanism is referred to (Steenbergen and Vrouwenvelder, 2003B).

Table A 3: Variables for slope instability (Steenbergen and Vrouwenvelder, 2003B)

| Variable nr. | symbol | description |
|---|---|---|
| 20 | $\Delta u$ | Deviation water levels |
| 21 | $c'$ | cohesion per layer |
| 22 | $\tan(\varphi')$ | friction angle per layer |
| 23 | $q$ | Model uncertainty Bishop |

#### 1.1.1.5 Heave/piping

In case of the mechanism heave/piping, the dike fails because sand under the dike is flushed away, see Figure A 3. Two mechanisms are involved. First, the impermeable layer will heave. Second, pipes will develop due to the hydraulic gradient and sand from below the dike will be washed away.

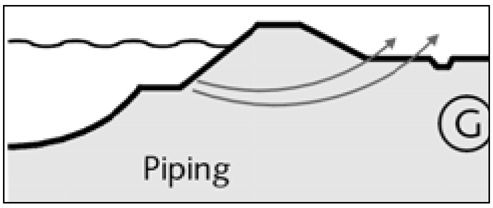


Figure A 3: Heave/piping (Technical Advisory Committee on Water Defences, 1998)

The following variables (above the geometry variables) apply to the mechanism heave/piping, see Table A 4 and Figure A 4. For more information about this mechanism is referred to (Steenbergen and Vrouwenvelder, 2003B).

Table A 4: Variables for heave/piping (Steenbergen and Vrouwenvelder, 2003B)

| Variable nr. | symbol | description |
|---|---|---|
| 41 | $d$ | Thickness covering layer |
| 137 | $h_b$ | Inner water level |
| 49 | $(\gamma_{hat}-\gamma_w)/\ \gamma_w$ | Apparent relative density of heaving soil |
| 50 | $\gamma_k/\gamma_w$ | Relative soil density sand (grain) |
| 43 | $L$ | Leakage length |
| 42 | $D$ | Thickness sand layer |
| 45 | $\kappa/d_{10}^2$ | Factor $C_{bear}$ |
| 47 | $d_{70}/d_{10}$ | Uniformity |
| 44 | $\theta$ | rolling resistance angle |
| 46 | $d_{70}$ | Grain size |
| 48 | $\eta$ | White's constant |
| 54 | $k$ | Specific permeability |
| 51 | $m_o$ | Model factor heave |
| 52 | $m_p$ | Model factor piping |
| 53 | $m_h$ | Model factor water level (damping) |

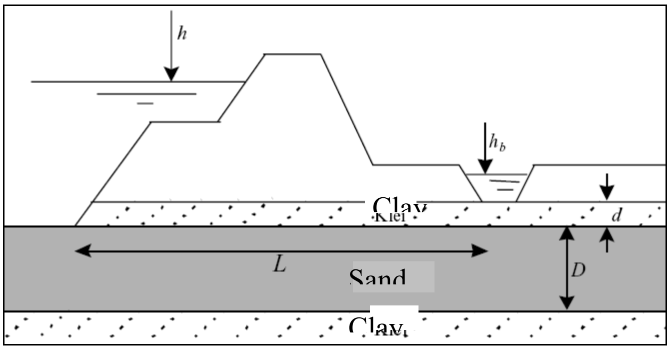


Figure A 4: Part of the variables in heave/piping (Steenbergen and Vrouwenvelder, 2003B)

### 1.1.1.6 Erosion revetment and erosion dike body

The mechanism erosion revetment/dike body occurs when first the revetment of a dike is eroded and secondly the body of the dike is eroded away, see . Several types of revetment have been considered: grass, stone pitching without filter, stone pitching with granular filter and asphalt.

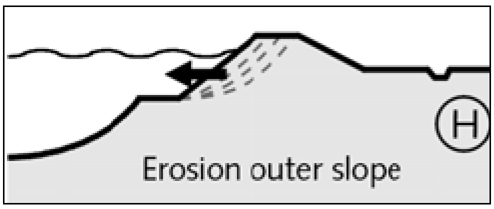


Figure A 5: Erosion revetment and erosion dike body

The following variables (above the geometry variables) apply to the mechanism erosion revetment and dike body, see Table A 5. For more information about this mechanism is referred to (Steenbergen and Vrouwenvelder, 2003B).

Table A 5: Variables for erosion revetment (Steenbergen and Vrouwenvelder, 2003B)

| Variable nr. | symbol | description |
|---|---|---|
| 62 | $L_K$ | Width covering clay layer |
| 63 | $L_{BK}$ | Width dike core at crest height |
| 65 | tan $\alpha_u$ | Angle outer slope |
| 66 | tan $\alpha_i$ | Angle inner slope |
| 70 | $c_{RK}$ | Coefficient erosion resistance covering layer |
| 71 | $c_{RB}$ | Coefficient erosion resistance dike core |
| 85 | $\alpha_z$ | Acceleration factor erosion rate |
| 86 | $\alpha_h$ | Declination erosion speed |
| 83 | $\beta_r$ | Angle in reduction factor r |
| *Grass* | | |
| 61 | $d_w$ | Root depth grass |
| 69 | $c_g$ | Coefficient erosion resistance grass |
| *Stone pitching, directly on clay* | | |
| 64 | $D$ | Stone pitching thickness |
| 67 | $\Delta$ | Relative density stone pitching |
| 68 | $c_k$ | Coefficient stone pitching on clay |
| *Stone pitching, with granular filter* | | |
| 64 | $D$ | Stone pitching thickness |
| 67 | $\Delta$ | Relative density stone pitching |
| 72 | $d_f$ | Thickness granular filter layer |
| 73 | $D_{f15}$ | Grain size 15% percentile filer |
| 74 | $s$ | Crack width |
| 75 | $c_f$ | Coefficient stone pitching on filter |
| 76 | $c_a$ | Coefficient in determination leakage length |
| 77 | $c_b$ | Coefficient in determination leakage length |
| 78 | $c_t$ | Coefficient in determination leakage length |
| 84 | $c_{gf}$ | Coefficient strength stone pitching |
| 87 | $c$ | Coefficient |
| *Asphalt revetment* | | |
| 79 | $D$ | Thickness asphaltic concrete |
| 80 | $\Delta$ | Relative density asphaltic concrete |
| 81 | $f_{MGWS}$ | Factor for normative water level |
| 82 | $h_{GWS}$ | Level average discharge |
| 88 | $h_{fo}$ | Height fictive bottom |
| 89 | $b$ | Parameter |
| 90 | $D_{n50}$ | Nominal average diameter revetment |
| 91 | $\psi_u$ | Revaluation factor |
| 92 | $\Phi_{SW}$ | Stability parameter |

#### 1.1.1.7 Piping structures

Piping of structures occurs in case sand below a hydraulic structure (for instance a sluice) is flushed away due to a hydraulic gradient, see Figure A 6.

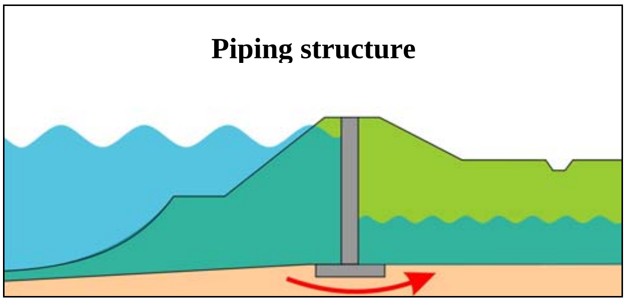


Figure A 6: Piping under a structure (FLORIS, 2006)

The following variables (above the geometry variables) apply to the mechanism piping structures, see Table A 6. For more information about this mechanism is referred to (Steenbergen and Vrouwenvelder, 2003B).

Table A 6: Variables for piping structures (Steenbergen and Vrouwenvelder, 2003B)

| Variable nr. | symbol | description |
|---|---|---|
| 114 | $m_L$ | Model factor |
| 115 | $m_c$ | Model factor |
| 111 | $L_v$ | Vertical leakage length |
| 112 | $L_h$ | Horizontal leakage length |
| 113 | $c_L$ | Lane's constant |
| 137 | $h_b$ | Inner water level |

#### 1.1.1.8 Structure not closed

The failure mechanism structure not closed occurs when the structure is not closed and when there is too much water flowing through the structure (for the surface of the retention area behind the structure), see Figure A 7.

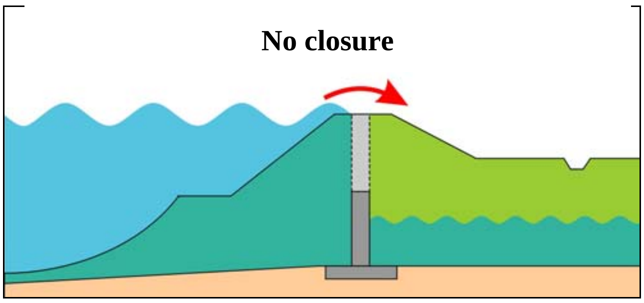


Figure A 7: Structure not closed (FLORIS, 2006)

The following variables (above the geometry variables) apply to the mechanism structure not closed, see Table A 7. For more information about this mechanism is referred to (Steenbergen and Vrouwenvelder, 2003B).

Table A 7: Variables for structure not closed (Steenbergen and Vrouwenvelder, 2003B)

| Variable nr. | symbol | description |
|---|---|---|
| 110 | $\beta_{ns}$ | Reliability closure |
| 107 | $m_{kom}$ | *Model factor* $V_{kom}$ |
| 108 | $m_{in}$ | *Model factor* $V_{in}$ |
| 109 | $c$ | Coefficient |
| 104 | $A_{kom}$ | surface retention area |
| 105 | $h_{pv}$ | Level raise |
| 102 | $B$ | Width structure |
| 103 | $h_{ok}$ | Water level in open condition |
| 101 | $A$ | Cross section discharge |
| 106 | $\mu$ | Discharge coefficient |

### 1.1.1.9 Dune erosion

The flood defence fails due to dune erosion in case the cross section is eroded below a threshold due to wave attack, see Figure A 8.

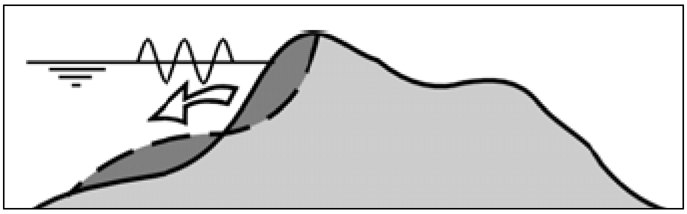

Figure A 8: Dune erosion (Technical Advisory Committee on Water Defences, 1998)

The following variables (above the geometry variables) apply to the mechanism dune erosion, see Table A 8. For more information about this mechanism is referred to (Steenbergen and Vrouwenvelder, 2003B).

Table A 8: Variables for dune erosion (Steenbergen and Vrouwenvelder, 2003B)

| Variable nr. | symbol | description |
|---|---|---|
| 122 | $M_D$ | Model factor |
| 123 | $d_{50}$ | Median grain size |

# IV-B: OVERVIEW OF RANDOM VARIABLES IN PC-RING

Computer program PC-ring is used in the Netherlands to calculate failure probabilities of dike rings. The different failure modes are described Appendix A, an overview of all random variables is provided in table B-1

*Table B-1: Overview of random variables in PC-Ring (Steenbergen and Vrouwenvelder, 2003A pp 48-50 and 2003B)*

| Variable nr. | symbol | description |
|---|---|---|
| **Geometry** | | |
| 1 | $h_d$ | Dike height |
| 2 | $h_B$ | Berm height |
| 3 | $B$ | Berm width |
| 4 | $h_t$ | Toe height |
| 5 | tan $\alpha_{u;b}$ | Angle outer slope (top) |
| 6 | tan $\alpha_{u;o}$ | Angle outer slope (bottom) |
| 7 | tan $\alpha_i$ | Angle inner slope |
| | | |
| **Overflow/overtopping** | | |
| 8 | $m_{qc}$ | Model factor critical overflow discharge |
| 9 | $k$ | Roughness inner slope |
| 10 | $f_b$ | Factor for determination $Q_b$ |
| 11 | $f_n$ | Factor for determination $Q_n$ |
| 12 | $m_{qo}$ | Model factor for occuring overflow discharge |
| 13 | $c'$ | Cohesion (Clay layer inner slope) |
| 14 | $\varphi'$ | Friction angle (Clay layer inner slope) |
| 15 | $\rho$ | Soil density (Clay layer inner slope) |
| 16 | $d_k$ | Layer thickness (Clay layer inner slope) |
| **Stability** | | |
| 20 | $\Delta$u | Deviation water levels |
| 21 | $c'$ | cohesion per layer |
| 22 | tan$(\varphi')$ | friction angle per layer |
| 23 | q | Model uncertainty Bishop |
| **Heave/piping** | | |
| 41 | $d$ | Thickness covering layer |
| 42 | $D$ | Thickness sand layer |
| 43 | $L$ | Leakage length |
| 44 | $\theta$ | rolling resistance angle |
| 45 | $\kappa/d_{10}^2$ | Factor $C_{bear}$ |
| 46 | $d_{70}$ | Grain size |
| 47 | $d_{70}/d_{10}$ | Uniformity |
| 48 | $\eta$ | White's constant |
| 49 | $(\gamma_{nat}-\gamma_w)/\ \gamma_w$ | Apparent relative density of heaving soil |
| 50 | $\gamma_k/\gamma_w$ | Relative soil density sand (grainl) |
| 51 | $m_o$ | Model factor heave |
| 52 | $m_p$ | Model factor piping |
| 53 | $m_h$ | Model factor water level (damping) |
| 54 | $k$ | Specific permeability |
| **Revetment** | | |
| 61 | $d_w$ | Root depth grass |

| Variable nr. | symbol | description |
|---|---|---|
| 62 | $L_K$ | Width covering clay layer |
| 63 | $L_{BK}$ | Width dike core at crest height |
| 64 | $D$ | Stone pitching thickness |
| 65 | $\tan \alpha_u$ | Angle outer slope |
| 66 | $\tan \alpha_i$ | Angle inner slope |
| 67 | $\Delta$ | Relative density stone pitching |
| 68 | $c_k$ | Coefficient stone pitching on clay |
| 69 | $c_g$ | Coefficient grass |
| 70 | $c_{RK}$ | Coefficient erosion covering layer |
| 71 | $c_{RB}$ | Coefficient erosion dike core |
| 72 | $d_f$ | Thickness granular filter layer |
| 73 | $D_{f15}$ | Grain size 15% percentile filer |
| 74 | $s$ | Crack width |
| 75 | $c_f$ | Coefficient stone pitching on filter |
| 76 | $c_a$ | Coefficient in determination leakage length |
| 77 | $c_b$ | Coefficient in determination leakage length |
| 78 | $c_t$ | Coefficient in determination leakage length |
| 79 | $D$ | Thickness asphaltic concrete |
| 80 | $\Delta$ | Relative density asphaltic concrete |
| 81 | $f_{MGWS}$ | Factor for normative water level |
| 82 | $h_{GWS}$ | Level average discharge |
| 83 | $\beta_r$ | Angle in reduction factor r |
| 84 | $c_{gf}$ | Coefficient strength stone pitching |
| 85 | $\alpha_z$ | Acceleration factor erosion rate |
| 86 | $\alpha_h$ | Declination erosion speed |
| 87 | $c$ | Coefficient |
| 88 | $h_{fo}$ | Height fictive bottom |
| 89 | $b$ | Parameter |
| 90 | $D_{n50}$ | Nominal diameter |
| 91 | $\psi_u$ | Revaluation factor |
| 92 | $\Phi_{SW}$ | Stability parameter |
| **No closure structure** | | |
| 101 | $A$ | Cross section discharge |
| 102 | $B$ | Width structure |
| 103 | $h_{ok}$ | Water level in open condition |
| 104 | $A_{kom}$ | surface retention area |
| 105 | $h_{pv}$ | Level raise |
| 106 | $m$ | Discharge coefficient |
| 107 | $m_{kom}$ | *Model factor* $V_{kom}$ |
| 108 | $m_{in}$ | *Model factor* $V_{in}$ |
| 109 | $c$ | Coefficient |
| 110 | $P_{ns}$ | Probability of no closure |
| **Piping structures** | | |
| 111 | $L_v$ | Vertical leakage length |
| 112 | $L_h$ | Horizontal leakage length |
| 113 | $c_L$ | Lane's constant |
| 114 | $m_L$ | Model factor |
| 115 | $m_c$ | Model factor |
| **Dunes** | | |
| 121 | $h_d$ | Dune height |
| 122 | $M_D$ | Model factor |
| 123 | $d_m$ | Median grain size |
| **General** | | |

| Variable nr. | symbol | description |
|---|---|---|
| 131 | $\Delta d$ | Error in determination ground level |
| 132 | $m_{gH}$ | Model factor Bretschneider for $H_s$ |
| 133 | $m_{gT}$ | Model factor Bretschneider for $T_s$ |
| 134 | $\Delta h_{loc}$ | Error in local water level |
| 135 | $\beta^*$ | Deviation wave direction |
| 136 | $t_s$ | Storm duration |
| 137 | $h_b$ | Inner water level |
| **Loads** | | |
| 140 | $u_A$ | Parameter magnitude discharge Lobith |
| 141 | $u_B$ | Parameter slope discharge Lobith |
| 142 | $u$ | Parameter h North Sea |
| 143 | $\sigma$ | Parameter h North Sea |
| 144 | $\gamma$ | Parameter h North Sea |
| 145 | $A$ | Parameter wind |
| 146 | $B$ | Parameter wind |
| 147 | $h_{MM}$ | Water level Maasmond |
| 148 | $v$ | Wind speed |
| 149 | $Q_{Lobith}$ | Discharge Lobith (Rijn) |
| 150 | $h_{Dlz}$ | Water level Delfzijl |
| 151 | $h_{OS}$ | Water level OS11 |
| 152 | $Q_{Vecht}$ | Water level Dalfsen (Vecht) |
| 153 | $Q_{IJssel}$ | Discharge Olst (IJssel) |
| 154 | $Q_{Lith}$ | Discharge Lith (Maas) |
| 155 | $\Delta h_{MK}$ | Prediction error water level Maeslantkering |
| 156 | $h_{IJsselmeer}$ | Water level IJsselmeer |
| 157 | $h_{Markermeer}$ | Water level Markermeer |
| 158 | $h_{HvH}$ | Water level Hoek van Holland |
| 159 | $h_{DH}$ | Water level Den Helder |
| 160 | $h_{Vlis}$ | Water level Vlissingen |
| 161 | $h_{Har}$ | Water level Harlingen |
| 162 | $h_{LO}$ | Water level Lauwersoog |
| 163 | $v_{SD}$ | Wind speed Schiphol / Deelen |
| 164 | $v_{IG}$ | Wind speed 'ligth island' Goeree |
| 165 | $v_{dK}$ | Wind speed de Kooy |
| 166 | $v_{Vlis}$ | Wind speed Vlissingen |
| 167 | $v_{TW}$ | Wind speed Terschelling West |
| 168 | $\Delta h_{OK}$ | Prediction error water level Oosterscheldekering |
| 169 | $t_{wo}$ | Duration wind setup |
| 170 | $\Delta t_{OS}$ | Phase difference |

## IV-C: SENSITIVITY COEFFICIENTS DIKE RING 7, 32 AND 36

The sensitivity coefficients of dike rings 7, 32 and 36 are shown in Table C-1, Table C-2 and Table C-3

*Table C-1: Sensitivity coefficients dike ring 7: Noordoostpolder*

| Variable # | Description | alfa | alfa^2 |
|---|---|---|---|
| 1 | Dike height h_d | 0.05100 | 0.00260 |
| 2 | Berm height h_B | 0.00600 | 0.00004 |
| 3 | Berm width B | 0.00000 | 0.00000 |
| 4 | Toe height h_t | 0.00100 | 0.00000 |
| 5 | Slope outer slope (top) | -0.01000 | 0.00010 |
| 6 | Slope outer slope (bottom) | 0.00000 | 0.00000 |
| 7 | Slope outer slope | -0.00300 | 0.00001 |
| 8 | Mode factor critical overflow discharge m_qc | 0.05200 | 0.00270 |
| 9 | Roughness inner slope k | 0.00700 | 0.00005 |
| 10 | Factor for determining Q_b f_b | 0.02200 | 0.00048 |
| 11 | Factor for determining Q_n f_n | 0.02700 | 0.00073 |
| 12 | Model factor occurring overflow discharge m_qo | -0.05700 | 0.00325 |
| 13 | Error position bottom | 0.00000 | 0.00000 |
| 14 | Model factor Bretschneider for Hs | 0.00000 | 0.00000 |
| 15 | Model factor Bretschneider for Ts | 0.00000 | 0.00000 |
| 16 | Error in local water level | 0.00000 | 0.00000 |
| 17 | Storm duration t_s | 0.00000 | 0.00000 |
| 18 | Level Lake IJssel | -0.32800 | 0.10758 |
| 19 | Wind speed Schiphol/Deelen | -0.86200 | 0.74304 |
| 20 | (null) | -0.37300 | 0.13913 |
| 21 | Discharge Lobith | 0.00000 | 0.00000 |
| 22 | Discharge Dalfsen | 0.00000 | 0.00000 |
| 23 | Discharge Olst | 0.00000 | 0.00000 |
| 24 | Root depth grass d_w | 0.00000 | 0.00000 |
| 25 | Widht covering layer of clay L_K | 0.00000 | 0.00000 |

| | | | |
|---|---|---|---|
| 26 | Widht dike core on crest height L_BK | 0.00000 | 0.00000 |
| 27 | Stone thickness D | 0.00000 | 0.00000 |
| 28 | Tangent alfa_u | 0.00000 | 0.00000 |
| 29 | Tangent alfa_i | 0.00000 | 0.00000 |
| 30 | Relative density stone | 0.00000 | 0.00000 |
| 31 | Coefficient stone pitching op klei c_k | 0.00000 | 0.00000 |
| 32 | Coefficient grass c_g | 0.00000 | 0.00000 |
| 33 | Coefficient erosion covering layer c_rk | 0.00000 | 0.00000 |
| 34 | Coefficient erosion dike core c_rb | 0.00000 | 0.00000 |
| 35 | Thickness granular filter layer d_f | 0.00000 | 0.00000 |
| 36 | Grain size15% percentile filter | 0.00000 | 0.00000 |
| 37 | Crack width s | 0.00000 | 0.00000 |
| 38 | Coefficient stone pitching on filter c_f | 0.00000 | 0.00000 |
| 39 | Coefficient in leakage length determination c_a | 0.00000 | 0.00000 |
| 40 | Coefficient in leakage length determination c_ b | 0.00000 | 0.00000 |
| 41 | Coefficient in leakage length determination c_t | 0.00000 | 0.00000 |
| 42 | Thickness asphalt concrete D | 0.00000 | 0.00000 |
| 43 | Relative density asphalt concrete | 0.00000 | 0.00000 |
| 44 | Factor f_MGWS | 0.00000 | 0.00000 |
| 45 | Height h_GWS | 0.00000 | 0.00000 |
| 46 | Angle in reduction factor r | 0.00000 | 0.00000 |
| 47 | Coefficient strength stone pitching c_gf | 0.00000 | 0.00000 |
| 48 | Acceleration erosion alfa_z | 0.00000 | 0.00000 |
| 49 | Damping factor alfa_h | 0.00000 | 0.00000 |
| 50 | Coefficient c | 0.00000 | 0.00000 |
| 51 | Height h_ fictive bottom | 0.00000 | 0.00000 |
| 52 | Parameter b | 0.00000 | 0.00000 |
| 53 | Nominal diameter | 0.00000 | 0.00000 |
| 54 | Upgrade factor | 0.00000 | 0.00000 |
| 55 | Stability parameter | 0.00000 | 0.00000 |

| | | |
|---|---|---|
| **Sum** | **-1.46700** | **0.99972** |

*Table C-2: Sensitivity coefficients dike ring 32: Zeeuws Vlaanderen*

| Variable Description | alfa | alfa^2 |
|---|---|---|
| Dike height h_d | 0.0883 | 0.0078 |
| Berm height h_B | 0.0563 | 0.0032 |
| Berm width B | 0.0000 | 0.0000 |
| Toe height h_t | 0.0055 | 0.0000 |
| Slope outer slope (top) tan(alfa_b) | 0.0185 | 0.0003 |
| Slope outer slope (bottom) tan(alfa_o) | 0.0150 | 0.0002 |
| Slope outer slope tan(alfa_i) | 0.0061 | 0.0000 |
| Roughness inner slope k | 0.0802 | 0.0064 |
| Factor f_b for determination Q_b (breaking waving) | 0.0106 | 0.0001 |
| Factor f_n for determination Q_n (non-breaking waving) | 0.0787 | 0.0062 |
| Model factor critical overflow discharge m_qc | 0.0075 | 0.0001 |
| Model factor occurring overflow discharge m_qo | -0.0827 | 0.0068 |
| Cohesion (clay inner slope) c` | | 0.0000 |
| Friction angle (clay inner slope) phi` | | 0.0000 |
| Soil weight (clay inner slope) rho | | 0.0000 |
| Layer thickness (clay inner slope) d_k | | 0.0000 |
| Error in position bottom Delta_d | 0.0000 | 0.0000 |
| Model factor Bretschneider for wave height m_gH | 0.0000 | 0.0000 |
| Model factor Bretschneider for wave period m_gT | 0.0000 | 0.0000 |
| Error in local water level Delta_hlok | 0.0000 | 0.0000 |
| Error in wave direction beta* | | 0.0000 |
| Storm duration t_s | 0.0299 | 0.0009 |
| Thickness covering layer d | 0.3170 | 0.1005 |
| Apparent weight soil with respect to uplift | 0.0005 | 0.0000 |
| Model factor uplift m_o | 0.0009 | 0.0000 |
| Model factor damping m_h | -0.0009 | 0.0000 |
| Root depth grass d_w | 0.0000 | 0.0000 |
| Width covering clay layer outer slope L_K | 0.0210 | 0.0004 |

| | | |
|---|---|---|
| Width dike core at crest level L_BK | 0.0216 | 0.0005 |
| Stone pitching thickness D | | 0.0000 |
| Slope outer slope dike core tan(alfa_u) | 0.1001 | 0.0100 |
| Slope inner slope dike core tan(alfa_i) | | 0.0000 |
| Relative density stone Delta | | 0.0000 |
| Coefficient for strength stone pitching on clay c_k | | 0.0000 |
| Coefficient for erosion resistance grass c_g | 0.0000 | 0.0000 |
| Coefficient for erosion resistance of covering layer c_RK | 0.3445 | 0.1187 |
| Coefficient for erosion resistance of the dike core c_RB | | 0.0000 |
| Thickness granular filter layer d_f | | 0.0000 |
| Grain size 15% percentile weight filter material D_f15 | | 0.0000 |
| Crack width s | | 0.0000 |
| Coefficient for strength stone pitching on filter c_f | | 0.0000 |
| Coefficient in determination leakage length c_a | | 0.0000 |
| Coefficient in determination leakage length c_b | | 0.0000 |
| Coefficient in determination leakage length c_t | | 0.0000 |
| Thickness asphalt layer D | | 0.0000 |
| Relative density asphalt layer | | 0.0000 |
| Factor f_MGWS | | 0.0000 |
| Height h_GWS | | 0.0000 |
| Angle of wave attack Beta_r | -0.0005 | 0.0000 |
| Coefficient for strength stone pitching c_gf | | 0.0000 |
| Measure of erosion acceleration in dike core alfa_z | 0.0000 | 0.0000 |
| Measure of erosion decrease with height alfa_h | 0.0000 | 0.0000 |
| Coefficient c | | 0.0000 |
| Height of fictive bottom h_fo | | 0.0000 |
| Parameter b | | 0.0000 |
| Nominal average diameter of pitching D_n50 | | 0.0000 |
| Upgrade factor Psi_u | | 0.0000 |
| Stability parameter Phi_sw | | 0.0000 |

| | | |
|---|---|---|
| Error in bottom determination Delta_d | 0.0000 | 0.0000 |
| Error in local water level Delta_hlok | 0.0000 | 0.0000 |
| Error in wave direction beta* | 0.0084 | 0.0001 |
| Storm duration t_s | -0.2811 | 0.0790 |
| Dune height h_d | | 0.0000 |
| Model factor m_D | | 0.0000 |
| Median grain size diameter d_m | | 0.0000 |
| **Sum** | **0.8454** | **0.3413** |

*Table C-3: Sensitivity coefficients dike ring 36: Land van Heusden / De Maaskant*

| Variable # | Description | alfa | alfa^2 |
|---|---|---|---|
| 1 | Dike height h_d | 0.00200 | 0.00000 |
| 2 | Berm height h_B | 0.00000 | 0.00000 |
| 3 | Berm width B | 0.00000 | 0.00000 |
| 4 | Toe height h_t | 0.00000 | 0.00000 |
| 5 | Slope outer slope (top) | 0.00000 | 0.00000 |
| 6 | Slope outer slope (bottom) | 0.00000 | 0.00000 |
| 7 | Slope outer slope | 0.00000 | 0.00000 |
| 8 | Model factor critical overflow discharge m_qc | 0.00000 | 0.00000 |
| 9 | Roughness inner slope k | 0.00000 | 0.00000 |
| 10 | Factor for determination Q_b f_b | 0.00000 | 0.00000 |
| 11 | Factor for determination Q_n f_n | 0.00000 | 0.00000 |
| 12 | Model factor occuring overflow discharge m_qo | -0.00100 | 0.00000 |
| 13 | Error in position bottom | 0.00400 | 0.00002 |
| 14 | Model factor Bretschneider for Hs | -0.02700 | 0.00073 |
| 15 | Model factor Bretschneider for Ts | 0.00000 | 0.00000 |
| 16 | Error in local water level | -0.06100 | 0.00372 |
| 17 | Storm duration t_s | -0.01100 | 0.00012 |
| 18 | Water level Maasmond | -0.01000 | 0.00010 |
| 19 | Discharge Lobith* | -0.90600 | 0.82084 |
| 20 | Discharge Lith* | -0.25100 | 0.06300 |
| 21 | Wind speed Schiphol/Deelen | -0.02100 | 0.00044 |
| 22 | (null) | -0.16100 | 0.02592 |
| 23 | Prediction error water level MK | -0.00700 | 0.00005 |
| 24 | Thickness covering layer d | 0.02800 | 0.00078 |
| 25 | Thickness sand layer D | -0.01100 | 0.00012 |
| 26 | Length leakage length L | 0.06600 | 0.00436 |
| 27 | Rolling friction angle theta | 0.05300 | 0.00281 |
| 28 | Factor C_Bear | 0.00000 | 0.00000 |
| 29 | Grain size d_70 | 0.11000 | 0.01210 |
| 30 | Uniformity d_70/d_10 | 0.00000 | 0.00000 |

| | | | |
|---|---|---|---|
| 31 | Constant van White | 0.19200 | 0.03686 |
| 32 | Apparent Relative volumetric mass soil | 0.00200 | 0.00000 |
| 33 | Relative volumetric weight sand | 0.02100 | 0.00044 |
| 34 | Model factor uplift | 0.00500 | 0.00003 |
| 35 | Model factor piping | 0.11400 | 0.01300 |
| 36 | Model factor damping | -0.00500 | 0.00003 |
| 37 | Specific permeability | -0.11000 | 0.01210 |
| 38 | Inner water level h_b | 0.03800 | 0.00144 |
| 39 | Root depth grass d_w | 0.01000 | 0.00010 |
| 40 | Width covering layer of clay L_K | 0.00000 | 0.00000 |
| 41 | Width dike core on crest height L_BK | 0.00000 | 0.00000 |
| 42 | Tangent alfa_u | 0.00000 | 0.00000 |
| 43 | Coefficient grass c_g | 0.00500 | 0.00003 |
| 44 | Coefficient erosion covering layer c_rk | 0.00000 | 0.00000 |
| 45 | Angle in reduction factor r | 0.00000 | 0.00000 |
| 46 | Acceleration erosion process alfa_z | 0.00000 | 0.00000 |
| 47 | Damping factor alfa_h | 0.00000 | 0.00000 |
| 48 | Unavailable wave direction | 0.00100 | 0.00000 |
| | **Sum** | **-0.93100** | **0.99914** |

* Dike ring 36 is not threatened by the river Rhine (which is measured in Lobith), but due to the structure of the load models in PC-Ring, the discharge (of the Rhine) in Lobith plays a fictive role. In fact the squared alfa value for the river Meuse should be $\alpha^2_{Meuse} = \alpha^2_{Lith} + \alpha^2_{Lobith}$ .

# V. Appendix 5: User manual reliability tool

## APPENDIX V-1: INSTALLATION GUIDE

### Software Installation procedure

These steps describe the procedure for installing the software - Steps 0 (if needed) and (3) will require local administrator rights for your PC. If you do not have such rights, you must ask somebody who does have these rights to perform the step(s).

(1) Create a folder on your hard-disk and copy the files from the ReliabiltyCalculator.zip file supplied. See Table 3 - Reliability Calculator files below for a list of the files.

The remainder of this document uses RelCalcFolder to refer to the path name of the folder which you have created here.

(2) If .NET Framework has not been installed already on your PC, install it now. To check, run Control Panel and choose Add or Remove Programs. If you see Microsoft .NET Framework 2.0, all is well. (You may have versions other than 2.0 but you must also have 2.0).

If not, you may download the package from http://www.microsoft.com/downloads/details.aspx?FamilyID=0856eacb-4362-4b0d-8edd-aab15c5e04f5&DisplayLang=en. You must then install it. This may require administrator rights. If you see .NET Framework 3.0 or 3.5, then you must also take an additional step – see (5).

(3) Locate the file regasm.exe on your PC. Start with your Windows folder (e.g. C:\Windows) and look in the subfolder Microsoft.NET\Framework\v2.0.50727.

(4) Start a Command Prompt window and run the following command. *C:\windows\Microsoft.NET\Framework\v2.0.50727\regasm /codebase RelCalcFolder\RelCalc.dll* Replace C:\windows\Microsoft.NET\Framework\v2.0.50727 with the path where you found regasm.exe.

(5) Skip this step unless you detected .NET Framework 3.0 or 3.5 at step 0 – (this step needs administrator permissions). Locate the folder containing EXCEL.EXE (maybe C:\Program Files\Microsoft Office\OFFICE11). Copy the file Excel.exe.config from RelCalcFolder to this folder. This file ensures that .NET objects used by Excel Visual Basic use .NET Framework 2.0. If there is an existing Excel.exe.config file, please seek advice before replacing it.

(6) Edit the file RelCalcFolder\Structure.csv with a Text editor such as Notepad or TextPad.. Replace the string d:\work\Reliability with the path for your RelCalcFolder and save the file.

(7) Start Microsoft Excel and open the file ReliabilityCalc.xls in RelCalcFolder. You can expect to see some error messages until you carry out the following.

*The following instructions are valid for Excel 2003. There should be corresponding features in other Excel versions.*

To ensure that you can run Visual Basic Macros, choose Tools / Options / Security /Macro Security… Select Medium (or Low, but this is not recommended). Now choose Tools / Macro / Visual Basic Editor. In the Project Explorer window, click on the line VBAProject (ReliabilityCalc.xls) or any of the Microsoft Excel Objects below. From the Tools menu on the Visual Basic Editor window, choose References. Click Browse… , find your RelCalcFolder , choose RelCalc.tlb and click Open. You should now see RelCalc with a tick under Available References. From the File menu, choose Close and return to Microsoft Excel. *S*ave the spreadsheet and your Reliability Calculator is available for use.

| Name | Description |
|---|---|
| **UserGuide.doc** | This document. |
| **ReliabilityCalc.xls** | EXCEL spreadsheet which forms the user interface. |
| **RelCalc.dll** | Reliability Calculator 'engine' used by the Reliability Calculator spreadsheet. |
| **RelCalc.dll** | Type library which defines the COM interface provided by |
| **LSESupport.dll** | DLL which includes the IndexOf function used by the LSE functions. |
| **LSESupport.lib** | Library file used when building the LSE function DLL. |
| **Task7_LSEs.dll** | DLL built using latest release of LSE functions from TU Delft. |
| | Also includes interim dummy LSE functions for Bb1.3a and Bb1.3b for use with the current Sheet Pile Wall fault tree. These interim functions always return zero i.e. 'no fail'. |
| **StatFunc.dll** | A DLL containing functions for generating random numbers according to specified distributions. |
| **FailureMode.csv** | A CSV file defining the Failure Modes and their supporting LSE functions. |

| | |
|---|---|
| **FailureModeParam.csv** | A CSV file defining the Parameter values required by the LSE for each Failure Mode. |
| **Parameter.csv** | A CSV file defining the names of all the current Parameters. |
| **Structure.csv** | A CSV file defining each structure and its associated Fault Tree file. |
| **FailureMode.ped** | A 'Primary Events database' for use with OpenFTA when defining further fault trees. |
| **SheetPileWall.fta** | A Fault Tree file for a Sheet Pile Wall structure. |
| **Excel.exe.config** | EXCEL configuration file required for PCs with .NET Framework 3.0 or later. |

**Table 4 - Reliability Calculator files**

## APPENDIX V-2: EXAMPLE LSE FROM FLOODSITE (TASK 4)

### Ba1.5aiii Uplifting of impermeable layers behind earth embankment

**Summary**: Uplifting behind embankments occurs if the difference between the local water level h, and the water level "inside", $h_b$ is larger than the critical water level $h_c$

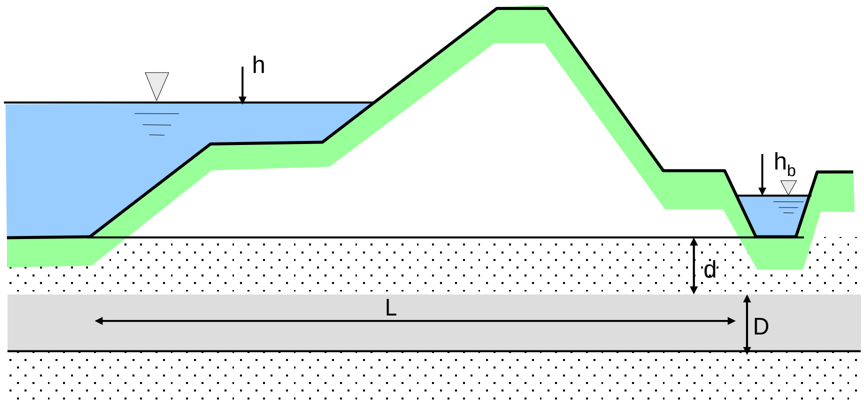


**Reliability equation:**

The reliability function is expressed by:

$$z = m_0 \cdot h_c - m_h \cdot \Delta h$$

where:

| | | |
|---|---|---|
| $h_c$ | = | critical water level [m] |
| $\Delta h$ | = | difference between local water depth in front of dike and water level in the floodplain [m] |
| $m_o$ | = | model uncertainty factor [-] |
| $m_h$ | = | model uncertainty factor for damping[-] |

**Loading equations:**

$$\Delta h = h - h_b$$

**Resistance (strength) equations:**

$$h_c = \frac{\gamma_{wet} - \gamma_w}{\gamma_w} d$$

**Parameter definitions:**

| | | |
|---|---|---|
| $\gamma_{wet}$ | = | saturated volumetric weight of the impermeable soil layers |
| $\gamma_w$ | = | volumetric weight of the water |
| d | = | thickness of the impermeable layers |
| h | = | water level on the river [m] |
| $h_b$ | = | water level in the floodplain [m] |

**Sources of failure mechanism equations / methods:**

| |
|---|
| Vrouwenvelder et al. (2001) |
| **Sources of uncertainties in failure equations / input parameters:**<br><br>Vrouwenvelder et al. (2001) |
| **Remarks:** |

# APPENDIX V-3: EXTENDING THE CALCULATOR

The key point about the Extensibility of the Calculator is that it is driven by the content of the four files defined in the Framework document - Parameter.csv, FailureMode.csv, FailureModeParam.csv, Structure.csv. These files must be in the same folder as the file ReliabilityCalc.xls.

These are simple CSV files and code has been supplied to TU Delft to enable them to generate the files from their internal spreadsheets.

They can also be edited using simple text editors such as Notepad.

However, a worksheet is also included for each file to enable you to edit the files within the Reliability Calculator.

Each sheet shows the values from the file and has a Load button and a Save button.

You need to be aware that the values in the sheets do not necessarily reflect those in the file (the file may have been edited outside the spreadsheet or the user didn't click Save having made some changes).

So, before you do any work on one of these sheets, click Load. This will load the values from the file into the sheet.

When you have made some changes, click Save. This will save the changes to the .csv file. When you next move to the Calculate sheet, click Reset to tell the Calculator to use the changed files.

Any additional advice for specific files is given in the following sub-sections.

### Structure

Initially, only one example structure (SheetPileWall) will be available from the structure drop down list in the Calculate sheet. To add additional specific structure fault trees to the calculator, the name of the structure and the name and location of the fault tree text file (.fta file) must be entered as a list in the Structure File sheet of the Reliability Calculator. When the Save button is clicked, this information is saved to the Structure.csv file.

### Failure Mode

If you add a Failure Mode to FailureMode.csv, you must also add one of the same name to the OpenFTA Event Database FailureMode.ped. This will allow the Failure Mode to be used in any fault Trees that you develop.

If you want to use the Failure Mode as a conditioning event, create a second Failure Mode with the same name but followed by a question mark. Again, this Failure Mode should be added to both FailureMode.csv and FailureMode.ped.

**Failure Mode Parameters**

Use the sheet labelled Fm_Parameters.

You will need to update this sheet (and save the file) if there is any change to the parameters used by an LSE function. Otherwise you may not be able to supply values for the parameter.

# APPENDIX V-4: PARAMETER DESCRIPTION AND LSE MAPPING

| Parameter | Unique fortran name | Description | Unit | LSE mapping | Example distribution | Distribution parameter 1 (Variation coefficient) | Distribution parameter 2 (Standard Deviation) | Distribution parameter 3 (name) |
|---|---|---|---|---|---|---|---|---|
| a | PierSlope | Slope of the pier from the downstream horizontal < 75° | ° | Da4.2a | | | | |
| A | Area | Area | m² | Cb1.2a | | | | |
| A | VariousEmpiricalCoeff | Coefficient used in various empirical formulae | - | Bc3.1a | | | | |
| A | LarsonCoeffA | Empirical factor according to Larson et al. 2004, A = 1.34.10-2 | - | Aa2.1b, Ba2.1bii, Ba2.1biii | | | | |
| A | IceCrushingArea | Area of ice crushing | m² | Da4.2b | | | | |
| Ac | CanalArea | Area of canal's cross section | m² | Bc2.1b, Bc2.1d, Ba3.1 | | | | |
| Ae | RockErosionArea | Erosion area on rock profile | m² | Ab2.1b,Bc2.1c,Ba2.4c | | | | |
| as | FlowDir | Flow direction | ° | Ba1.4, Bb1.4 | | | | |
| As | ShipArea | Area of ship's cross section | m² | Bc2.1b, Bc2.1d | | | | |
| l | ApronW | Width of apron | m | Bc3.1a | | | | |
| b | LarsonCoeffB | Empirical factor according to Larson et al. 2004, b = 3.19.10-4 | - | Aa2.1b, Ba2.1bii, Ba2.1biii | | | | |
| b | LocGeometryRatio | Ratio of local geometry b = 0 for head-on impact | - | Da4.2b | | | | |

| Parameter | Unique fortran name | Description | Unit | LSE mapping | Example distribution | Distribution parameter 1 (Variation coefficient) | Distribution parameter 2 (Standard Deviation) | Distribution parameter 3 (name) |
|---|---|---|---|---|---|---|---|---|
| b | SegmentWidth | Width of segment, element or slice | m | Bc2.3b | | | | |
| B | ChannelWidth | Channel width | m | Bc2.1b, Bc2.1d | | | | |
| B | CrestWidth | Crest width | m | Aa2.1b,Aa2.4,Ba2.4i, Ba2.4c,Ba2.4d,Ba2.5, Ba1.5bii, Ba1.1, Ba1.5bii, Ba2.1bii, Ba2.1bii | lognormal [1] | | 0.20 | |
| BB | BermWidth | Berm width | m | Ca2.1b, Aa2.4, Ba1.1<br>Ba1.5bii,Ba1.5dii, Ba2.5 | normal | | 0.15 | |
| Bw | StrucWidthToeLevel | Structure width, often at toe level | m | Ba1.6, Da2.5 | | | | |
| C | AMassCoeff | Added mass coefficient | - | Da4.3 | | | | |
| C | Chezy | Chezy coefficient | $m^{1/2}/s$ | Ba2.4b, Bc3.1c | | | | |
| C | WaveProp | Propagation celerity of waves | m/s | Aa2.4, Ba1.1, Ba1.5bii<br>Ba1.5dii, Ba2.5 | | | | |
| C, c' | DrainedSoilCohesion | Drained cohesion of soil | N/ m² | Ba1.4 | normal [2b]<br>lognormal [1]<br>lognormal [2c] | 0.2 | 0.5 | 0.3 |

| Parameter | Unique fortran name | Description | Unit | LSE mapping | Example distribution | Distribution parameter 1 (Variation coefficient) | Distribution parameter 2 (Standard Deviation) | Distribution parameter 3 (name) |
|---|---|---|---|---|---|---|---|---|
| cE | GrassQual | Grass quality after Verheij et al., 1998 | $m.s^{-1}$ | Ba2.1a, Ba2.1biii | | | | |
| Cf | SBedFri | Friction of sand bed | - | Aa2.4, Ba2.4d | | | | |
| Ck | CreepCoeff | Creep coefficient | - | Ba1.5aii, Cc1.5, Ba1.5bii, Ba1.5dii | normal [1] | | 0.1 | |
| cRK | CRK | Factor representing the erosion sensitivity of the clay cover | - | Ba2.1b, Bc2.1h | lognormal [1] | | | 0.3 |
| cT | TurbCoeff | turbulence coefficient | - | Bc3.1b, Bc3.1d | | | | |
| cV | DissCoeff | Dissipation coefficient | - | Aa1.1, Ba1.1, Ba2.5 | | | | |
| cw | CW | Cohesion due to root penetration | kPa | Ba2.3 | | | | |
| d | FriCoeff | Friction coefficient | - | Cc1.2aii | | | | |
| d | PileDia | Diameter of the pile | m | Da4.2c | | | | |
| d | Depth | Depth | m | Ba2.4b | normal | | 0.1 | |
| d | LayerThick | Thickness of certain layer, element | m | Ba1.5d,Bc2.1d,Bc2.1k Bc2.3a, Bc2.3b | lognormal [1] | | | 0.3 |
| D' | BaskThick | Basket or mattress thickness | m | Bc2.1m | | | | |
| D50 | D50 | Sieve diameter, diameter of stone which exceeds the 50% value of | m | Ba1.5c, Aa2.1b Ab2.1a, Ba2.1bii, | lognormal | | | |

| Parameter | Unique fortran name | Description | Unit | LSE mapping | Example distribution | Distribution parameter 1 (Variation coefficient) | Distribution parameter 2 (Standard Deviation) | Distribution parameter 3 (name) |
|---|---|---|---|---|---|---|---|---|
| | | sieve curve | | Ba2.1biii | | | | 0.5 |
| d70 | D70 | 70%-pass grain diameter | m | Ba1.5ai | lognormal [1] | | | 0.15 |
| D85 | D85 | 85% value of sieve curve | m | Ba1.5c | | | | |
| Df15 | Df15 | 15% non-exceedance diameter of filter layer from grading curve, indicating permeability of the filter | m | Ba1.5c | lognormal [1] | 0.02 | | 0.1 |
| dk | Dk | Thickness of remaining clay layer | m | Bc1.1, Ba2.1a, Ba2.1b, Bc2.1h | | | | |
| dgen | Dgen | General erosion, long term degradation of the bed level | | | | | | |
| Dn15 | Dn15 | Nominal mean diameter, Dn50= M15/rr1/3 | m | Bc1.5 | normal [3] | | | 0.25 |
| Dn50 | Dn50 | Nominal mean diameter, Dn50= M50/rr1/3 | m | Bc1.5, Aa2.4, Ab2.1b, Ba1.1, Ba1.5bii, Ba1.5dii, Ba2.4c, Ba2.4iii,Ba2.5,Bc2.1a, Bc2.1c,Bc2.1g,Bc2.1m Bc3.1b, Bc3.1c, | normal | | | |

| Parameter | Unique fortran name | Description | Unit | LSE mapping | Example distribution | Distribution parameter 1 (Variation coefficient) | Distribution parameter 2 (Standard Deviation) | Distribution parameter 3 (name) |
|---|---|---|---|---|---|---|---|---|
| | | | | Bc3.1d, Ca2.1b | | | | 0.05 |
| do | D0 | The water level in front of or at upstream of the dyke | m | Bc1.1 | | | | |
| dr | GapDepth | Depth of gap | m | Ba2.3 | | | | |
| dw | GrassRootsDepth | Depth of the grass roots | m | Ba2.3 | lognormal [1] | | | 0.2 |
| dw | DuneWidth | Width of the dune | m | Aa2.1a | | | | |
| DWT | DWT | Dead-weight tonnage of the vessel | t | Da4.1 | | | | |
| d_zs | Dzs | Depth of slope affected by flow | | Ba1.4, Bb1.4 | | | | |
| e'bu | ConcStrain | Ultimate strain of the concrete | - | Cc1.2c, Cc2.2b | | | | |
| e'pl | ConcPlast | Plasticity strain of the concrete | - | Cc1.2c, Cc2.2b | | | | |
| es | Es | Fraction of air pore | - | Ba1.5dii | | | | |
| f | StabCoeff | Stability coefficient, general, mainly dependent on structure type, tanα and friction | - | Bc2.1d, Bc2.1m | | | | |
| f'b | ConcreteStrength | Cubic pressure strength of the concrete | kN/m² | Cc1.2c, Cc1.2d Cc2.2b, Ca2.3 | lognormal[2d] | | | 0.15 |
| f2 | DecCoeff | Coefficient for deceleration of | - | Aa2.4, Ba2.4d | | | | |

| Parameter | Unique fortran name | Description | Unit | LSE mapping | Example distribution | Distribution parameter 1 (Variation coefficient) | Distribution parameter 2 (Standard Deviation) | Distribution parameter 3 (name) |
|---|---|---|---|---|---|---|---|---|
| | | erosion process | | Ba1.5bii, Ba1.5dii | | | | |
| fA | Fa | Factor for mean force due to wave impact | - | Ba2.3 | | | | |
| fb | ConcTensStrength | Cubic tensile strength of the concrete | kN/m² | Cc1.2d | lognormal[2d] | | | 0.2 |
| fc | CurFriFact | Friction factor for current | - | Ba2.4i | | | | |
| fg | GrassRevQ | Quality factor for grass revetment | - | Aa1.1, Ba1.1, Ba2.4i | normal | | | 0.2 |
| fG | SoilMassF | Factor for force due to mass of soil | - | Ba2.3 | | | | |
| fp | Fp | 'Peak' frequency of wave spectrum | s-1 | Ba2.3 | | | | |
| fpmax | Fpmax | Factor for pmax | - | Ba2.3 | | | | |
| fs | YieldStress | Yield stress of the steel, net of any factoring | kN/m² | Cb1.2a,Cb1.2c Cc1.2c, Cc2.2b, Ca2.3 | lognormal[2d] | | | 0.1 |
| g | Grav | Gravitational acceleration, 9.81 m/s2 | m/s² | Aa1.1, Ba1.1, Bc1.1 Cc1.2aii, Cc1.2b Cc1.2c,Aa2.1b,Ab2.1a | deterministic | | | |

| Parameter | Unique fortran name | Description | Unit | LSE mapping | Example distribution | Distribution parameter 1 (Variation coefficient) | Distribution parameter 2 (Standard Deviation) | Distribution parameter 3 (name) |
|---|---|---|---|---|---|---|---|---|
| | | | | Ab2.1b,Bc2.1c,Bc2.1d Bc2.1h, Bc2.1m, Ca2.2a,Cc2.2a,Cc2.2b, Ba2.3,Bc2.3b,Ca2.3, Aa2.4,Ba2.4i,Ba2.4iii, Ba2.4b,Ba2.4c,Ba2.4d, Ba2.5, Da2.5, Bc3.1b, Bc3.1c,Bc3.1d,Ba2.1a, Ba2.1b,Bc2.1a | | | | |
| g | RedFG | Reduction factor; g = gf gb , taking into account the effects of oblique wave attack. | - | Ba2.4iii Ba2.4c | | | | |
| gd | SoilDryWeight | Volumetric weight of the dry soil | kN/m3 | Cb1.2a,Cb1.2c,Cb1.2d Cc1.2aii,Cc1.2b | normal | | | 0.05 |
| gf | SlopeRough | Roughness of the seaward slope | - | Ba2.4iii, Ba2.4c | lognormal [1] | | | 0.25 |
| gf-c | Gfc | Roughness at the crest | - | Ba2.4iii,Ba2.4c | | | | |
| gfg | GammaFg | Unit weight of the fine grained natural soil beneath the embankment saturated | kg/m3 | Bb1.2 | normal | | 0.2 | |
| gG | Gg | Velocity coefficient | - | Ba2.1a, Ba2.1biii | | | | |

| Parameter | Unique fortran name | Description | Unit | LSE mapping | Example distribution | Distribution parameter 1 (Variation coefficient) | Distribution parameter 2 (Standard Deviation) | Distribution parameter 3 (name) |
|---|---|---|---|---|---|---|---|---|
| gs | GammaS | Volumetric weight of saturated soil | kN/m3 | Cb1.2a,Cb1.2c,Cb1.2d<br>Cc1.2aii,Cc1.2b, Cc1.2d,Ba1.5aiii<br>Bc2.3b,Ba2.4b | normal | | 0.2 | |
| gsat | GammaSat | Unit weight of the saturated part of the embankment | kg/m3 | Bb1.2 | normal | | 0.2 | |
| gunsat | GammaUnsat | Unit weight of the unsaturated part of the embankment | kg/m3 | Bb1.2 | normal | | 0.2 | |
| gw | GwaterL | Groundwater level | m | Cb1.2a,Cb1.2c,Cb1.2d<br>Cc1.2aii, Cc1.2b<br>Ba1.5aii, Cc1.5 | normal | | 0.1 | |
| gw | GammaW | Volumetric weight of water | kN/m3 | Bb1.2,Cb1.2a,Cb1.2c<br>Cb1.2d,Cc1.2aii,<br>Cc1.2b,Cc1.2d,Ba2.4b<br>Ba1.5aiii, Ba2.3 | normal [1] | | 0.1 | |
| Dimp | Dimp | thickness impermeable layers | | Ba1.5aiii | lognormal [1]<br>normal [2b] | | 0.3<br>0.2 | |
| h | Height | Height of a element, segment | m | Cc1.2c,Cc2.2a,Cc2.2b | | | | |

| Parameter | Unique fortran name | Description | Unit | LSE mapping | Example distribution | Distribution parameter 1 (Variation coefficient) | Distribution parameter 2 (Standard Deviation) | Distribution parameter 3 (name) |
|---|---|---|---|---|---|---|---|---|
| h | IceThick | Ice thickness | m | Da4.2a, Da4.2c | | | | |
| h | WaterL | River water level | m | Aa1.1, Aa2.1a, Aa2.4<br>Ab2.1a, Ab2.1b, Ba1.1<br>Ba1.5ai, Ba1.5aii<br>Ba1.5aiii, Ba1.5b<br>Ba1.5bii, Ba1.5dii<br>Ba1.6, Ba2.1a, Ba2.1b<br>Ba2.1bii, Ba2.1biii<br>Ba2.3, Ba2.4b,Ba2.4c<br>Ba2.4i, Ba2.4iii, Ba2.5<br>Bc2.1a, Bc2.1b,Bc2.1c<br>Bc2.1g,Bc2.1h, Bc2.1j<br>Bc2.1m,Bc2.3a,Bc2.3b<br>Ca2.1a,Ca2.2a, Ca2.2b<br>Ca2.3, Cb1.2a, Cb1.2c<br>Cb1.2d,Cc1.2aii,Da2.5<br>Cc1.2b,Cc1.2c, Cc1.2d | deterministic | | | |

| Parameter | Unique fortran name | Description | Unit | LSE mapping | Example distribution | Distribution parameter 1 (Variation coefficient) | Distribution parameter 2 (Standard Deviation) | Distribution parameter 3 (name) |
|---|---|---|---|---|---|---|---|---|
| | | | | Cc1.5, Cc2.2a, Cc2.2b | | | | |
| h | WaterD | Water depth | m | Aa2.4, Ba1.1, Ba1.5bii<br>Ba2.5, Bc2.1a, Bc2.1b<br>Bc2.1d, Bc3.1a, Ca2.1b, Ca2.2b | lognormal | | | 0.15 |
| H | IncRWaveH | Incident regular wave height | m | Ca2.1a | | | | |
| h´ | WDToe | Water depth at the toe including the coverlayer | m | Aa2.1b,Aa2.4, Ba1.5bii, Ba1.5dii Ba2.1bii, Ba2.1biii Ba2.4d, Bb1.2, Ca2.1b Ca2.2a, Ca2.2b | | | | |
| hb | Hb | Water level in the floodplain / dike ring | m | Ba1.5aiii, Ca2.2a,<br>Ca2.2b, Ba1.5ai | normal [1] | | 0.1 | |
| hc | Hc | Water depth above structure crest | m | Bc1.1 | | | | |
| $h_{crest}$ | | | m | Ba2.1bii, Ba2.1biii<br>Ba2.4b,Ba2.4c, Ba2.4i<br>Ba2.4iii, Ba2.5, Ca2.3<br>Cb1.2c, Cc1.2aii<br>Cc1.2b, Cc1.2c,Cc1.2d | normal [1] | | 0.1 | |

| Parameter | Unique fortran name | Description | Unit | LSE mapping | Example distribution | Distribution parameter 1 (Variation coefficient) | Distribution parameter 2 (Standard Deviation) | Distribution parameter 3 (name) |
|---|---|---|---|---|---|---|---|---|
| | Hcrest | Crest height above SWL | | Cc2.2a, Cc2.2b, Da2.5 | | | | |
| hf0 | Hf0 | | 0 | Bc2.1j, Bc2.3a | normal [1] | | 0.1 | |
| hgp | Hgp | Crest height of the dune which respects to SWL | m | Aa2.1a | | | | |
| Hm0 | Hm0 | Significant wave height calculated from the spectrum, Hmo=4√mo | m | Ca2.1a | | | | |
| hs | HMobSoil | Height of the mobilised soil | m | Cc1.2aii,Cc1.2b | | | | |
| Hs | WaveHeight | Significant wave height | m | Aa2.1a, Aa2.1b, Aa2.4 Ab2.1a, Ab2.1b, Ba1.1 Ba1.5bii, Ba1.5dii Ba2.1a,Ba2.1bii,Ba2.3 Ba2.1biii, Ba2.4b, Ba2.4c,Ba2.4d,Ba2.4i, Ba2.4iii,Ba2.5,Bc2.1a, Bc2.1b,Bc2.1c,Bc2.1g, Bc2.1h,Bc2.1m,Bc2.3b Bc3.1a,Ca2.1b,Ca2.2a, Ca2.2b, Ca2.3, Cc1.2c Cc2.2a, Cc2.2b, Da2.5 | | | | |

| Parameter | Unique fortran name | Description | Unit | LSE mapping | Example distribution | Distribution parameter 1 (Variation coefficient) | Distribution parameter 2 (Standard Deviation) | Distribution parameter 3 (name) |
|---|---|---|---|---|---|---|---|---|
| ht | DStrToe | Water depth at structure toe | m | Ba1.5b | | | | |
| hwlr | Hwlr | Allowable water level rise | m | Ba1.6,Da2.5 | | | | |
| i | HydG | hydraulic gradient | - | Ba1.4,Bb1.4,Bc3.1c | | | | |
| k | CollisionContact | Effective contact stiffness of the collision | kg/s2 | Da4.3 | | | | |
| k | Darcy | Permeability coefficient according to Darcy | m/s | Ba1.5ai | normal/lognormal<br>lognormal[2b]<br>lognormal[2b] | (clay)<br>(sand) | 1.0E-08<br>1.0E-05 | 0.2<br>1.6<br>0.5 |
| k | CorePerm | Permeability of core material | m/s | Ba1.5b | normal/lognormal | | | 0.2 |
| k | RouF | Roughness factor by Strickler | m | Aa1.1,Ba1.1 | normal<br>lognormal | 0.015 | | 0.1<br>0.25 |
| k* | EmpF | Empirical factor , e.g. k* = 1.0, see Schüttrumpf 2001 | - | Aa2.1b, Ba2.1bii, Ba2.1biii | | | | |
| Ka | ActGrainFCoeff | Coefficient for active horizontal grain force | - | Cb1.2a,Cb1.2c,Cb1.2d<br>Cc1.2aii,Cc1.2b, Cc1.2d | lognormal [4] | | | 0.1 |

| Parameter | Unique fortran name | Description | Unit | LSE mapping | Example distribution | Distribution parameter 1 (Variation coefficient) | Distribution parameter 2 (Standard Deviation) | Distribution parameter 3 (name) |
|---|---|---|---|---|---|---|---|---|
| kd, kf | KdKf | Coefficients for consideration of the crest width Bk, and sharpcrestedness of the weir Rk | - | Aa1.1, Ba1.1, Ba2.5 | | | | |
| kh | VelProF | velocity profile factor | - | Bc3.1b,Bc3.1d | | | | |
| Kp | PassGrainFCoeff | Coefficient for passive horizontal grain force | - | Cb1.2a,Cb1.2c,Cb1.2d Cc1.2aii, Cc1.2b, Cc1.2d | lognormal [4] | | | 0.1 |
| ksl | Ksl | Slope reduction factor for critical bed shear stress, ksl=kl.kd | - | Bc3.1b Bc3.1d | | | | |
| kt | Kt | Turbulence amplification factor for current velocity | - | Bc3.1b Bc3.1d | | | | |
| kλ | KLamda | Coefficients | - | Cc1.2d | | | | |
| kn | Kn | Coefficients | - | Cc1.2d | | | | |
| l | Hslid | Length of horizontal sliding surface beneath embankment | m | Bb1.2 | | | | |
| L | Espan | Effective span distance between the supports | m | Ca2.3 | | | | |
| L | Slab | Length of the concrete slab | m | Cc1.2c,Cc1.2d,Cc2.2b | | | | |

| Parameter | Unique fortran name | Description | Unit | LSE mapping | Example distribution | Distribution parameter 1 (Variation coefficient) | Distribution parameter 2 (Standard Deviation) | Distribution parameter 3 (name) |
|---|---|---|---|---|---|---|---|---|
| L1 | SPileLong | The level of the longest sheet pile cut off | m | Cc1.2aii, Cc1.2b | normal [1] | | 0.1 | |
| L1 | SPileToeLev | The toe level of the sheet pile | m | Cb1.2a,Cb1.2c,Cb1.2d | normal [1] | | 0.1 | |
| L3 | SPileShort | The level of the shortest sheet pile cut off | m | Cc1.2aii, Cc1.2b | normal [1] | | 0.1 | |
| LKh | HorSeepageLength | horizontal seepage length | m | Ba1.5ai,Ba1.5aii,Cc1.5 | normal [1] | | | 0.1 |
| LKv | Lkv | Vertical seepage length | m | Ba1.5aii, Cc1.5 | normal [1] | | | 0.1 |
| Ls | ShipL | Length of the ship | m | Bc2.1b,Bc2.1d | | | | |
| lt | Lt | Partial length of the dike at the inner toe | - | Aa2.4, Ba2.4d, Ba2.3, Ba1.5bii, Ba1.5dii | | | | |
| m | MOutS | Mean outer slope | - | Aa2.1b,Bc2.1b,Bc2.1j<br>Bc2.3, Ba2.4d, Bc2.3a, Ba2.1bii, Ba2.1biii | normal<br>normal [1] | | | 0.15<br>0.05 |
| m | TangF | Ratio of tangential force to normal force in the contact area | - | Da4.2b | | | | |
| M | MIceF | Mass of the ice feature | kg | Da4.2b | | | | |
| m0 | m0Flow | m0 coefficient | | Aa2.4, Ba2.4d, Ba1.5bii, Ba1.5dii | | | | |
| mf | Mf | Mass of the fluid displaced by | kg | Da4.3 | | | | |

| Parameter | Unique fortran name | Description | Unit | LSE mapping | Example distribution | Distribution parameter 1 (Variation coefficient) | Distribution parameter 2 (Standard Deviation) | Distribution parameter 3 (name) |
|---|---|---|---|---|---|---|---|---|
| | | the object | | | | | | |
| ml | Ml | Mass of the storm debris | kg | Da4.3 | | | | |
| n | MInSlope | Mean inner slope | 0 | Aa2.1b,Ba2.4i, Ba2.1bii, Ba2.1biii | normal | | | 0.05 |
| N | N | nf · D15f/D50b, where nf = porosity of filter material | - | Bc1.5 | | | | |
| N | NbWaveStorm | Number of waves over the duration Tr of a storm, record, or test, N=Tr/Tm | - | Ab2.1b, Bc2.1c, Ba2.4c | | | | |
| Nod | Nod | Number of displaced units per width Dn across armour face | - | Bc2.1a Ca2.1b | | | | |
| p | ICP | Effective ice crushing pressure | kN/m² | Da4.2a | | | | |
| p | P | Net uniformly distributed pressure acting on the member in the case of the front wall, p is the arithmetic sum of the applied wave loading and the internal cell pressure | Mpa | Ca2.3 | | | | |
| D | | Particle size, or typical dimension | | Aa2.4, Ba1.1, Ba2.5, Ba1.5bii, Ba1.5dii | | | | |

| Parameter | Unique fortran name | Description | Unit | LSE mapping | Example distribution | Distribution parameter 1 (Variation coefficient) | Distribution parameter 2 (Standard Deviation) | Distribution parameter 3 (name) |
|---|---|---|---|---|---|---|---|---|
| | PartSize | | | | | | | |
| p | Poro | Porosity | 0 | Aa2.4, Ba2.4d, Ba1.5bii, Ba1.5dii | deterministic | | | |
| P | Pparam | Permeability parameter 0.1<P<0.6 | - | Ab2.1b, Bc2.1c | | | | |
| q | MORate | Mean overtopping rate | l/s.m | Ba2.4d | | | | |
| Q | MeanOvertopDis | Mean overtopping discharge per metre run of crest | m3/s.m | Ba1.6, Da2.5 | | | | |
| qG | Qg | Grass quality (between 0 and 1) | - | Bc2.1b | normal | 0.2 | | |
| qM | Qm | Material quality 1,0 for Sand | - | Bc2.1b | | | | |
| r | R | Reduction factor for oblique wave attack | - | Bc2.1h | deterministic | | | |
| R | GraDis | Distance to the center of gravity from the point of impact | m | Da4.2b | | | | |
| R | HyRad | Hydraulic radius | m | Bc3.1c | | | | |
| Rg | Rg | Radius of gyration of the ice feaure about the vertical axis through its center of gravity | m | Da4.2b | | | | |
| rr | SteelArea | Area ratio of steel reinforcement | - | Ca2.3 | normal | 0.01 | | |

| Parameter | Unique fortran name | Description | Unit | LSE mapping | Example distribution | Distribution parameter 1 (Variation coefficient) | Distribution parameter 2 (Standard Deviation) | Distribution parameter 3 (name) |
|---|---|---|---|---|---|---|---|---|
| | | with respect to the concrete cross-sectional area D | | | | | | |
| Rw | Rw | A reduction factor, depending on on the slope angle | - | Bc2.1j , Bc2.3a | | | | |
| s | DiShip | Distance from the ship's sailing line | m | Bc2.1b, Bc2.1d | | | | |
| sB | CtrlVar | Control variable inner slope | - | Ba2.4i | | | | |
| Sd | Sd | Non-dimensional damage, $Sd=Ae/Dn50^2$ calculated from mean profiles or separately for each profile line, then averaged | - | Ab2.1b Bc2.1c | normal [6] | | 0.02 | |
| Su | Su | Undrained shear strength of the fine grained soil | $kN/m^2$ | Bb1.2 | normal | | 0.2 | |
| t | T | Period of constant loading | s | Ba1.6, Da2.5 | | | | |
| t0 | T0 | Start time of erosion if inner slope | h | Aa2.4, Ba2.4d, Ba1.5bii, Ba1.5dii | | | | |
| ta, tu, tf | TTT | Thickness of armour and underlayer or filter layer in direction normal face | m | Bc2.1k | | | | |
| tano | Tano | Slope of the initial dune profile | - | Aa2.1a | | | | |

| Parameter | Unique fortran name | Description | Unit | LSE mapping | Example distribution | Distribution parameter 1 (Variation coefficient) | Distribution parameter 2 (Standard Deviation) | Distribution parameter 3 (name) |
|---|---|---|---|---|---|---|---|---|
| | | simplified | | | | | | |
| tans | Tans | Slope of the initial dune profile simplified | - | Aa2.1a, Aa2.4, Ba1.1, Ba1.5bii, Ba1.5dii, Ba2.5 | | | | |
| tl | Tl | Toe level of initial dune profile | m | Aa2.1a, Ab2.1a, Ba3.1 | normal | | 0.2 | |
| Tm | Tm | Mean wave period | s | Aa2.4, Ba1.1<br>Ba1.5bii, Ba1.5dii<br>Ba2.4i, Ba2.5, Bc2.3b | | | | |
| Tm-1,0 | EneWPer | Spectral wave period, also called the energetic wave period | s | Aa2.1b, Aa2.4, Ba1.1, Ba1.5bii, Ba1.5dii, Ba1.2bii, Ba1.2biii, Ba2.4i, Ba2.4iii<br>Ba2.4b, Ba2.4d, Ba2.5 | | | | |
| Tp | WavePeriod | Spectral peak period, inverse of peak frequency | s | Aa2.1a,Aa2.1b,Ab2.1a Ab2.1b,Ba2.1a,Ba2.1b<br>Ba2.1bii, Ba2.1biii<br>Ba2.3, Ba2.4d, Bc2.1a<br>Bc2.1b,Bc2.1c, Bc2.1g<br>Bc2.1h,Bc2.1m,Ca2.1a | deterministic | | | |

| Parameter | Unique fortran name | Description | Unit | LSE mapping | Example distribution | Distribution parameter 1 (Variation coefficient) | Distribution parameter 2 (Standard Deviation) | Distribution parameter 3 (name) |
|---|---|---|---|---|---|---|---|---|
| | | | | Ca2.3, Cc1.2c, Cc2.2a Cc2.2b, Da2.5 | | | | |
| Tp | Tp | Spectral peak period, inverse of peak frequency | s | Ba2.4c | normal | | | 0.2 |
| Tr | Tr | Root tensile strength | $kN/m^3$ | Ba2.4b | | | | |
| TR | StormD | Duration of wave record, test or sea state | 0 | Aa1.1,Ba1.1,Ba1.5d, Ba1.5d,Aa2.1b,Ba2.1a Ba2.1b,Bc2.1b,Bc2.1h Aa2.4,Ba2.4i,Ba2.4d | lognormal [1] | | | 0.1 |
| u | VesVel | Vessel velocity | m/s | Da4.1 | | | | |
| U | HDMCV | Horizontal depth-mean current velocity | m/s | Bc3.1b, Bc3.1d | | | | |
| ub | Ub | Near bed velocity | m/s | Bc3.1b, Bc3.1d | | | | |
| ul | Ul | Velocity of the storm debris | m/s | Da4.3 | | | | |
| v | SFVel | Seepage flow velocity | m/s | Ba1.5d | | | | |
| v | IceVel | velocity of the ice feature | m/s | Da4.2b | | | | |
| V | Vol | Volume | $m^3$ | Da4.2b | | | | |
| vs | Vs | Ship’s speed | m/s | Bc2.1db, Bc2.1d | | | | |

| Parameter | Unique fortran name | Description | Unit | LSE mapping | Example distribution | Distribution parameter 1 (Variation coefficient) | Distribution parameter 2 (Standard Deviation) | Distribution parameter 3 (name) |
|---|---|---|---|---|---|---|---|---|
| w | SPartVel | Fall velocity of the sand particles. | m/s | Aa2.1a | | | | |
| w | ShingleBeachWidth | Width of shingle beach, determined as narrow / wide and condition grade | m | Ab2.1a | lognormal | | 0.5 | |
| W | WSuW | Water surface width | m | Ba3.1 | | | | |
| wa | Wa | Distance between two tie rods | m | Cb1.2a | | | | |
| $x_u$ | Xu | x- coordinate of leaking point at the inner berm | m | Ba1.5b, Ba1.5bii | | | | |
| xw | Xw | x- coordinate of intersection point of still water level and outer slope | m | Ba1.5b, Ba1.5bii | | | | |
| y | StructImp | 'importance-of-structure' factor >1: engineering judgement factor | - | Ba2.4iii | | | | |
| Y | Y | Eccentricity of the center of gravity from the point of impact | | Da4.2b | | | | |
| y | Eccent | Eccentricity ship in canal | m | Bc2.1b, Bc2.1d | | | | |
| Zo | Z0 | Initial, unscoured bed level adjacent to toe of protection | m | Ba3.1 | | | | |

| Parameter | Unique fortran name | Description | Unit | LSE mapping | Example distribution | Distribution parameter 1 (Variation coefficient) | Distribution parameter 2 (Standard Deviation) | Distribution parameter 3 (name) |
|---|---|---|---|---|---|---|---|---|
| α | TieRAng | Angle of inclination of the tie rod | ° | Cb1.2a | | | | |
| α | Sang | Angle of the slope | - | Ab2.1b, Ba2.1b | | | | |
| α, β | ABeta | Cofficients for determination of horizontal wave load | - | Cc1.2c,Cc2.2a,Cc2.2b Ca2.3 | | | | |
| αi | InsSlopeAng | Angle of the inner slope | º | Aa1.1,Ba1.1,Aa2.4 Ba2.4i,Ba2.4b,Ba2.4c Ba2.4d, Ba1.5bii, Ba1.5dii | normal [1] | | | 0.05 |
| αo | OutSlopeAng | Angle of the outer slope | º | Aa2.1b, Aa2.4, Ba1.1, Ba1.4, Ba2.3, Ba2.4c, Ba1.5bii, Ba1.5dii, Ba2.1bii, Ba2.1biii, Ba2.4d,Ba2.4i,Ba2.5, Ba2.4iii, Bb1.4, Bc1.4 Bc1.5,Bc2.1b, Bc2.1c, Bc2.1d,Bc2.1g,Bc2.1h Bc2.1m, Bc2.3b | normal [1] | | | 0.05 |
| β | WaveObliquity | Angle of wave attack with respect to the structure | ° | Aa2.1a, Aa2.1b, Aa2.4 Ab2.1a, Ab2.1b, Ba1.1 Ba1.5bii, Ba1.5dii | normal [1] | | | 15 |

| Parameter | Unique fortran name | Description | Unit | LSE mapping | Example distribution | Distribution parameter 1 (Variation coefficient) | Distribution parameter 2 (Standard Deviation) | Distribution parameter 3 (name) |
|---|---|---|---|---|---|---|---|---|
| | | | | Ba2.1a, Ba2.1b, Ba2.3<br>Ba2.1bii, Ba2.1biii<br>Ba2.4iii,Ba2.5, Bc2.1a<br>Bc2.1b, Bc2.1c,Bc2.1d<br>Bc2.1g,Bc2.1h,Bc2.1m<br>Bc2.3b, Ca2.1a,Ca2.1b<br>Ca2.2a, Ca2.2b, Ca2.3<br>Cc2.2a, Cc2.2b, Da2.5 | | | | |
| β1 | Beta1 | Internal friction angle of sand | ° | Aa2.4, Ba2.4d<br>Ba1.5bii, Ba1.5dii | | | | |
| Γf | RFSloR | Reduction factor for slope roughness wave run-up, wave overtopping | - | Ba2.4b | normal | | 0.1 | |
| γw | WaUWei | water unit weight | $kN/m^3$ | Ba1.4,Bb1.4,Bc1.4<br>Bc2.1j, Bc2.3a | normal [1] | | | 0.01 |
| Δ | BuDen | Relative buoyant density of material, i.e. for rock Δ=ρr/ρw – 1 | - | Aa2.4, Ab2.1b, Ba1.1, Ba1.5bii, Ba1.5dii,<br>Ba2.4iii, Ba2.4c, | lognormal [1] | | | 0.02 |

| Parameter | Unique fortran name | Description | Unit | LSE mapping | Example distribution | Distribution parameter 1 (Variation coefficient) | Distribution parameter 2 (Standard Deviation) | Distribution parameter 3 (name) |
|---|---|---|---|---|---|---|---|---|
| | | | | Bc2.1c, Ba2.4d,Bc2.1g | | | | |
| Δ | CoDen | Relative density of cover layer, Δ = (ρr-ρw)/ρw | - | Bc1.1,Bc2.1a,Bc2.1d Bc2.1m,Bc3.1b, Bc3.1c,Bc3.1d | lognormal [1] | | | 0.02 |
| ζ | ShipGeo | Coefficient of proportionality, representing the ship's geometry. | - | Bc2.1b Bc2.1d | | | | |
| η | WhiteConst | Drag force factor (Constante of White) | - | Ba1.5ai | lognormal [1] | | | 0.15 |
| θ | Rolling | Rolling resistance angle of sand grains | ° | Ba1.5ai | lognormal [1] | | 3 | |
| Θ | RootAng | Root angle of shear rotation | ° | Ba2.4b | | | | |
| Λ | LeaLen | Leakage length | m | Bc1.5 | | | | |
| λ1, λ2, λ3 | Lambda | Modification factors, depending on the geometry and the nature of the wall | - | Ca2.2a | | | | |
| μ | SlidF | Sliding factor | - | Ca2.2a,Ca2.2b, Cc2.2a | | | | |
| ρ | SandDensity | Density of the sand | $kg/ m^3$ | Ba1.5ai | normal [1] | | | 0.05 |
| ρ | Rho | Volumetric weight of the soil | $kN/ m^3$ | Ba1.4, Bb1.4 | normal [1] | | | 0.05 |

| Parameter | Unique fortran name | Description | Unit | LSE mapping | Example distribution | Distribution parameter 1 (Variation coefficient) | Distribution parameter 2 (Standard Deviation) | Distribution parameter 3 (name) |
|---|---|---|---|---|---|---|---|---|
| ρa | RhoA | Density of the revetment | $kg/m^3$ | Bc1.4, Bc2.1j, Bc2.3a | normal [1] | | | 0.05 |
| ρg | RhoG | Density of the subsoil | $kg/m^3$ | Bc1.4 | normal [1] | | | 0.05 |
| ρr, rc | ConcreteDensity | Mass density of rock / concrete | $kg/m^3$ | Cc1.2aii,Cc1.2b<br>Ca2.2a,Ca2.2b,Cc2.2a | normal [1] | | | 0.05 |
| ρt | RhoT | Density of the top layer | $kg/m^3$ | Bc2.1k | normal [1] | | | 0.05 |
| ρw | RhoW | Mass density of sea water | $kg/m^3$ | Ba1.5ai,Bc2.3a,Bc2.3b<br>Bc2.1k,Bc2.3d, Ca2.2a<br>Ca2.2b,Cc2.2a,Cc2.2b<br>Ca2.3, Cc1.2c | normal [1] | | | 0.05 |
| υ | Upsi | Kinematic viscosity | m²/s | Ba1.5ai | deterministic | | | |
| φ’ | IntFriction | Angle of internal friction | ° | Bc1.5 | lognormal<br>normal [1]<br>normal [2c]<br>normal [2a] | | <br>2<br><br> | 0.15<br><br>0.1<br>0.2 |
| tan(φ’) | tan(IntFriction) | | | Bc1.5 | lognormal [5] | | | 0.15 |
| φ’ | SoilAngleFriction | Effective soil angle of friction | ° | Ba1.4, Bb1.4, Bc1.4 | lognormal | | | |

| Parameter | Unique fortran name | Description | Unit | LSE mapping | Example distribution | Distribution parameter 1 (Variation coefficient) | Distribution parameter 2 (Standard Deviation) | Distribution parameter 3 (name) |
|---|---|---|---|---|---|---|---|---|
| | | | | Bc2.3a, Ba2.4b | | | | 0.15 |
| φb | PotHead | potential head induced in the filter or a gabion | m | Bc1.5 | | | | |
| ψcr | PsiCR | idem, critical value hydraulic stability | - | Bc3.1c | | | | |
| ψcr | ProElem | mobility parameter of protection element | - | Bc3.1b, Bc3.1d | | | | |
| d | TwoMat | Friction angle between two materials | - | Ba2.3 | lognormal | | 5 | |
| fsc | PhiSC | Stability correction factor for current-exposed stones | - | Bc3.1b, Bc3.1d | | | | |
| fsw | PhiSW | Stability correction factor for wave-exposed stones | - | Bc2.1g, Bc2.1m | | | | |
| fu | PhiU | Stability upgrading factor depending on system | - | Bc2.1g, Bc2.1m | | | | |
| Dn50;core | Dn50Core | Dn50 of the structure core in Van Gent et al. | m | Ab2.1b, Bc2.1c | | | | |
| c_geotextile | cGeotex | Coefficient in Bc1.5 in erosion of subsoil through revetment or geotextile | - | Bc1.5 | | | | |

| Parameter | Unique fortran name | Description | Unit | LSE mapping | Example distribution | Distribution parameter 1 (Variation coefficient) | Distribution parameter 2 (Standard Deviation) | Distribution parameter 3 (name) |
|---|---|---|---|---|---|---|---|---|
| k_si | Ksi | Breaker index in Bc2.1b erosion of revetment by shipwaves | - | Bc2.1b | | | | |
| Rc,rear | Rc_rear | crest freeboard relative to the water level at rear side of the crest | m | Ba2.4c | | | | |
| Ar/A | ARootRatio | Area root ratio in Ba2.4b, erosion clay inner slope by wave overtopping | - | Ba2.4b | | | | |
| u^/(g*delta* Dn50) | DimFlowU | Dimensionless flow velocity | - | Ba2.4iii | | | | |
| rc | RcBend | radius of curvature of bend | m | Ba3.1 | | | | |
| A_sat | ASat | Area of the saturated part of the embankment | m | Bb1.2 | | | | |
| A_unsat | AUnsat | Area of the unsaturated part of the embankment | $m^2$ | Bb1.2 | | | | |
| A_fg | AFg | Area of the fine grained soil underneath the embankment | $m^2$ | Bb1.2 | | | | |
| indicator drained/undr | DrainUndrain | choice for 0=drained or 1=undrained condition | | Bb1.2 | deterministic | | | |

| Parameter | Unique fortran name | Description | Unit | LSE mapping | Example distribution | Distribution parameter 1 (Variation coefficient) | Distribution parameter 2 (Standard Deviation) | Distribution parameter 3 (name) |
|---|---|---|---|---|---|---|---|---|
| ained | | | - | | | | | |
| Qadm | Qadm | Admissable wave overtopping rate | l/s.m | Ba2.5 | | | | |
| β | AngleShearGap | Angle of shear gap | rad or ° | Ba2.3 | | | | |
| fF | Ff | Coefficient | - | Ba2.3 | | | | |
| Cu,adm | CuAdm | Admissable cohesion in local clay failure due to wave impact | | Ba2.3 | | | | |
| beta_r | betaR | angle of wave obliquity for which reduction is taken into account | | Ba2.1b, Ba2.1bii, Ba2.1biii | | | | |
| v0 | Vel0 | flow velocity at the riverside crest of the embankment | | Ba1.6 | | | | |
| Cw | CoeffW | Coefficient | | Ba1.6 | | | | |
| CL | CoeffL | Coefficient | | Ba1.6 | | | | |
| CR | CoeffR | Coefficient | | Ba1.6 | | | | |
| Cm | CoeffM | Coefficient | | Ba1.6 | | | | |
| Cn | CoeffN | Coefficient | | Ba1.6 | | | | |
| kd | Kd_KdKf | Coefficient for the consideration | | Ba1.6 | | | | |

| Parameter | Unique fortran name | Description | Unit | LSE mapping | Example distribution | Distribution parameter 1 (Variation coefficient) | Distribution parameter 2 (Standard Deviation) | Distribution parameter 3 (name) |
|---|---|---|---|---|---|---|---|---|
| | | of the crest width Bk | | | | | | |
| kf | Kf_KdKf | Coefficient for the sharpcrestedness of the weir Rk | | Ba1.6 | | | | |
| KD | KdHudson | KD coefficient in Hudson's formula | - | Ab2.1b, Bc2.1c | normal [6]<br>normal [6] | 4<br>3.5 | 8<br>8 | breaking waves |
| d_zs | Depth1 | Depth of slope affected by flow | | Bc1.1 | | | | |
| d1 | FreeSubmerged | The water level at downstream of the dike | | Bc1.1 | deterministic | | | |
| Free / Submerged weir | Hvert | Switch to indicate a free or submerged weir | | Bc1.4 | | | | |
| H | Lhor | Water level difference between outside water level and level in embankment | m | Bc1.4 | | | | |
| l | PresSwitch | Horizontal distance between intersections between: 1) inside water level and revetment 2)outside water level and revetment | | Bc2.1j, Bc2.3a | | | | |

| **Parameter** | **Unique fortran name** | **Description** | **Unit** | **LSE mapping** | **Example distribution** | **Distribution parameter 1 (Variation coefficient)** | **Distribution parameter 2 (Standard Deviation)** | **Distribution parameter 3 (name)** |
|---|---|---|---|---|---|---|---|---|
| | | | m | | | | | |
| pressure switch | Hgws | Maximum uplift pressure lower than average outside water level (0), higher than average outside water level (1), or highest of the two (2) | | Bc2.1j, Bc2.3a | normal [1] | | 0.5 | |
| hGWS | FMGWS | Average water level | | Bc2.1j, Bc2.3a | lognormal [1] | 0.5 | | 0.13 |
| fMGWS | DeqReqHs | Factor to derive the design water level hMGWS | | Bc2.1k | | | | |
| Deq;req;Hs | StaticDynamic | Required equivalent thickness of top layer as a function of Hs | | Bc2.1m | | | | |
| switch | FCoeffFric | Static stability or dynamic stability limit state equation for Bc2.1m | | Bc2.3a | | | | |
| f | PilEscMay | coefficient for friction | | Bc3.1b, Bc3.1d | | | | |
| switch | NormIncRegIrreg | Choice for Pilarczyk / Escarameia and May models | | Ca2.1a | deterministic | | | |
| L | SmReq | incident regular wavelength | | Ca2.1a | | | | |
| switch | TopSill | Normally incident, nonbreaking, regular (0) or irregular (1) waves | | Aa2.4, Ba1.1<br>Ba1.5bii,Ba1.5dii, | | | | |

| Parameter | Unique fortran name | Description | Unit | LSE mapping | Example distribution | Distribution parameter 1 (Variation coefficient) | Distribution parameter 2 (Standard Deviation) | Distribution parameter 3 (name) |
|---|---|---|---|---|---|---|---|---|
| | | | | Ba2.5, Ca2.2a | | | | |
| Sm;req | HStruc | Required scour width | | Ca2.2a | | | | |
| d | Ts | Water depth above the top layer of the sill (Goda) | | Ca2.2a,Ca2.2b, Bc3.1a | | | | |
| KD | Kdiff | Diffraction coefficient | | Aa2.1a, Aa2.1b, Aa2.4 Ab2.1a,Ab2.1b, Ba1.1, Ba1.5bii, Ba1.5dii, Ba2.1a Ba2.1b, Ba2.3, Ba2.4biii, Bc2.1a, Ba2.5, Bc2.1b, Bc2.1c, Bc2.1g,Bc2.1h,Bc2.1m Bc2.3b,Ca2.1a,Ca2.1b, Ca2.2a, Ca2.2b, Ca2.3, Cc2.2a, Cc2.2b | | | | |
| θ0 | Theta0 | angle between wave crests and depth lines on deep water | | Aa1.1, Aa2.1b, Aa2.4 Ba1.1, Aa2.1a, Aa2.1b Ba1.5bii, Ba1.5dii, Aa2.4, Ab2.1a,Ab2.1b Ba1.1, Ba2.1a, Ba2.1b Ba1.5bii, Ba1.5dii, | | | | |

| Parameter | Unique fortran name | Description | Unit | LSE mapping | Example distribution | Distribution parameter 1 (Variation coefficient) | Distribution parameter 2 (Standard Deviation) | Distribution parameter 3 (name) |
|---|---|---|---|---|---|---|---|---|
| | | | | Ba2.1bii, Ba2.1biii,<br>Ba2.3, Ba2.4iii, Ba2.5, Bc2.1a,Bc2.1b,Bc2.1c, Bc2.1g,Bc2.1h,Bc2.1m Bc2.3b,Ca2.1a,Ca2.1b, Ca2.2aCa2.2b, Ca2.3, Cc2.2a Cc2.2b, Da2.5 | | | | |
| θ1 | Theta1 | angle between wave crests and depth lines on location of interest | | Aa1.1, Aa2.1b, Aa2.4<br>Ba1.1, Aa2.1a, Aa2.1b<br>Ba1.5bii, Ba1.5dii<br>Ab2.1a, Ab2.1b, Ba1.1<br>Ba1.5bii, Ba1.5dii, Ba2.1a, Ba2.1b, Ba2.1bii, Ba2.1biii<br>Ba2.3, Ba2.4iii, Ba2.5, Bc2.1a,Bc2.1b,Bc2.1c, Bc2.1g,Bc2.1h,Bc2.1m Bc2.3b,Ca2.1a,Ca2.1b, Ca2.2aCa2.2b, Ca2.3, Cc2.2a Cc2.2b, Da2.5 | | | | |
| hb | Hb5Hd | Water depth at 5Hd dinstance of | | Ca2.2a | | | | |

| Parameter | Unique fortran name | Description | Unit | LSE mapping | Example distribution | Distribution parameter 1 (Variation coefficient) | Distribution parameter 2 (Standard Deviation) | Distribution parameter 3 (name) |
|---|---|---|---|---|---|---|---|---|
| | | the wall | | | | | | |
| Bstruc | WidthFoun | Width of the foundation of the structure | | Ca2.2a,Ca2.2b, Cc2.2a Cc1.2aii, Cc1.2b | normal [2d] | | 0.004 | |
| $l_R$ | Lr | Effective width | m | Ba2.3 | | | | |
| V | VolStruc | Volume of the structure | | Ca2.2a, Ca2.2b,Cc2.2a | | | | |
| Tl | WallToe | Level of the foundation of the structure | | Aa2.4, Ab2.1b, Ba1.1 Ba1.5bii, Ba1.5dii Ba2.1a, Ba2.1b, Ba2.3 Ba2.1bii, Ba2.1biii Ba2.3, Ba2.4iii, Ba2.5 Bc2.1a,Bc2.1b,Bc2.1c Bc2.1g,Bc2.1h,Bc2.1j Bc2.1m,Bc2.3a, Bc2.3b,Ca2.1a,Ca2.2a, Ca2.2b,Ca2.3, Cc2.2a, Cc2.2b,Da2.5 | normal [1] | | 0.1 | |
| α | LongTAlp | coefficient which takes account of the long-term effects on the compressive strength and of the | | Ca2.3 | | | | |

| Parameter | Unique fortran name | Description | Unit | LSE mapping | Example distribution | Distribution parameter 1 (Variation coefficient) | Distribution parameter 2 (Standard Deviation) | Distribution parameter 3 (name) |
|---|---|---|---|---|---|---|---|---|
| | | unfavourable effects resulting from the way in which the load is applied | | | | | | |
| β | ABeta2 | Cofficient for determination of horizontal wave load, combined with ABeta | - | Cc2.1c, Ca2.3, Cc2.2a, Cc2.2b | | | | |
| As | ReinStArea | Area of reinforcement steel in concrete | | C.c1.2d, C.c2.2b | | | | |
| RedFuFh | RedFuFh | Reduction factor of the horizontal wave pressures Fh0.1% | | Cc2.2a | | | | |
| As | StorArea | Area of reinforcement steel in concrete | | Ba1.6, Da2.5 | | | | |
| A | AdmWOver | Storage area behind the structure | | Ba1.6, Da2.5 | deterministic | | | |
| switch;qadm | ABroadShort | Switch for admissable q (0) or h (1) | | Ba1.6 | deterministic | | | |
| switch,A | ResStreF | A for broad crest (0) or short crested weir (1) | | Da4.1 | | | | |
| Fr | PierWidth | Resulting overall strength against ship collision | | Da4.2a | | | | |

| Parameter | Unique fortran name | Description | Unit | LSE mapping | Example distribution | Distribution parameter 1 (Variation coefficient) | Distribution parameter 2 (Standard Deviation) | Distribution parameter 3 (name) |
|---|---|---|---|---|---|---|---|---|
| D | HeadEcc | The width of the pier under ice collision | | Da4.2b | deterministic | | | |
| switch;head/ eccentric | ResStrePier | Switch for head-on collission (0) or eccentric impact (1) | | Da4.2a | | | | |
| Fr | ResStreColl | Overall strength pier in ice accumulation circumstances | | Da4.2b | | | | |
| Fr | ResStreAttach | Overall strength structure in colliding ice circumstances | | Da4.2c | | | | |
| Fr | ResStreDebris | Overall strength structure in ice attachment circumstances | | Da4.3 | | | | |
| Fr | Ktheta | Overall strength structure in debris circumstances | | Cc1.2d | | | | |
| kθ | SectionMod | coefficient | | Cb1.2c | lognormal[2d] | | | 0.01 |
| z | OverPercen | Section modulus of sheet pile wall | | Aa1.1, Ba1.1, Ba2.4i | | | | |
| P | BreakSlope | Proportion of time overtopping during the storm duration | | Bc3.1a | deterministic | | | |
| D20f | D20f | 20% value of sieve curve filter | | Ba1.5c | | | | |
| D20b | D20b | 20% value of sieve curve base layer | | Ba1.5c | | | | |

| Parameter | Unique fortran name | Description | Unit | LSE mapping | Example distribution | Distribution parameter 1 (Variation coefficient) | Distribution parameter 2 (Standard Deviation) | Distribution parameter 3 (name) |
|---|---|---|---|---|---|---|---|---|
| c1 | FilterC1 | Filter coefficient c1 | | Ba1.5c | | | | |
| c2 | FilterC2 | Filter coefficient c2 | | Ba1.5c | | | | |
| g | Grading | Switch whether the material is uniformly (0) or wide graded (1) | | Ba1.5c | | | | |
| mR | MAA1_1R | Aa1.1 model uncertainty factor strength | | Aa1.1 | | | | |
| mS | MAA1_1S | Aa1.1 model uncertainty factor loading | | Aa1.1 | | | | |
| mR | MAA2_1AR | Aa2.1a model uncertainty factor strength | | Aa2.1a | | | | |
| mS | MAA2_1AS | Aa2.1a model uncertainty factor loading | | Aa2.1a | | | | |
| mR | MAA2_1BR | Aa2.1b model uncertainty factor strength | | Aa2.1b | | | | |
| mS | MAA2_1BS | Aa2.1b model uncertainty factor loading | | Aa2.1b | | | | |
| mR | MAA2_4R | Aa2.4 model uncertainty factor strength | | Aa2.4 | | | | |
| mS | MAA2_4S | Aa2.4 model uncertainty factor loading | | Aa2.4 | | | | |

| Parameter | Unique fortran name | Description | Unit | LSE mapping | Example distribution | Distribution parameter 1 (Variation coefficient) | Distribution parameter 2 (Standard Deviation) | Distribution parameter 3 (name) |
|---|---|---|---|---|---|---|---|---|
| mR | MAB2_1AR | Ab2.1a model uncertainty factor strength | | Ab2.1a | | | | |
| mS | MAB2_1AS | Ab2.1a model uncertainty factor loading | | Ab2.1a | | | | |
| mR | MAB2_1BR | Ab2.1b model uncertainty factor strength | | Ab2.1b | | | | |
| mS | MAB2_1BS | Ab2.1b model uncertainty factor loading | | Ab2.1b | | | | |
| mR | MBA1_1R | Ba1.1 model uncertainty factor strength | | Ba1.1 | | | | |
| mS | MBA1_1S | Ba1.1 model uncertainty factor loading | | Ba1.1 | | | | |
| mR | MBA1_4R | Ba1.4 model uncertainty factor strength | | Ba1.4 | | | | |
| mS | MBA1_4S | Ba1.4 model uncertainty factor loading | | Ba1.4 | | | | |
| mR | MBA1_5AIIR | Ba1.5aii model uncertainty factor strength | | Ba1.5aii | | | | |
| mS | MBA1_5AIIS | Ba1.5aii model uncertainty factor loading | | Ba1.5aii | | | | |

| Parameter | Unique fortran name | Description | Unit | LSE mapping | Example distribution | Distribution parameter 1 (Variation coefficient) | Distribution parameter 2 (Standard Deviation) | Distribution parameter 3 (name) |
|---|---|---|---|---|---|---|---|---|
| mR | MBA1_5AIIIR | Ba1.5aiii model uncertainty factor strength | | Ba1.5aiii | lognormal [1] | 1.2 | | 0.1 |
| mS | MBA1_5AIIIS | Ba1.5aiii model uncertainty factor loading | | Ba1.5aiii | | | | |
| mR | MBA1_5BR | Ba1.5b model uncertainty factor strength | | Ba1.5b | | | | |
| mS | MBA1_5BS | Ba1.5b model uncertainty factor loading | | Ba1.5b | | | | |
| mR | MBA1_5DR | Ba1.5d model uncertainty factor strength | | Ba1.5d | | | | |
| mS | MBA1_5DS | Ba1.5d model uncertainty factor loading | | Ba1.5d | | | | |
| mR | MBA1_6R | Ba1.6 model uncertainty factor strength | | Ba1.6 | | | | |
| mS | MBA1_6S | Ba1.6 model uncertainty factor loading | | Ba1.6 | | | | |
| mR | MBA2_1AR | Ba2.1a model uncertainty factor strength | | Ba2.1a | | | | |
| mS | MBA2_1AS | Ba2.1a model uncertainty factor loading | | Ba2.1a | | | | |

| Parameter | Unique fortran name | Description | Unit | LSE mapping | Example distribution | Distribution parameter 1 (Variation coefficient) | Distribution parameter 2 (Standard Deviation) | Distribution parameter 3 (name) |
|---|---|---|---|---|---|---|---|---|
| mR | MBA2_1BR | Ba2.1b model uncertainty factor strength | | Ba2.1b | | | | |
| mS | MBA2_1BS | Ba2.1b model uncertainty factor loading | | Ba2.1b | | | | |
| mR | MBA2_3R | Ba2.3 model uncertainty factor strength | | Ba2.3 | | | | |
| mS | MBA2_3S | Ba2.3 model uncertainty factor loading | | Ba2.3 | | | | |
| mR | MBA2_4BR | Ba2.4b model uncertainty factor strength | | Ba2.4b | | | | |
| mS | MBA2_4BS | Ba2.4b model uncertainty factor loading | | Ba2.4b | | | | |
| mR | MBA2_4CR | Ba2.4c model uncertainty factor strength | | Ba2.4c | | | | |
| mS | MBA2_4DR | Ba2.4c model uncertainty factor loading | | Ba2.4d | | | | |
| mR | MBA2_4CS | Ba2.4d model uncertainty factor strength | | Ba2.4c | | | | |
| mS | MBA2_4DS | Ba2.4d model uncertainty factor loading | | Ba2.4d | | | | |

| Parameter | Unique fortran name | Description | Unit | LSE mapping | Example distribution | Distribution parameter 1 (Variation coefficient) | Distribution parameter 2 (Standard Deviation) | Distribution parameter 3 (name) |
|---|---|---|---|---|---|---|---|---|
| mR | MBA2_4IR | Ba2.4i model uncertainty factor strength | | Ba2.4i | | | | |
| mS | MBA2_4IS | Ba2.4i model uncertainty factor loading | | Ba2.4i | | | | |
| mR | MBA2_4IIIR | Ba2.4iii model uncertainty factor strength | | Ba2.4iii | | | | |
| mS | MBA2_4IIIS | Ba2.4iii model uncertainty factor loading | | Ba2.4iii | | | | |
| mR | MBA2_5R | Ba2.5 model uncertainty factor strength | | Ba2.12 | | | | |
| mS | MBA2_5S | Ba2.5 model uncertainty factor loading | | Ba2.13 | | | | |
| mR | MBA3_1R | Ba3.1 model uncertainty factor strength | | Ba3.1 | | | | |
| mS | MBA3_1S | Ba3.1 model uncertainty factor loading | | Ba3.1 | | | | |
| mR | MBB1_2R | Bb1.2 model uncertainty factor strength | | Bb1.2 | | | | |
| mS | MBB1_2S | Bb1.2 model uncertainty factor loading | | Bb1.2 | | | | |

| Parameter | Unique fortran name | Description | Unit | LSE mapping | Example distribution | Distribution parameter 1 (Variation coefficient) | Distribution parameter 2 (Standard Deviation) | Distribution parameter 3 (name) |
|---|---|---|---|---|---|---|---|---|
| mR | MBb1_4R | Bb1.4 model uncertainty factor strength | | Bb1.4 | | | | |
| mS | MBb1_4S | Bb1.4 model uncertainty factor loading | | Bb1.4 | | | | |
| mR | MBC1_1R | Bc1.1 model uncertainty factor strength | | Bc1.1 | | | | |
| mS | MBC1_1S | Bc1.1 model uncertainty factor loading | | Bc1.1 | | | | |
| mR | MBC1_4R | Bc1.4 model uncertainty factor strength | | Bc1.4 | | | | |
| mS | MBC1_4S | Bc1.4 model uncertainty factor loading | | Bc1.4 | | | | |
| mR | MBC1_5R | Bc1.5 model uncertainty factor strength | | Bc1.5 | | | | |
| mS | MBC1_5S | Bc1.5 model uncertainty factor loading | | Bc1.5 | | | | |
| mR | MBC2_1AR | Bc2.1a model uncertainty factor strength | | Bc2.1a | | | | |
| mS | MBC2_1AS | Bc2.1a model uncertainty factor loading | | Bc2.1a | | | | |

| Parameter | Unique fortran name | Description | Unit | LSE mapping | Example distribution | Distribution parameter 1 (Variation coefficient) | Distribution parameter 2 (Standard Deviation) | Distribution parameter 3 (name) |
|---|---|---|---|---|---|---|---|---|
| mR | MBC2_1BR | Bc2.1b model uncertainty factor strength | | Bc2.1b | | | | |
| mS | MBC2_1BS | Bc2.1b model uncertainty factor loading | | Bc2.1b | | | | |
| mR | MBC2_1CR | Bc2.1c model uncertainty factor strength | | Bc2.1c | | | | |
| mS | MBC2_1DR | Bc2.1c model uncertainty factor loading | | Bc2.1d | | | | |
| mR | MBC2_1CS | Bc2.1d model uncertainty factor strength | | Bc2.1c | | | | |
| mS | MBC2_1DS | Bc2.1d model uncertainty factor loading | | Bc2.1d | | | | |
| mR | MBC2_1GR | Bc2.1g model uncertainty factor strength | | Bc2.1g | | | | |
| mS | MBC2_1GS | Bc2.1g model uncertainty factor loading | | Bc2.1g | | | | |
| mR | MBC2_1HR | Bc2.1h model uncertainty factor strength | | Bc2.1h | | | | |
| mS | MBC2_1HS | Bc2.1h model uncertainty factor loading | | Bc2.1h | | | | |

| Parameter | Unique fortran name | Description | Unit | LSE mapping | Example distribution | Distribution parameter 1 (Variation coefficient) | Distribution parameter 2 (Standard Deviation) | Distribution parameter 3 (name) |
|---|---|---|---|---|---|---|---|---|
| mR | MBC2_1JR | Bc2.1j model uncertainty factor strength | | Bc2.1j | | | | |
| mS | MBC2_1JS | Bc2.1j model uncertainty factor loading | | Bc2.1j | | | | |
| mR | MBC2_1KR | Bc2.1k model uncertainty factor strength | | Bc2.1k | | | | |
| mS | MBC2_1KS | Bc2.1k model uncertainty factor loading | | Bc2.1k | | | | |
| mR | MBC2_1MR | Bc2.1m model uncertainty factor strength | | Bc2.1m | | | | |
| mS | MBC2_1MS | Bc2.1m model uncertainty factor loading | | Bc2.1m | | | | |
| mR | MBC2_3AR | Bc2.3a model uncertainty factor strength | | Bc2.3a | | | | |
| mS | MBC2_3AS | Bc2_3a model uncertainty factor loading | | Bc2.3a | | | | |
| mR | MBC2_3BR | Bc2_3b model uncertainty factor strength | | Bc2.3b | | | | |
| mS | MBC2_3BS | Bc2_3b model uncertainty factor loading | | Bc2.3b | | | | |

| Parameter | Unique fortran name | Description | Unit | LSE mapping | Example distribution | Distribution parameter 1 (Variation coefficient) | Distribution parameter 2 (Standard Deviation) | Distribution parameter 3 (name) |
|---|---|---|---|---|---|---|---|---|
| mR | MBC3_1AR | Bc3_1a model uncertainty factor strength | | Bc3.1a | | | | |
| mS | MBC3_1AS | Bc3_1a model uncertainty factor loading | | Bc3.1a | | | | |
| mR | MBC3_1BR | Bc3_1b model uncertainty factor strength | | Bc3.1b | | | | |
| mS | MBC3_1BS | Bc3_1b model uncertainty factor loading | | Bc3.1b | | | | |
| mR | MBC3_1CR | Bc3_1c model uncertainty factor strength | | Bc3.1c | | | | |
| mS | MBC3_1CS | Bc3_1c model uncertainty factor loading | | Bc3.1c | | | | |
| mR | MBC3_1DR | Bc3_1d model uncertainty factor strength | | Bc3.1d | | | | |
| mS | MBC3_1DS | Bc3_1d model uncertainty factor loading | | Bc3.1d | | | | |
| mR | MCA2_1AR | Ca2.1a model uncertainty factor strength | | Ca2.1a | | | | |
| mS | MCA2_1AS | Ca2.1a model uncertainty factor loading | | Ca2.1a | | | | |

| Parameter | Unique fortran name | Description | Unit | LSE mapping | Example distribution | Distribution parameter 1 (Variation coefficient) | Distribution parameter 2 (Standard Deviation) | Distribution parameter 3 (name) |
|---|---|---|---|---|---|---|---|---|
| mR | MCA2_1BR | Ca2.1b model uncertainty factor strength | | Ca2.1b | | | | |
| mS | MCA2_1BS | Ca2.1b model uncertainty factor loading | | Ca2.1b | | | | |
| mR | MCA2_2AR | Ca2.2a model uncertainty factor strength | | Ca2.2a | | | | |
| mS | MCA2_2AS | Ca2.2a model uncertainty factor loading | | Ca2.2a | | | | |
| mR | MCA2_2BR | Ca2.2b model uncertainty factor strength | | Ca2.2b | | | | |
| mS | MCA2_2BS | Ca2.2b model uncertainty factor loading | | Ca2.2b | | | | |
| mR | MCA2_3R | Ca2.3 model uncertainty factor strength | | Ca2.3 | | | | |
| mS | MCA2_3S | Ca2.3 model uncertainty factor loading | | Ca2.3 | | | | |
| mR | MCB1_2AR | Cb1.2a model uncertainty factor strength | | Cb1.2a | | | | |
| mS | MCB1_2AS | Cb1.2a model uncertainty factor loading | | Cb1.2a | | | | |

| Parameter | Unique fortran name | Description | Unit | LSE mapping | Example distribution | Distribution parameter 1 (Variation coefficient) | Distribution parameter 2 (Standard Deviation) | Distribution parameter 3 (name) |
|---|---|---|---|---|---|---|---|---|
| mR | MCB1_2CR | Cb1.2c model uncertainty factor strength | | Cb1.2c | | | | |
| mS | MCB1_2CS | Cb1.2c model uncertainty factor loading | | Cb1.2c | | | | |
| mR | MCB1_2DR | Cb1.2d model uncertainty factor strength | | Cb1.2d | | | | |
| mS | MCB1_2DS | Cb1.2d model uncertainty factor loading | | Cb1.2d | | | | |
| mR | MCC1_2AIIR | Cc1.2aii model uncertainty factor strength | | Cc1.2aii | | | | |
| mS | MCC1_2AIIS | Cc1.2aii model uncertainty factor loading | | Cc1.2aii | | | | |
| mR | MCC1_2BR | Cc1_2b model uncertainty factor strength | | Cc1.2b | | | | |
| mS | MCC1_2BS | Cc1_2b model uncertainty factor loading | | Cc1.2b | | | | |
| mR | MCC1_2CR | Cc1_2c model uncertainty factor strength | | Cc1.2c | | | | |
| mS | MCC1_2CS | Cc1_2c model uncertainty factor loading | | Cc1.2c | | | | |

| Parameter | Unique fortran name | Description | Unit | LSE mapping | Example distribution | Distribution parameter 1 (Variation coefficient) | Distribution parameter 2 (Standard Deviation) | Distribution parameter 3 (name) |
|---|---|---|---|---|---|---|---|---|
| mR | MCC1_2DR | Cc1_2d model uncertainty factor strength | | Cc1.2d | | | | |
| mS | MCC1_2DS | Cc1_2d model uncertainty factor loading | | Cc1.2d | | | | |
| mR | MCC1_5R | Cc1.5 model uncertainty factor strength | | Cc1.5 | | | | |
| mS | MCC1_5S | Cc1.5 model uncertainty factor loading | | Cc1.5 | | | | |
| mR | MCC2_2AR | Cc2.2a model uncertainty factor strength | | Cc2.2a | | | | |
| mS | MCC2_2AS | Cc2.2a model uncertainty factor loading | | Cc2.2a | | | | |
| mR | MCC2_2BR | Cc2.2b model uncertainty factor strength | | Cc2.2b | | | | |
| mS | MCC2_2BS | Cc2.2b model uncertainty factor loading | | Cc2.2b | | | | |
| mR | MDA2_5R | Da2.5 model uncertainty factor strength | | Da2.5 | | | | |
| mS | MDA2_5S | Da2.5 model uncertainty factor loading | | Da2.5 | | | | |

| Parameter | Unique fortran name | Description | Unit | LSE mapping | Example distribution | Distribution parameter 1 (Variation coefficient) | Distribution parameter 2 (Standard Deviation) | Distribution parameter 3 (name) |
|---|---|---|---|---|---|---|---|---|
| mR | MDA4_1R | Da4.1 model uncertainty factor strength | | Da4.1 | | | | |
| mS | MDA4_1S | Da4.1 model uncertainty factor loading | | Da4.1 | | | | |
| mR | MDA4_2AR | Da4.2a model uncertainty factor strength | | Da4.2a | | | | |
| mS | MDA4_2AS | Da4.2a model uncertainty factor loading | | Da4.2a | | | | |
| mR | MDA4_2BR | Da4.2b model uncertainty factor strength | | Da4.2b | | | | |
| mS | MDA4_2BS | Da4.2b model uncertainty factor loading | | Da4.2b | | | | |
| mR | MDA4_2CR | Da4.2c model uncertainty factor strength | | Da4.2c | | | | |
| mS | MDA4_2CS | Da4.2c model uncertainty factor loading | | Da4.2c | | | | |
| mR | MDA4_3R | Da4.3 model uncertainty factor strength | | Da4.9 | | | | |
| mS | MDA4_3S | Da4.3 model uncertainty factor loading | | Da4.10 | | | | |

| Parameter | Unique fortran name | Description | Unit | LSE mapping | Example distribution | Distribution parameter 1 (Variation coefficient) | Distribution parameter 2 (Standard Deviation) | Distribution parameter 3 (name) |
|---|---|---|---|---|---|---|---|---|
| mR | MBA1_5AIR | Ba1.5ai model uncertainty factor strength | | Ba1.5ai | lognormal [1] | 0.7 | | 0.1 |
| mS | MBA1_5AIS | Ba1.5ai model uncertainty factor loading | | Ba1.5ai | | | | |
| D | WaterCondLayer | Thickness of the wate conductive layer underneath the embankments | | Ba1.5ai | normal [1] | | | 0.1 |
| Bb | BermLevel | Berm level in outside slope | m | Aa2.4, Ba1.1, Ba1.5bii Ba1.5dii, Ba2.5 | normal [1] | | 0.2 | |
| Sdrock | SdRock | switch for calculation damage level of rock armour from RockErosionArea and Dn50 (0) or for the indication of the damage level Sd (1) | | Bc2.1c, Ab2.1b | deterministic | | | |
| | OutSlopeAngLow | Angle of the lower part of the outside slope in case of a berm | | Aa2.4, Ba1.1, Ba1.5bii Ba1.5dii, Ba2.5 | | | | |
| | WallAng | Angle in relation to gamma_v to take the influence of a vertical crown wall into account | | Aa2.4, Ba1.1, Ba1.5bii Ba1.5dii, Ba2.5 | | | | |
| | NumRun | Number of the wave run up | | Aa2.4, Ba1.1, Ba2.5, | | | | |

| Parameter | Unique fortran name | Description | Unit | LSE mapping | Example distribution | Distribution parameter 1 (Variation coefficient) | Distribution parameter 2 (Standard Deviation) | Distribution parameter 3 (name) |
|---|---|---|---|---|---|---|---|---|
| | | model | | Ba1.5bii, Ba1.5dii | | | | |
| | Fwind | Factor taking the effect of wind on the overtopping discharge into account (EurOtop Manual) | | Aa2.4, Ba1.1, Ba1.5bii Ba1.5dii, Ba2.5 | | | | |
| | BatterWall510 | (0) for 5:1 battered wall (1) for 10:1 battered wall | | Aa2.4, Ba1.1, Ba1.5bii Ba1.5dii, Ba2.5 | | | | |
| | gamma_f | Shape factor in overtopping models, see Eurotop manual | | Aa2.4, Ba1.1, Ba1.5bii Ba1.5dii, Ba2.5 | | | | |
| | MBA2_1BIIR | Ba2.1bii model uncertainty factor strength | | Ba2.1bii | | | | |
| | MBA2_1BIIS | Ba2.1bii model uncertainty factor loading | | Ba2.1bii | | | | |
| | MBA2_1BIIIR | Ba2.1biii model uncertainty factor strength | | Ba2.1bii | | | | |
| | MBA2_1BIIIS | Ba2.1biii model uncertainty factor loading | | Ba2.1bii | | | | |
| | ShipWindWaves | Switch for ship waves (0) or wind waves (1) | | Bc2.1b | | | | |
| | MBA1_5BIIR | Ba1.5bii model uncertainty | | Ba1.5bii | | | | |

| Parameter | Unique fortran name | Description | Unit | LSE mapping | Example distribution | Distribution parameter 1 (Variation coefficient) | Distribution parameter 2 (Standard Deviation) | Distribution parameter 3 (name) |
|---|---|---|---|---|---|---|---|---|
| | | factor strength | | | | | | |
| | MBA1_5BIIS | Ba1.5bii model uncertainty factor loading | | Ba1.5bii | | | | |
| | MBA1_5DIIR | Ba1.5dii model uncertainty factor strength | | Ba1.5dii | | | | |
| | MBA1_5DIIS | Ba1_5dii model uncertainty factor loading | | Ba1.5dii | | | | |
| Df50 | Df50 | 50 percentile in the filter | m | Ba1.5c | | | | |
| | FineGrainLayer | Layer thickness of fine grained | | Bb1.2 | | | | |
| | BottomLevelDeep | Bottom level at deep water, to derive water depth at deep water | | Ca2.2a | | | | |
| num | Num | the type of embankment, determining the type of overtopping model | - | Aa2.4, Ba1.1, Ba2.5, Ba1.5bii, Ba1.5dii | | | | |
| no_k_hor | KnotsNumber | the number of knots in the grid in horizontal direction | - | Ab2.1b, Bc2.1c | | | | |
| d1 | d1 | dimension concrete wall/sheet pile wall | - | Cc1.2aii, Cc1.2b | normal [2d] | | 0.004 | |
| d2 | d2 | dimension concrete wall/sheet pile wall | - | Cc1.2aii, Cc1.2b | normal [2d] | | 0.004 | |

| Parameter | Unique fortran name | Description | Unit | LSE mapping | Example distribution | Distribution parameter 1 (Variation coefficient) | Distribution parameter 2 (Standard Deviation) | Distribution parameter 3 (name) |
|---|---|---|---|---|---|---|---|---|
| | | | | Cc1.2d | | | | |
| d3 | d3 | dimension concrete wall/sheet pile wall | - | Cc1.2aii, Cc1.2b | normal [2d] | | 0.004 | |
| d4 | d4 | dimension concrete wall/sheet pile wall | - | Cc1.2aii, Cc1.2b<br>Cc1.2d | normal [2d] | | 0.004 | |
| d5 | d5 | dimension concrete wall/sheet pile wall | - | Cc1.2aii , Cc1.2b | normal [2d] | | 0.004 | |
| d6 | d6 | dimension concrete wall/sheet pile wall | - | Cc1.2aii , Cc1.2b | normal [2d] | | 0.004 | |
| d7 | d7 | dimension concrete wall/sheet pile wall | - | Cc1.2aii , Cc1.2b | normal [2d] | | 0.004 | |
| d8 | d8 | dimension concrete wall/sheet pile wall | - | Cc1.2aii , Cc1.2b | normal [2d] | | 0.004 | |
| d9 | d9 | dimension concrete wall/sheet pile wall | - | Cc1.2aii , Cc1.2b | normal [2d] | | 0.004 | |
| ds | ds | distance from outer concrete fibre to heart of the reinforcement | - | Cc1.2c, Cc2.2b<br>Ca2.3 | lognormal[2d]<br>(normal+0.005) | | 0.01 | |
| h1 | h1 | Level of elevation in front of riverside of concrete wall | - | Cb1.2a,Cb1.2c,Cb1.2d | normal [1] | | 0.1 | |

| Parameter | Unique fortran name | Description | Unit | LSE mapping | Example distribution | Distribution parameter 1 (Variation coefficient) | Distribution parameter 2 (Standard Deviation) | Distribution parameter 3 (name) |
|---|---|---|---|---|---|---|---|---|
| | | | | Cc1.2aii, Cc1.2b, Cc1.2d | | | | |
| h3 | h3 | Level of elevation of ground behind concrete wall on landward side | - | Cb1.2a,Cb1.2c,Cb1.2d Cc1.2aii, Cc1.2b, Cc1.2d | normal [1] | | 0.1 | |

[1] Vrouwenvelder et al.

[2a] CUR 140

[2b] CUR 141

[2c] CUR 162

[2d] CUR 190

[3] IGBE

[4] Christian & Baecher

[5] Leidraad

[6] lecture notes CT5310 probabilistic design in hydraulic engineering

## APPENDIX V-5: DETAILED INSTRUCTIONS FOR INTERFACE OPERATION

The Calculator is started by opening the EXCEL spreadsheet ReliabilityCalc.xls. There are five tabbed worksheets, of which the prime one is that labelled Calculate, as shown in Figure 3 (The remaining four are used to update the files defining Failure Modes, Parameters etc. These may be used for 'extending' the Calculator – see Appendix 3.).

In outline, the process is:

(1) Click Reset button if any of the underlying files (Parameter.csv, FailureMode.csv, FailureModeParam.csv, Structure.csv) have changed since the sheet was last shown.

(2) Choose a structure from the drop-down box.

(3) If you have changed the structure, click on Load Parameter Names.

This will regenerate the names under PARAMETERS to reflect the parameters used by the LSE functions for the failure Modes used in the fault Tree for the structure.

Currently, the values from the previous structure are not cleared automatically. You need to do this yourself.

(4) For each parameter, enter a value and, optionally, a Statistical distribution and its parameters.

Currently, the permitted values in the Distribution column are blank (fixed value), N (Normal) and LN (Log Normal). Other options will be added at a later release.

The value in the Value column is either the fixed value (Distribution is blank) or the Mean value (other Distributions).

The Distribution Parameters columns allow up to 4 further parameters for a statistical distribution. The current distributions (Normal or Log Normal) only require the first column to be filled – with the standard deviation for the distribution.

(5) Review the Convergence Control parameters and change them if you wish. These are used to control how the Reliability Calculator determines whether it has a converged value for the annual probability of failure.

For any 'sample', the Calculator generates values for each parameter- either the fixed value of a random value according to the prescribed distribution.

It then evaluates the Fault Tree for the structure using these values for the parameters passed to the LSE functions and determines whether or not the structure will fail.

After a number of samples, the non-annualised failure rate is simply the number of failures divided by the number of samples.

After Min samples and every Interval samples, the failure rate is calculated and compared with the previously calculated value. If the 2 failure rates satisfy the following relationship, then convergence has been detected at this interval.

$$Abs\left(1-\frac{Rate1}{Rate2}\right) < Factor$$

Factor is the value of the Convergence Factor.

If Rate2 is very small (less than Factor) then the relationship is

$$Abs(Rate1 - Rate2) < Factor$$

In normal use, once convergence has been detected then the calculator has a value.

However, you can ensure tighter convergence control by supplying an integer value greater than one for Successive Intervals. In this case, convergence must be detected for that number of successive intervals before a final value is determined. This can be used if you suspect that convergence is being detected too early 'by chance'.

The Calculator will also terminate if it reaches MaxSamples. The 'rate of failure' value at the last interval will be returned.

(6) Review the other Control parameters and change them if you wish. For maximum efficiency, use Yes for Optimise and No for both Log each Sample and Log each LSE call.

| | |
|---|---|
| Events per year | Used as a multiplier of 'failure rate' to produce Annual Probability of Failure. If the assumption is that the load occurrence rate is 1 per year then this is set to 1 and the failure rate=annual probability of failure |
| Optimise | Should normally be set to Yes. This ensures that the Calculator will only call an LSE function if it's essential. For example, if it evaluates an OR gate and the LSE function for the first Failure Mode within the gate indicates 'failure' then there is no need to call the LSE functions for the other Failure Modes within the same gate.<br><br>You may find it useful to set Optimise to No if you are logging each LSE call (see section 0) and you want to monitor the results of the LSE function even where they are irrelevant. |
| Log each Sample | Controls how much information is logged by the Calculator – see section 0 |
| Log each LSE call | ditto |

(7) Press Calculate button.

The values under RESULTS will clear while the calculation proceeds. When the calculation completes, the results will be shown as follows

Annual Reliability 1.0 minus the Annual Probability of Failure

| | |
|---|---|
| Annual Probability of Failure | Calculated Fail rate times Events per year |
| Converged | Yes or No |
| Convergence Factor | The proximity of the last 2 failure rates checked. If Converged is Yes, the value will be less than the Convergence Factor in CONVERGENCE CONTROL. |
| Samples | The number of Samples checked. If Converged is No, this will be the same as Max Samples. |
| Time Taken (s) | Time taken by the Calculator. |

**Log messages**

In order to assist the investigation of the results produced by the Calculator, a log file is produced with messages as follows:

Currently, the log file is produced in the folder C:\TEMP which must exist. The name of the file is pcname_nnnn.log, where pcname is the name of your PC and nnnn is a number derived from the process id of the EXCEL instance you are using. This normally ensures that you can accumulate log files for several runs and delete them at your leisure.

Log files are simple text files viewable by tools such as Notepad.

(1) At the start of each Calculate run, 2 messages show the fixed values and the distributions to be used.

(2) Each time convergence is checked, a message shows the Sample and Failure counts, the current and previous 'rate of failure' and an indication of the proximity of the two. The line includes a message if full convergence was detected.

(3) Two additional messages are produced for each Sample if you have chosen Yes for Log each Sample.

One shows the specific values used for each parameter. The other shows the resulting failure indication – True or False.

(4) An additional message is produced for each LSE function call if you have chosen Yes for Log each LSE call. This gives the Failure Mode name, the LSE function name and the value returned by the function.

If your Optimise value is Yes, you may find that some Failure Modes are not evaluated since they were found to be unnecessary for the final result.

## APPENDIX V-6: SPECIFICATION CSV FILES

### Parameter.csv

The file `Parameter.csv` contains one line per parameter value which specifies the unique name of the parameter.

The order of the parameters determines the order in which they are stored in the `VALUES` array passed to an LSE function. However, an LSE Function should not rely on this. It should always call `'IndexOf'`.

### Failure Mode.csv

The file `FailureMode.csv` contains one line per Failure Mode. Each line has 3 columns as follows.

| Column | Description |
|---|---|
| **FailureModeName** | A unique name for the Failure Mode.<br>This name must match that used in the FTA Event Database. |
| **LSEFuncDLL** | The Filename of the DLL which includes the LSE function for this Failure Mode.<br>If possible, this should be the full pathname of the DLL including drive and directories.<br>If not, the DLL must be in the same directory as the Reliability Tool or in one of the directories listed in the PATH environment variable. |
| **LSEFuncName** | The name of the LSE Function. |

### Failuremodeparam.csv

The file `FailureModeParam.csv` contains one or more lines per Failure Mode and identifies which Parameters are used by the LSE Function for the Failure Mode. Each line has 2 columns as follows.

| Column | Description |
|---|---|
| **FailureModeName** | The unique name for the Failure Mode.<br>This name must be one of those included in the Failure Mode file – see 0. |
| **ParamName** | The name of a Parameter used by the LSE Function for this Failure Mode. |

| | |
|---|---|
| | The name must match one of those in the Parameter file – see 0. |

*This file may not be used in early implementations of the Reliability Tool software. Instead, a sheet will be provided for the user showing a grid of Parameter Names versus Failure Modes.*

## Structure.csv

The file `Structure.csv` contains one line per structure type. Each line has 2 columns as follows.

| Column | Description |
|---|---|
| **StructureName** | The unique name for the Structure Type.<br>This name will be used by the Reliability Tool user. |
| **FTAFile** | The filename of the OpenFTA file which defines the relevant Failure Modes and the logic which links them.<br>If possible, this should be the full pathname of the file including drive and directories.<br>If not, the file must be in the same directory as the Reliability Tool. |